Model Development Report: Mattole River Watershed

SUBMITTED TO:

State Water Resources Control Board
1001 I Street, 14th Floor
Sacramento, CA 95814

PREPARED BY:

Paradigm Environmental
9320 Chesapeake Drive, Suite 100
San Diego, CA 92123

DECEMBER 5, 2025

THIS PAGE INTENTIONALLY LEFT BLANK

Contents

Figures

Tables

1 INTRODUCTION

This report provides a detailed discussion of the development and configuration of a hydrology model which was developed for the Mattole River watershed to support decision making by the California State Water Resources Control Board (Water Board) regarding water supply, demand, and use. In April 2021, Governor Gavin Newsom issued a state of emergency proclamation for specific watersheds across California in response to exceptionally dry conditions throughout the state. The April 2021 proclamation, as well as subsequent proclamations, directed the Board to address these emergency conditions to ensure adequate, minimal water supplies for critical purposes. To support Water Board actions to address emergency conditions, hydrologic modeling and analysis tools are being developed to contribute to a comprehensive decision support system that assesses water supply and demand, and the flow needs for watersheds throughout California.

This model development report builds on the Mattole River watershed modeling work plan (SWRCB 2024) which has additional information on the model background and over-arching model approach; the Loading Simulation Program in C++ (LSPC) was used to simulate hydrology within the watershed. The model provides an evaluation platform for (1) simulating existing instream flows that integrate current water management activities and consumptive uses, (2) evaluating the range of impacts of alternative management scenarios. Key components necessary for the development of this model are detailed in this report. Model development refers to basic building blocks for defining the surface water model domain. It includes catchment delineation, reach segments (cross-sections, hydraulic characteristics, and routing network), and Hydrologic Response Units (HRUs). Model development also includes creating and assigning representative climate forcing inputs.

- Section 2 describes the Catchment Delineation and Hydraulic Network. Catchments are the highest resolution spatial boundaries in the model. Delineated catchments were compiled from best-available topographic layers and refined as needed to align outlets with monitoring gauges. Hydraulic routing features include reaches, lakes/reservoirs, and other network routing elements that convey flow and pollutants from one catchment to another.
- Section 3 describes the Hydrologic Response Units. HRUs are the smallest spatial unit within the model, representing unique combinations of spatial data layers including land use/land cover, hydrologic soil group, and slope that characterize hydrologic behavior.
- Section 4 describes climate forcing inputs. Forcing inputs include precipitation and potential evapotranspiration that drive the model's rainfall-runoff response.
- Section 5 describes the representation of surface water withdrawals and irrigation in the model.
- Section 6 presents an evaluation of the observed water balance within the watershed.
- Sections 7 and 8 detail the model calibration and validation procedures and results.

2 CATCHMENT NETWORK

2.1 Catchment Delineation

The United States Geological Survey (USGS) delineates watersheds nationwide based on surface hydrological features and organizes the drainage units into a nested hierarchy using hydrologic unit codes (HUC). These HUCs have a varying number of digits to denote scale ranging from 2-digit HUCs (largest) at the regional scale to 12-digit HUCs (smallest) at the subwatershed scale. The Mattole River watershed is defined as a HUC-8 watershed that comprises 15 HUC-12 subwatersheds.

For units smaller than HUC-12 subwatersheds, the National Hydrography Dataset Plus v2 (NHDPlus) has further discretized the watershed into catchments ranging in size between 0.003 square miles to about 6 square miles. Where necessary, catchments were either merged to eliminate braiding in the stream network or sub-delineated using the hydrologically conditioned 30-meter resolution digital elevation model (DEM), flow direction, and flow accumulation rasters available with the NHDPlus dataset to better represent points of interest. Catchments were merged in 17 cases; sub-delineation was necessary in 1 case where a catchment had disconnected reach segments with points of diversion. Table 2-1 presents summary statistics of NHDPlus catchment sizes by HUC-12 subwatershed. Figure 2-1 is a map of HUC-12 subwatersheds and NHDPlus catchments within the Mattole River HUC-8 watershed.

Table 2-1. Summary of finalized NHDPlus catchments within the Mattole River watershed HUC-12 subwatersheds

HUC-12	HUC-12 Name	Catchment Count	Catchment Minimum (acres)	Catchment Average (acres)	Catchment Maximum (acres)	Catchment Total (acres)
180101070101	Upper Bear River	54	2.7	580.1	2,621.8	31,327.0
180101070102	Lower Bear River	28	2.0	771.1	3,375.5	21,590.7
180101070201	Bear Creek	15	11.7	921.2	3,825.6	13,818.6
180101070202	Headwaters Mattole River	94	3.3	333.0	1,492.9	31,305.6
180101070203	Upper Mattole River	70	2.4	259.7	1,187.8	18,177.9
180101070204	Honeydew Creek	19	2.2	578.7	2,791.7	10,995.6
180101070205	Middle Mattole River	48	18.0	527.0	2,037.3	25,294.2
180101070206	Upper North Fork	27	261.5	621.1	1,333.4	16,768.5
180101070207	Squaw Creek	18	101.0	589.4	1,944.2	10,608.5
180101070208	North Fork	36	17.1	671.5	1,964.6	24,174.8
180101070209	Lower Mattole River	74	4.4	521.1	2,622.0	38,559.7
180101070301	Guthrie Creek	27	2.7	582.6	2,482.1	15,731.1
180101070302	Davis Creek	39	90.7	515.0	1,555.0	20,084.2
180101070401	Cooskie Creek	37	45.9	540.5	1,543.2	19,996.7
180101070402	Big Flat Creek	44	2.4	489.5	1,775.4	21,535.9
	Total	**630**	**--**	**--**	**--**	**319,968.9**

1. Note that the total area of NHDPlus catchments is 77 acres (0.02%) smaller than the raster-based area summaries presented later in this report because the raster layers have a coarser resolution (i.e., 30-m grid) than the vector catchment layer.

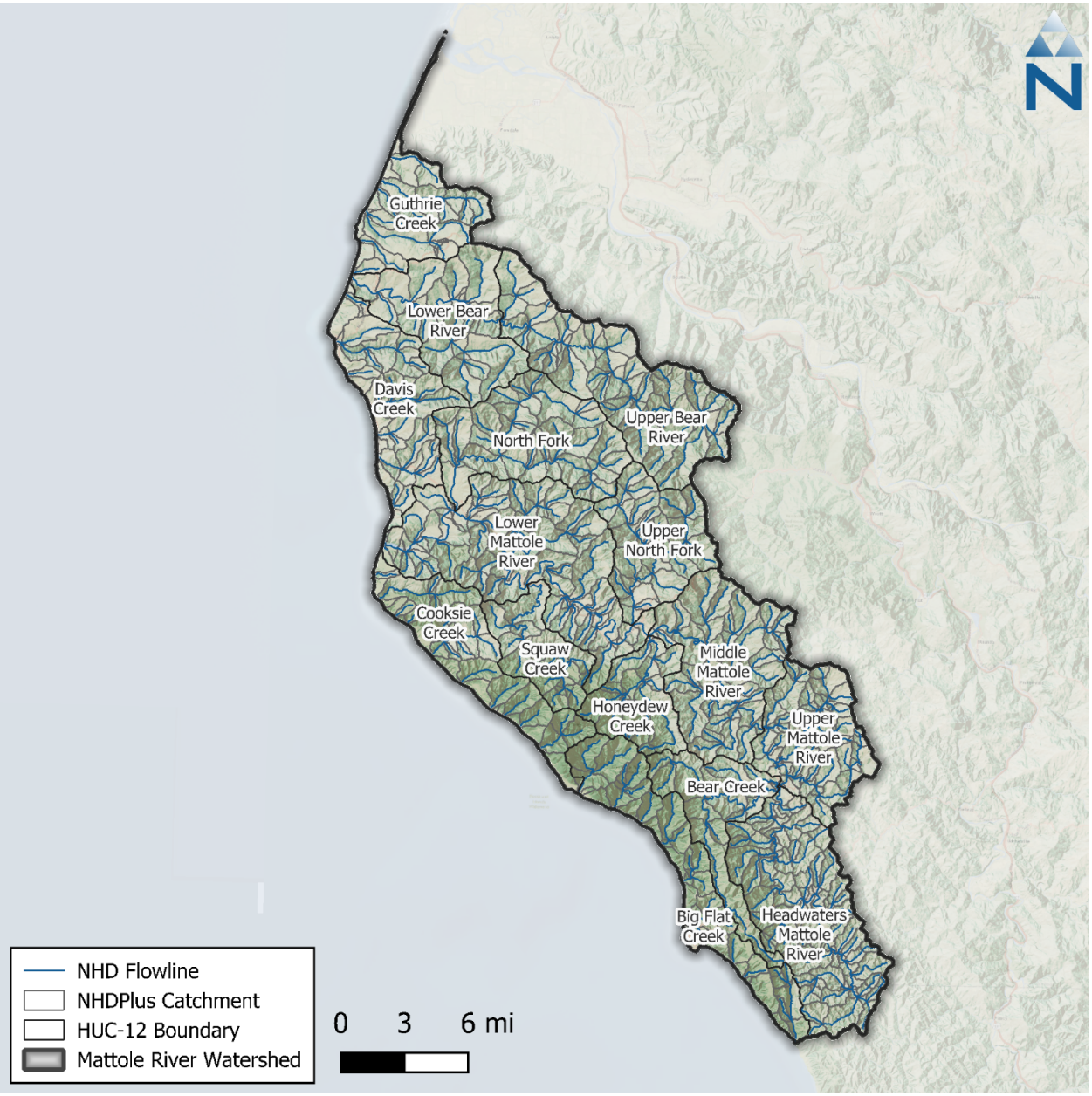

Figure 2-1. Final NHDPlus catchment segmentation for the Mattole River watershed.

2.2 Routing & Connectivity

Once catchments have been delineated, the connectivity of flow within and between each catchment needs to be specified so that water can be routed from upstream to downstream areas. Within the Mattole River watershed model, surface flow is conveyed through a reach network with no more than one representative reach segment for each catchment; note that some catchments draining directly to the coast do not have a stream segment. Within a catchment, water from all other upstream physical conveyances is routed directly to the top of and through the representative stream segment.

The reach network for the Mattole River watershed is based on the NHD flowlines available with the NHDPlus dataset. These flowlines were edited as described in Section 2.1 to eliminate braiding and are shown in Figure 2-1. There were also 4 coastal catchments that had a Point of Diversion (POD)

for surface water withdrawal, but no NHD flowline; stream segments were added to these catchments based on aerial imagery. Within the NHDPlus schema, catchments can be related to flowlines through the catchment *FEATUREID* and flowline *COMID*. The flowline *COMID* was joined to the PlusFlowlineVAA (value-added attributes) table available with the NHDPlus dataset to determine flow routing.

2.3 Stream Characteristics

The discharge for each stream segment is calculated in LSPC using Manning's equation, presented below as Equation 1:

$$Q = VA = (\frac{1.49}{n})AR^{\frac{2}{3}}\sqrt{S} \qquad \text{Equation 1}$$

where (A) is the cross-sectional area in square feet, (R) is the hydraulic radius in feet, (V) is the velocity in feet per second, (S) is the longitudinal slope, and (n) is the channel roughness coefficient.

Length and slope are derived from the PlusFlowlineVAA table, which includes precalculated reach characteristics based on local conditions. For reaches that were merged, split, or edited, the slope was recalculated as the length-weighted average slope (derived from the DEM described in Section 3.4) based on the new reach length. The default cross-section representation in LSPC is a symmetrical trapezoidal channel defined using the terms shown in Figure 2-2. Stream segments are represented in the model as having the same cross-section for the entire reach length. Numerous studies have developed empirical relationships between stream channel geometry and upstream contributing area (Bent & Waite 2013; McCandless 2003a, 2003b; McCandless & Everett 2002); these were used to derive channel geometry for each stream segment in LSPC. An initial estimate of $n = 0.04$ representing natural streams with vegetation was used for all reach segments and may be updated as needed during model calibration (Arcement & Schneider 1989).

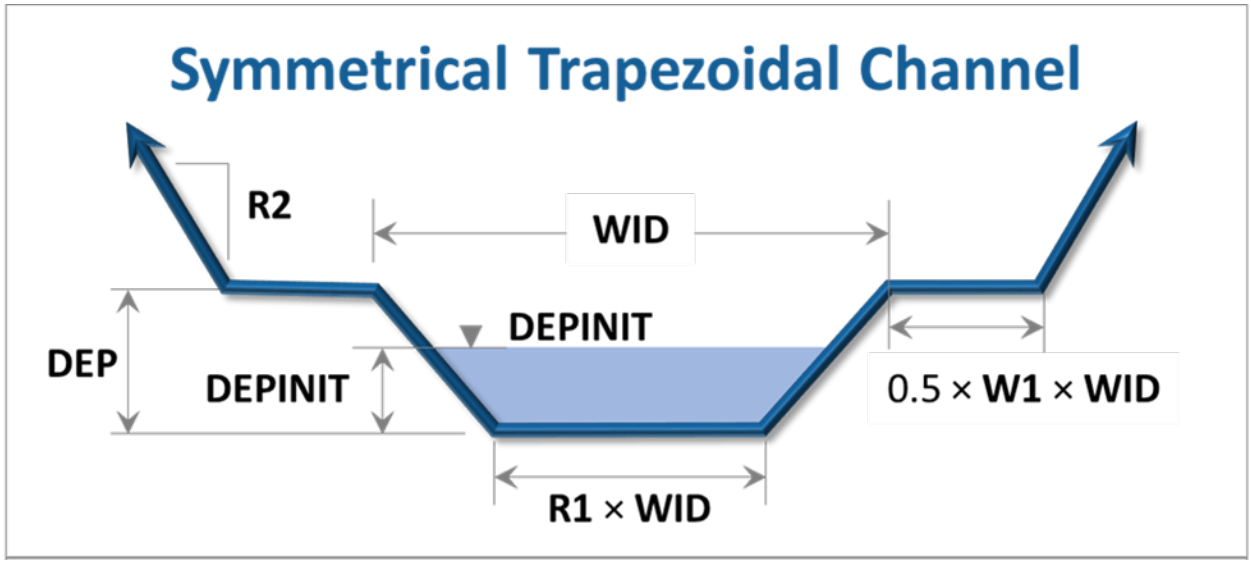

WID	Estimated Bankfull-Width	**R1**	Ratio of channel bottom width to **WID**
DEP	Estimated Bankfull-Depth	**R2**	Side slope for floodplain
DEPINIT	Initial water depth	**W1**	Floodplain width parameter

Figure 2-2. Example cross-section representation in LSPC.

3 HYDROLOGIC RESPONSE UNITS

Within LSPC, the land is categorized into HRUs, which are the core hydrologic modeling land units in the watershed model. Each HRU represents areas of similar physical characteristics attributable to certain processes. The HRU development process uses data types that are typically closely associated with hydrology (and water quality, when applicable) in the watershed. For the Mattole River watershed, this includes data such as land cover, cropland, soil type, and slope. The HRUs are developed by overlaying these datasets in raster format and identifying the unique combinations over the catchments. Ultimately, some consolidation of HRUs was implemented to balance the model computational efficiency and optimal spatial resolution, resulting in a set of meaningful HRUs for model configuration. Percent tree canopy was also summarized as a secondary attribute by HRU and used to estimate initial values for the interception storage and lower-zone evapotranspiration rate for model configuration.

Table 3-1 lists the spatial data used in the HRU analysis along with the corresponding data sources. The following subsections summarize the data that were used to develop each of these spatial layers and the processes for consolidating them as HRUs.

Table 3-1. Summary of input datasets detailing data source and type

GIS Layer	Data Source	Site	Description	Date Downloaded
Digital Elevation Model	USGS 3D Elevation Program (3DEP)	Science Base	2024 – 27.66m resolution grid	August 1, 2024
Land Cover	MRLC (NLCD)	MRLC	2021 – 30m resolution grid	June 30, 2023
Cropland	USDA (CDL)	USDA	2022 – 30m resolution grid	January 2, 2023
Percent Imperviousness	MRLC (NLCD)	MRLC	2021 – 30m resolution grid	June 30, 2023
Percent Tree Canopy	MRLC	MRLC	2021 – 30m resolution grid	October 5, 2023
Soil Survey Geographic Database (SSURGO)	USDA (NRCS)	USDA	2022 – polygon layer	October 5, 2023
U.S. General Soil Map (STATSGO2)	USDA (NRCS)	USDA	2016 – polygon layer	December 29, 2022

3.1 Land Cover

The land cover data were obtained from the 2021 National Land Cover Database (NLCD) maintained by the Multi-Resolution Land Consortium (MRLC), a joint effort between multiple federal agencies. The primary objective of the MRLC NLCD is to provide a current data product in the public domain with a consistent characterization of land cover across the United States. The 2021 NLCD provides a 16-class scheme at a 30-meter grid resolution.

Table 3-2 summarizes the NLCD 2021 land cover distribution for the Mattole River watershed; Figure 3-1 shows the land cover for the Mattole River watershed. Evergreen forest is the dominant land cover classification, covering approximately 63% of the watershed area. When combined, evergreen forest, the undeveloped categories of deciduous forest, mixed forest, shrub/scrub, and grassland/herbaceous account for close to 95% of the total watershed area. Developed land cover makes up less than 4% of

the total watershed area and is classified mostly as "Developed, Open Space," which suggests that much of the developed area is dispersed. None of the total watershed areas are categorized as cultivated cropland. For HRU development, similar NLCD classes (e.g., forest) were grouped.

Table 3-2. Distribution of 2021 NLCD land cover classes within the Mattole River watershed

NLCD Class	Description	Model Group[1]	Area (acres)	Area (%)
22	Developed, Low Intensity	Developed_Low_Intensity	1,079.3	0.3%
23	Developed, Medium Intensity	Developed_Medium_Intensity	529.5	0.2%
24	Developed, High Intensity	Developed_High_Intensity	86.5	0.0%
21	Developed, Open Space	Developed_Open_Space	9,989.7	3.1%
31	Barren Land (Rock/Sand/Clay)	Barren	2,589.8	0.8%
41	Deciduous Forest	Forest	7,913.2	2.5%
42	Evergreen Forest	Forest	201,847.4	63.1%
43	Mixed Forest	Forest	18,139.8	5.7%
52	Shrub/Scrub	Scrub	38,328.9	12.0%
71	Grassland/Herbaceous	Grassland	36,578.2	11.4%
81	Pasture/Hay	Pasture	111.0	0.0%
82	Cultivated Crops	Agriculture	0.0	0.0%
90	Woody Wetlands	Forest	540.4	0.2%
95	Emergent Herbaceous Wetlands	Grassland	1919.7	0.6%
11	Open Water	Water	392.7	0.1%
		Total	**320,046.3**	**100.0%**

1. Developed land cover will be refined and redistributed into effective Developed_Impervious and Developed_Pervious areas as described in Section 3.6.1. All other model groups are mapped for consolidation as shown.

Color Gradient: Lowest | Low | Med | High | Highest

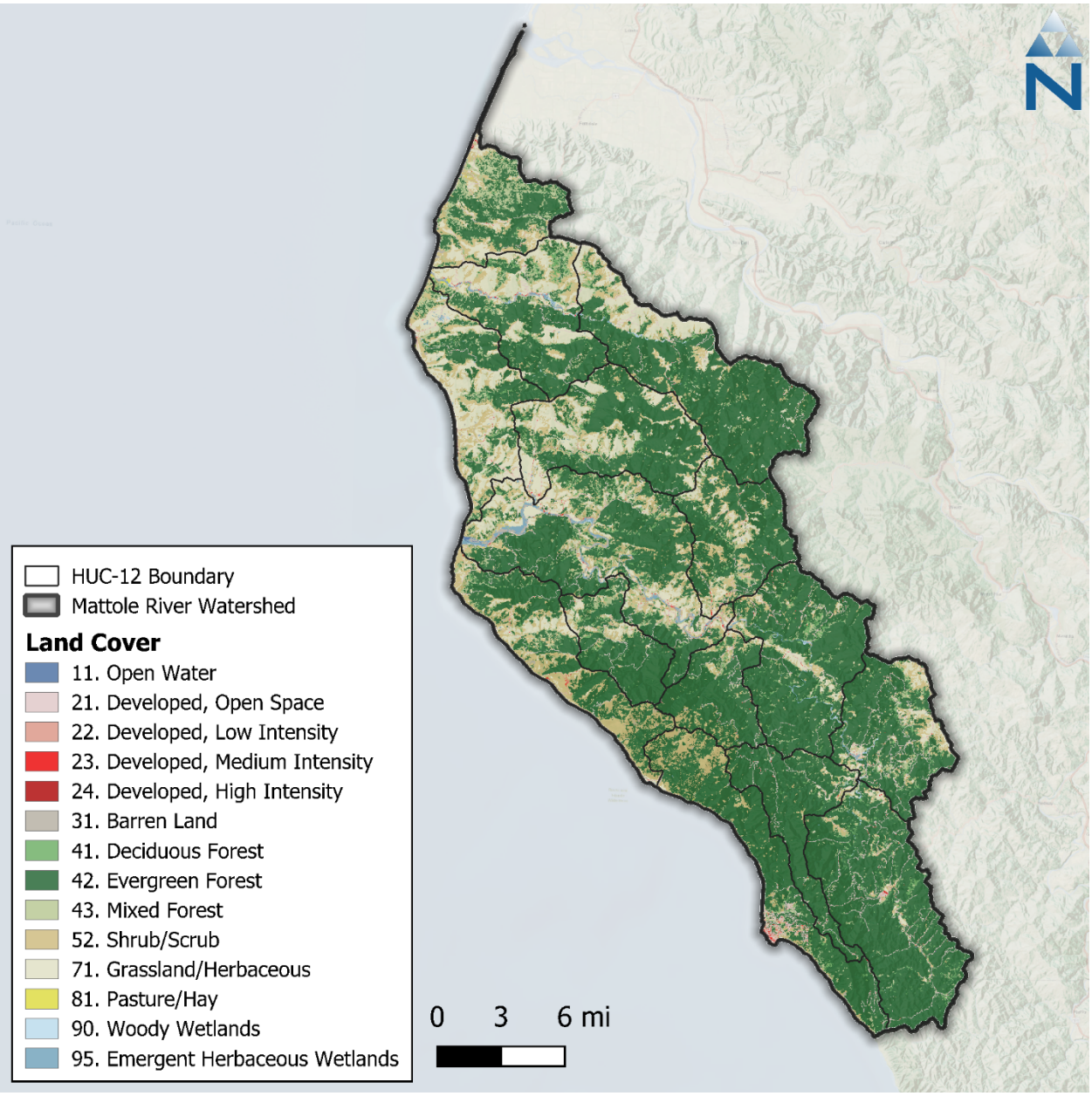

Figure 3-1. NLCD 2021 land cover within the Mattole River watershed.

3.2 Agriculture and Crops

Land cover data for the Mattole River watershed (see Section 3.1) were analyzed to identify predominant cropland vegetation classes. This analysis revealed that only 0.03% of the watershed area was classified as Pasture/Hay (class 81), 12% was classified as Shrub/Scrub (class 52), and 11% was classified as Grassland/Herbaceous (class 71); of these areas, a portion may include areas of cultivated crops that were not automatically recognized through processing of the remote sensing data or include cultivated crops on a rotating schedule. To reflect these situations, supplemental information published by the United States Department of Agriculture (USDA) was used.

The USDA Cropland Data Layer (CDL) is an annually updated raster dataset that geo-references crop-specific land use (USDA 2024). The dataset comes as a 30-meter resolution raster with a linked

lookup table of 85 standard crop types that can be used to classify agricultural land. Figure 3-2 shows the spatial distribution of these classes through the study area and Table 3-3 summarizes their areal coverage. The CDL Land use layer was intersected with the NLCD Land Cover layer, and CDL Agriculture and Pasture land use classifications overwrote the original NLCD classifications. The combined Land Use/Land Cover (LULC) increased "Cropland" to nearly 201 acres (0.1%), which was classified as "Agriculture" in the final HRU layer—"Pasture" area was also updated to match CDL land use. The LULC intersection redistributes HRU area between originally classified Grassland, Pasture, and Agriculture categories from NLCD.

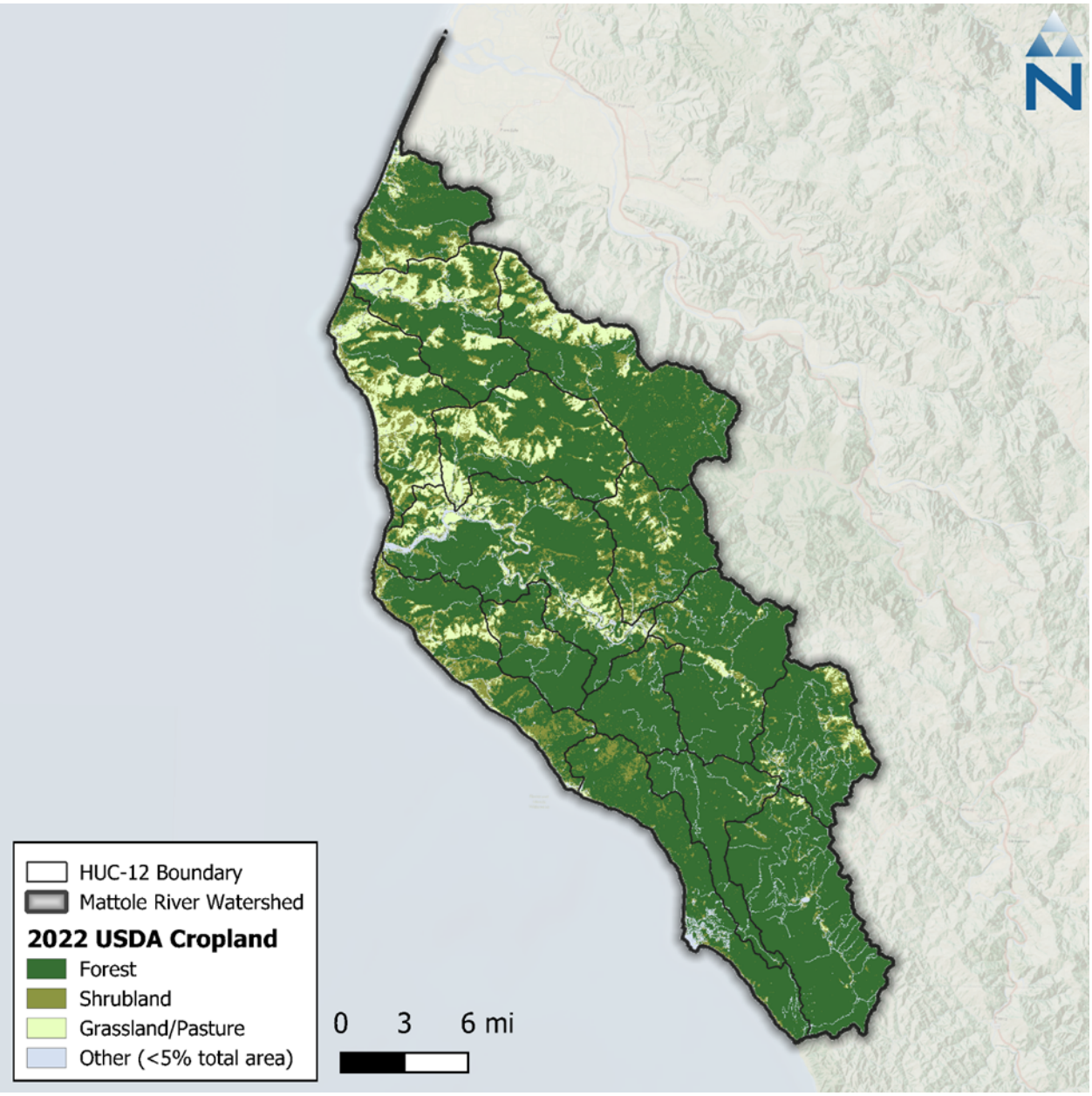

Figure 3-2. USDA 2022 Cropland Data within the Mattole River watershed.

Table 3-3 USDA 2022 Cropland Data summary within the Mattole River watershed

Crop Type	Area (acres)	Area (%)
Forest	230,449.3	72.0%
Shrubland	44,295.1	13.8%
Grassland/Pasture	28,365.7	8.9%
Cropland	200.8	0.1%
Other (<5% Total Area by Category)	16,735.4	5.2%
Total	**320,046.3**	**100.0%**

Color Gradient: Lowest | Low | Medium | High | Highest

3.3 Soils

Soil data for the Mattole River watershed were obtained from the Soil Survey Geographic Database (SSURGO) published by the Natural Resource Conservation Service (NRCS). Four primary hydrologic soil groups (HSG) are used to characterize soil runoff potential. Group A generally has the lowest runoff potential, whereas Group D has the highest runoff potential. The SSURGO soils database is composed of a GIS polygon layer of map units and a linked tabular database with multiple layers of soil properties.

Table 3-4 and Figure 3-3 present summaries of the SSURGO hydrologic soil groups for the Mattole River watershed. The dominant soil group in the watershed is Group B (64%), containing moderately well to well-drained silt loams and loams. Group C (34%) is the next most common soil group in the watershed, containing sandy clay loam that typically has low infiltration rates. Group D, with the lowest infiltration rates, makes up approximately 0.7% of the watershed. Less than 1% of the watershed areas have mixed soils. For modeling purposes, mixed soils will be grouped with the nearest primary group as follows: A/D → B, B/D → C, and C/D → D. About 19% of the watershed HSG area is classified as unknown in the SSURGO database and reside primarily within mountainous areas (see Figure 3-3). For these areas, the corresponding HSG from the STATSGO dataset was used to supplement the data gaps (primarily B and C, as shown in Figure 3-4); this reduced the unknown soil areas to about 0.3%. Since most of the soil in the watershed is Group B, the remaining unknown soil areas are also considered to be Group B in this analysis.

Table 3-4. NRCS Hydrologic soil groups in the Mattole River watershed

Soil Group	Model Group	Area (acres)	Area (%)
A	A	1,213.8	0.4%
A/D	B	283.8	0.1%
B	B	204,882.7	64.0%
B/D	C	119.0	0.0%
C	C	109,552.4	34.2%
C/D	D	793.3	0.2%
D	D	2,330.5	0.7%
Unclassified	B	870.9	0.3%
Total		**320,046.3**	**100.0%**

Color Gradient: Lowest | Low | Medium | High | Highest

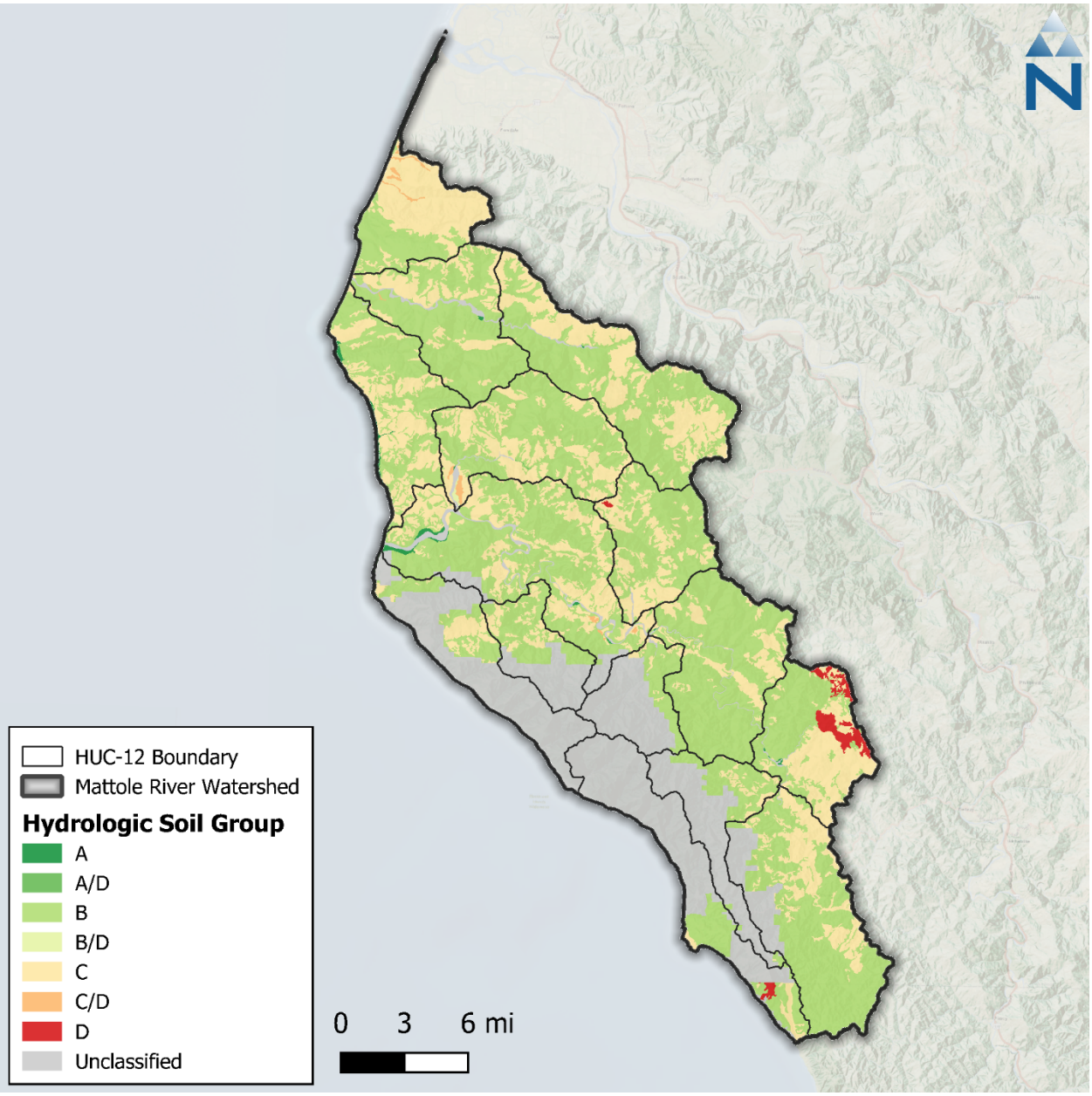

Figure 3-3. SSURGO hydrologic soil groups within the Mattole River watershed.

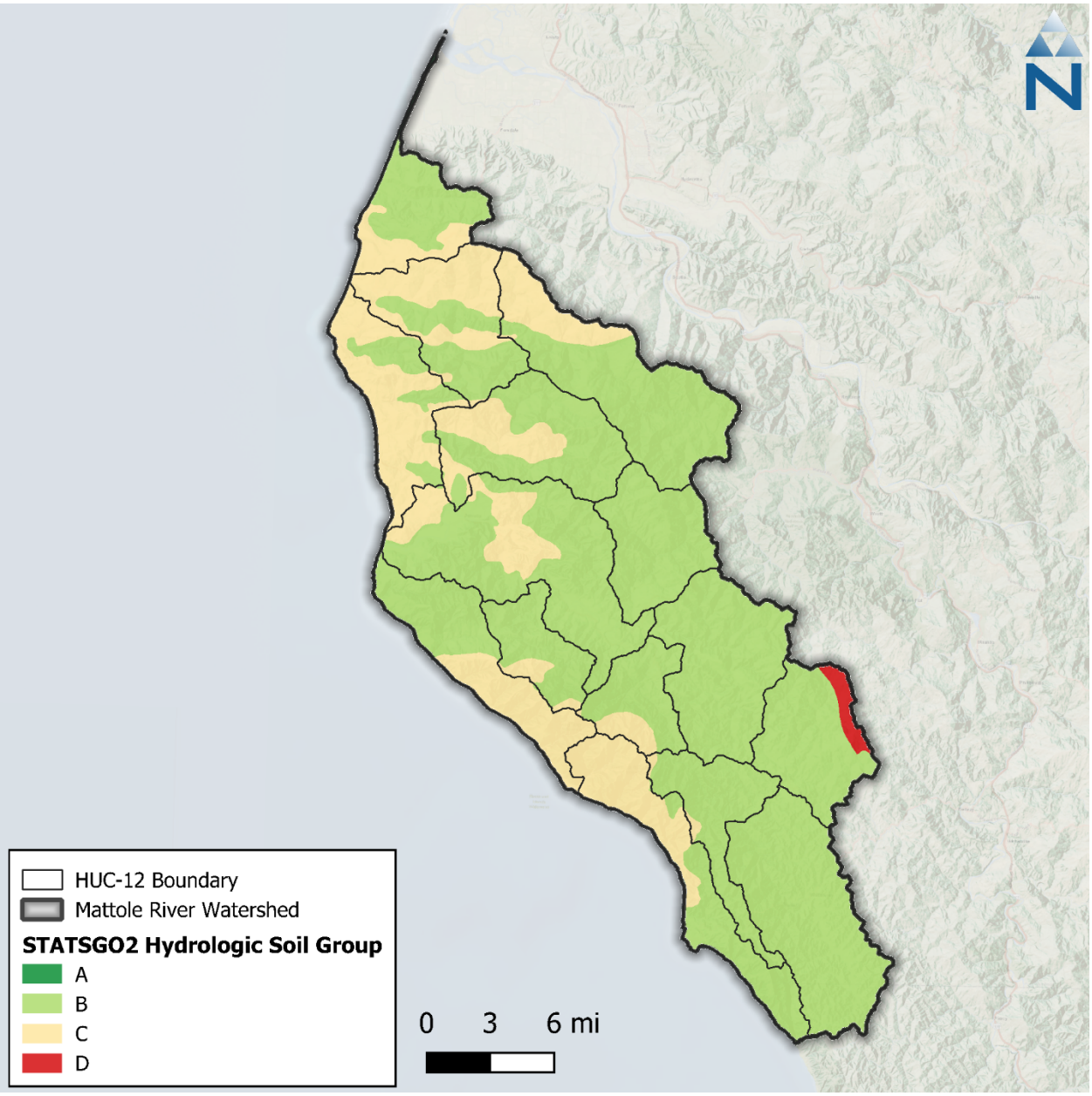

Figure 3-4. STASTGO hydrologic soil groups within the Mattole River watershed.

3.4 Elevation and Slope

The United States Geological Survey (USGS) 3D Elevation Program (3DEP) publishes DEMs expressing landscape elevation through a raster grid data product with a 1 arc-second (approximately 30-meter) horizontal resolution. The 1 arc-second data covering the Mattole River watershed had a resolution of 27.66-meters and thus was resampled to 30-meters for consistency with the rest of the datasets for the HRU analysis. The Mattole River watershed ranges in elevation from sea level along the shoreline in the west to over 1,200 meters at the highest elevation peaks in the central portion of the watershed along the north and south.

The 30-meter DEM was used to generate a slope (percent rise) raster for the watershed. Figure 3-5 illustrates the cumulative distribution function (CDF) of the slope raster values across the model

domain as a percentage of the total watershed land area (i.e., excluding major water bodies). The CDF was used to identify appropriate bins for HRU slope categories during the HRU definition process. Slopes were categorized as low (< 5%), medium (5% to 15%), and high (>15%) according to their distribution and overlap with the land cover layer. Table 3-5 and Figure 3-6 present the distribution of slope categories within the watershed.

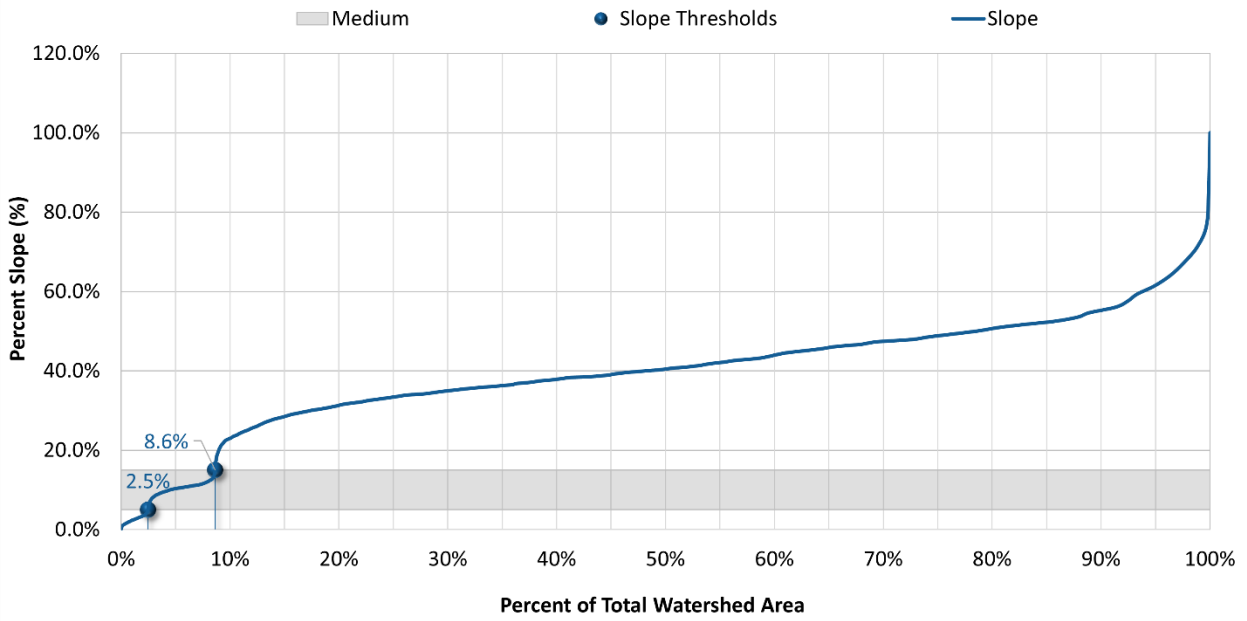

Figure 3-5. Cumulative distribution of slope categories within the Mattole River watershed.

Table 3-5. Distribution of slope categories within the Mattole River watershed

Slope (%)	Slope Category	HRU Group	Area (acres)	Area (%)
0-5	Low	Low	7,863.2	2.5%
5-15	Medium	Med	19,778.1	6.2%
>15	High	High	292,396.0	91.4%
		Total	**320,046.3**	**100.0%**

Color Gradient: Lowest | Low | Medium | High | Highest

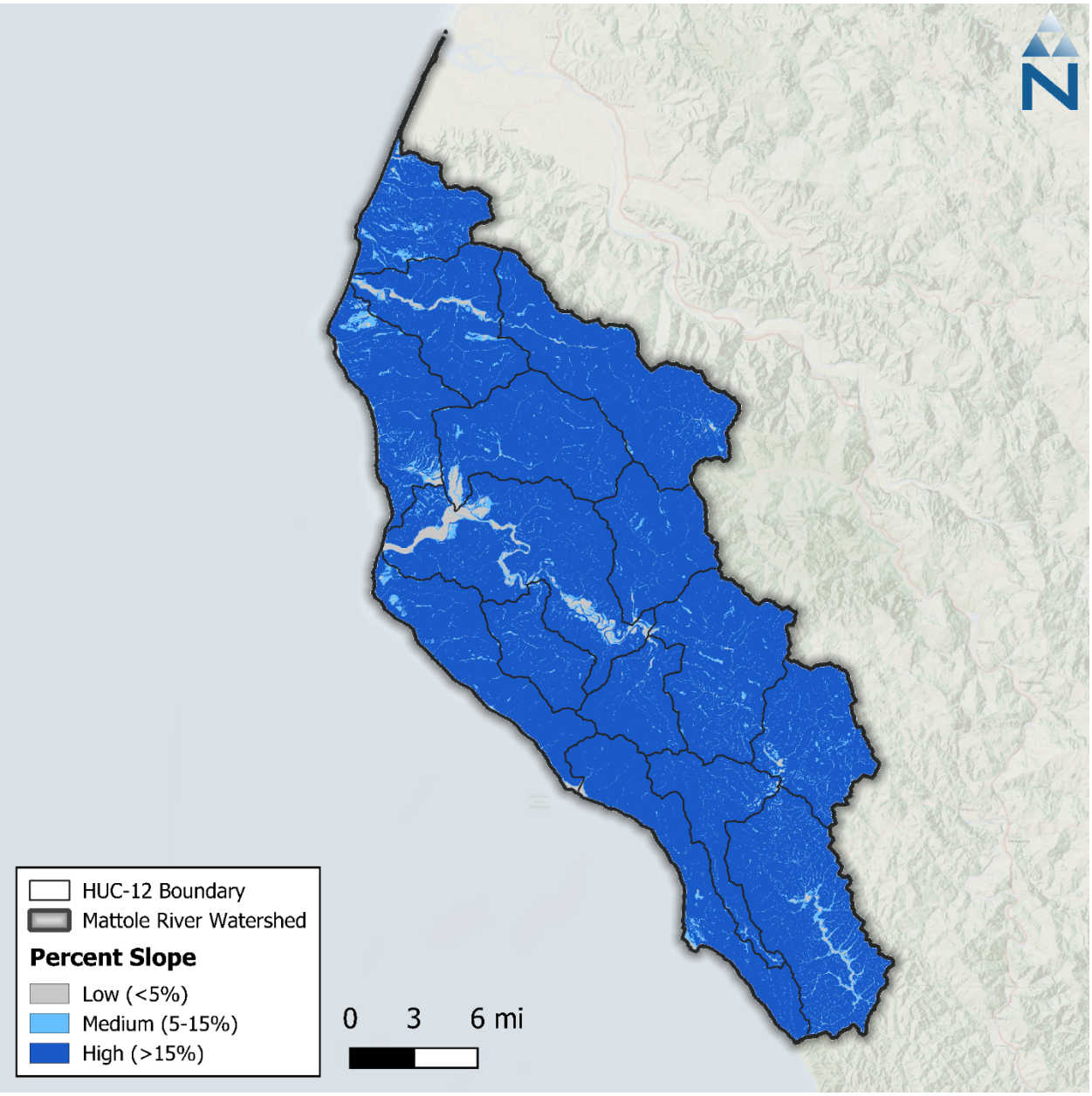

Figure 3-6. Percent Slope derived from the DEM within the Mattole River watershed.

3.4.1 Length and Slope of Overland Flow

Overland flow lengths on high slopes are generally shorter and more direct and have faster travel times, but generally longer and less direct with slower travel times on lower slopes. It was found during previous modeling efforts that using an empirical relationship shown in Figure 3-7, derived by inversely scaling length of overland flow (LSUR) with slope of overland flow (SLSUR), improved model prediction of peak flow timing. Figure 3-8 is the resulting cumulative distribution of LSUR and SLSUR in the Mattole River watershed. Longer flow lengths on shallow sloped areas increase the opportunity for attenuation, surface storage, and infiltration. On the other hand, shorter flow lengths on steeper slopes retain the flashiness where applicable.

Similar modeling efforts have historically used discrete/fixed values and ranges for SLSUR and LSUR to better manage the degrees of freedom among model variables. However, because SLSUR can be measured by HRU from remotely-sensed data, applying a relationship to also estimate LSUR as a function of SLSUR preserves some natural variability throughout the watershed that (1) can provide some improvement relative to initial hydrology prediction using constant values and (2) helps to reduce the chance of adjusting other parameters during calibration that are better explained by the influence of LSUR and SLSUR.

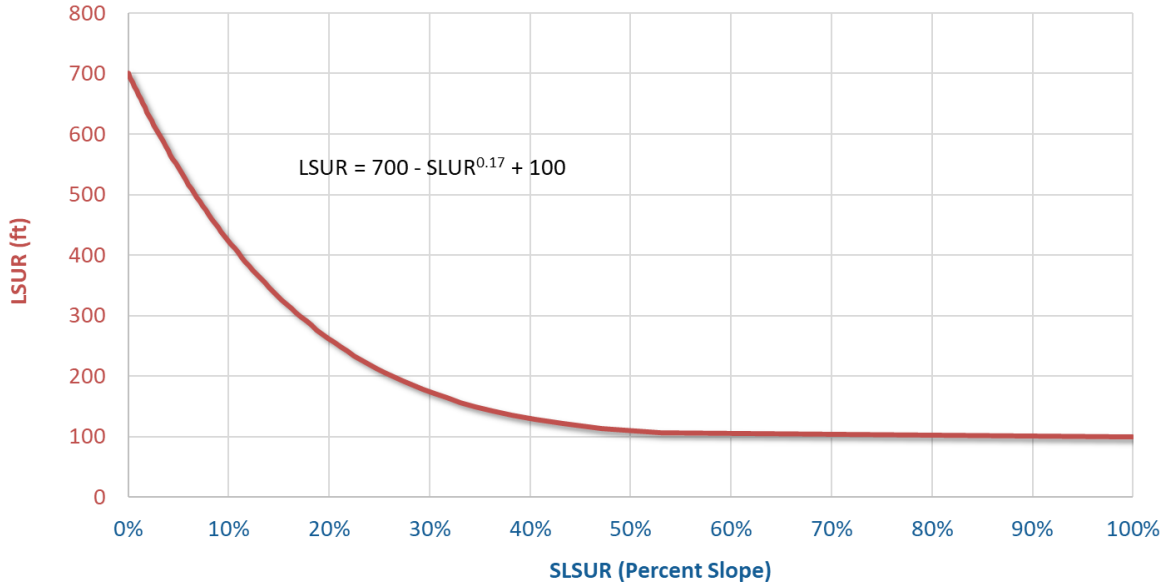

Figure 3-7. Empirical relationship of LSUR vs. SLSUR.

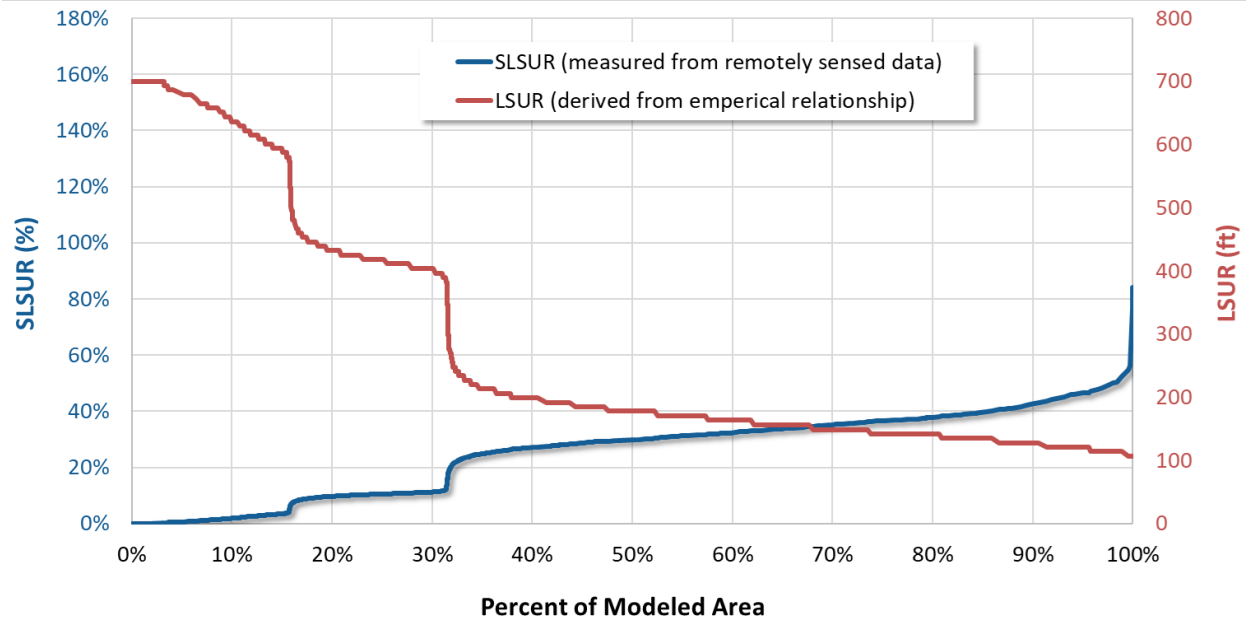

Figure 3-8. Cumulative distribution of LSUR and SLSUR in the Mattole River watershed derived from the generalized empirical relationship.

3.5 Secondary Attributes

Secondary attributes can be included in the HRU development process to provide additional information not directly mapped in the HRU categories. Secondary attributes used for the Mattole River watershed include impervious and tree canopy cover percentages, as well as the distribution of tree species within the watershed. The impervious cover percentage is used for the translation of mapped impervious cover to effective impervious cover, while percent canopy estimates can inform certain hydrologic parameters but won't be represented in the HRUs as a category. The tree species distribution allows additional refinement of forest area to help represent the watershed's recovery from logging.

3.5.1 Impervious Cover

MRLC publishes a developed impervious cover dataset as a companion to the NLCD land cover. This dataset is also provided as a raster with a 30-meter grid resolution. Impervious cover is expressed in each raster pixel as a percentage of the total area ranging from 0 to 100 percent. Figure 3-9 shows the NLCD impervious 2021 cover dataset for the Mattole River watershed. Because this data set provides impervious cover estimates for areas classified as developed, non-zero values closely align with developed areas (NLCD classification codes 21 through 24).

The percentage impervious cover was used in HRU development to further group developed land cover classes into pervious or impervious and to distinguish between mapped impervious area (MIA) and effective impervious area (EIA), as discussed in Section 3.6.1.

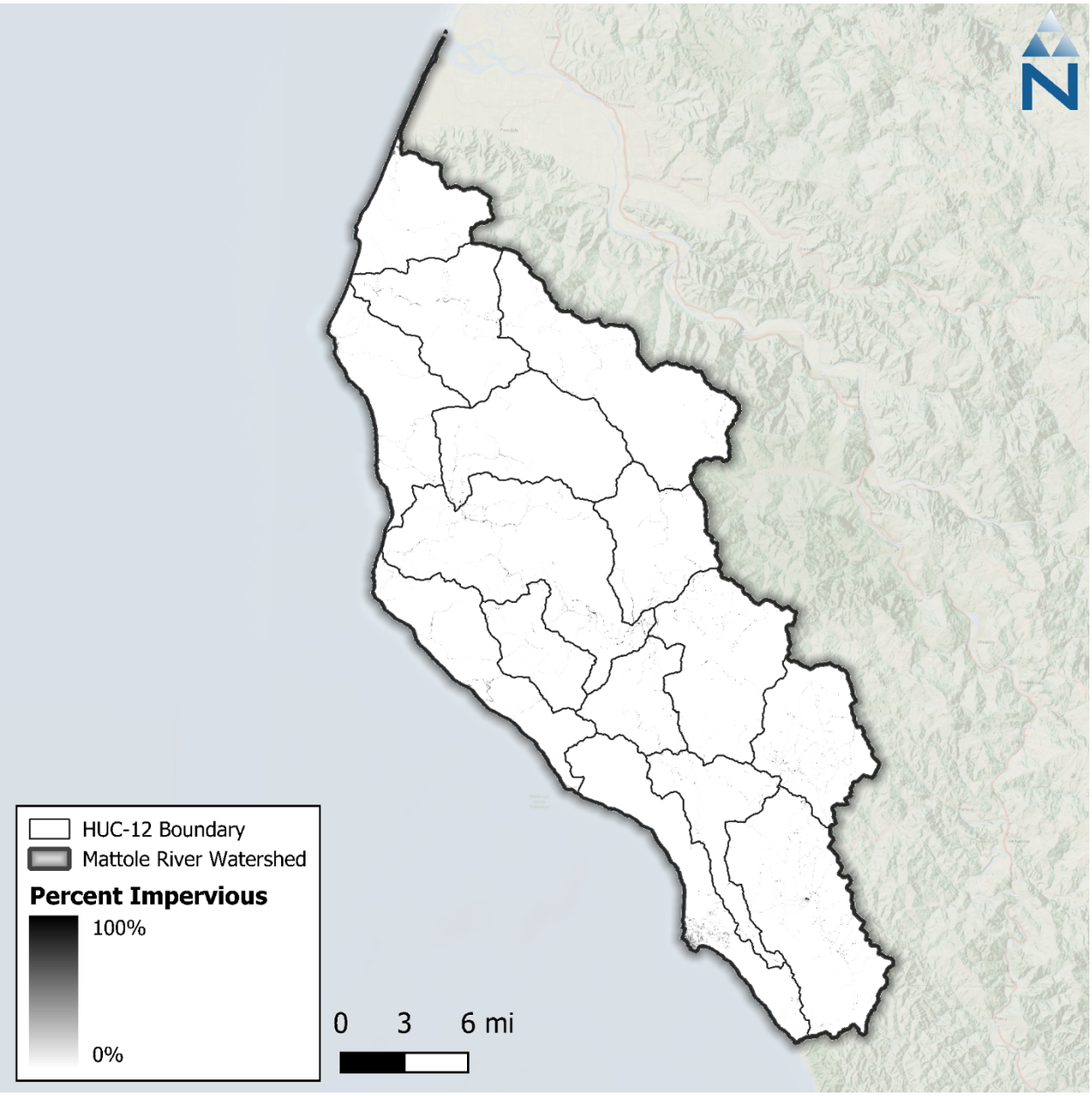

Figure 3-9. NLCD 2021 percent impervious cover in the Mattole River watershed.

3.5.2 Tree Canopy

MRLC publishes a tree canopy dataset as a companion to the NLCD land cover dataset that estimates the percentage of tree canopy cover spatially. The United States Forest Service (USFS) developed the underlying data model, which is available through its partnership with the MRLC. This dataset is also provided as a raster with a 30-meter grid resolution. Similar to the impervious cover dataset, each raster grid cell expresses the percentage of grid cell area covered by tree canopy with values ranging from 0 to 100 percent. The Mattole watershed has the highest canopy coverage of 90% toward the southwestern border (Figure 3-10). Tree canopy cover data was used to inform model parameters such as interception storage and lower-zone evapotranspiration rates.

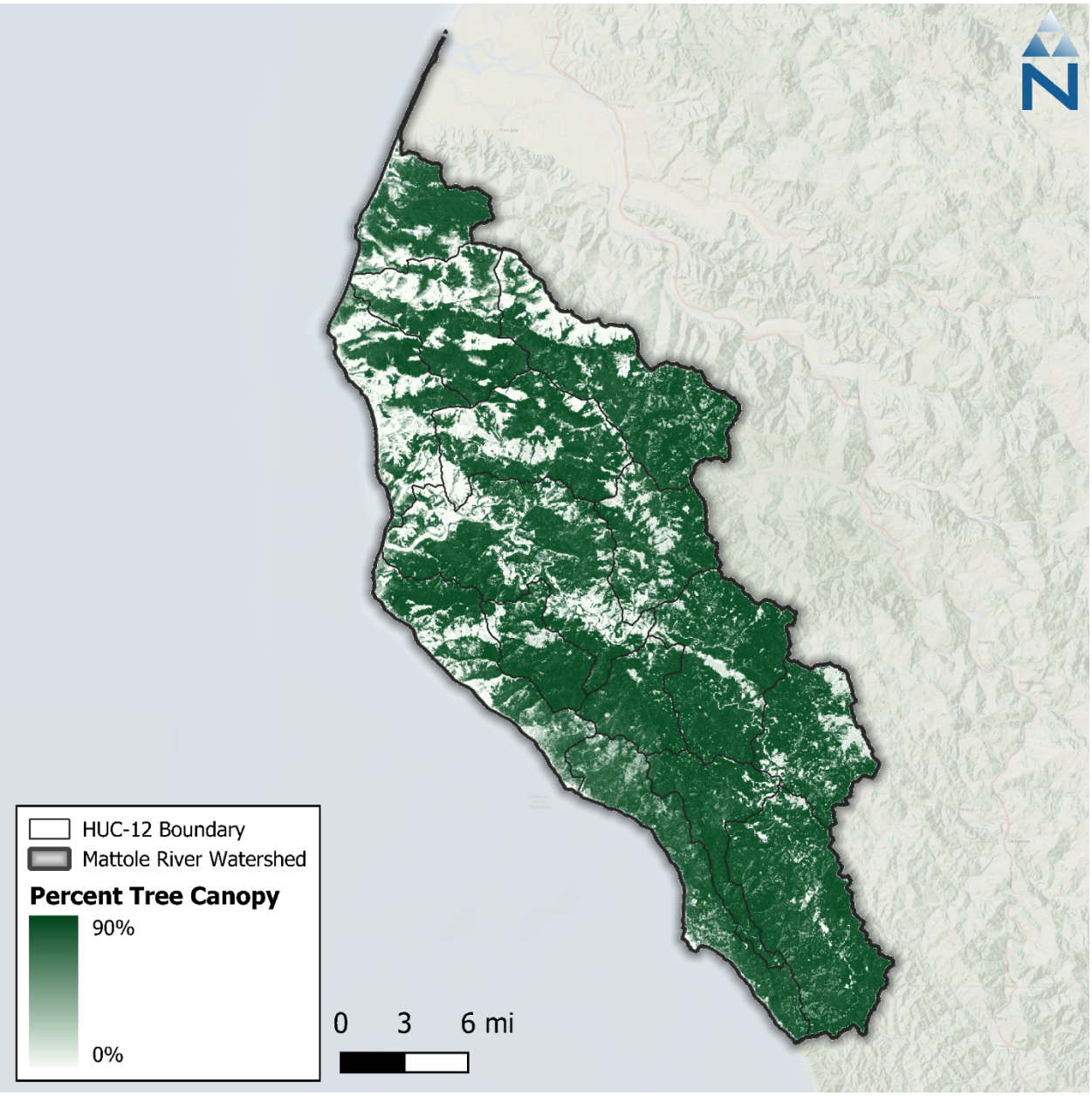

Figure 3-10. NLCD 2021 percent tree canopy cover in the Mattole River watershed.

3.5.3 Tree Type

The USFS publishes the TreeMap dataset, which describes CONUS-wide tree species distribution and forest structure as a raster with a 30-meter grid resolution (Riley et al. 2022). The 2022 TreeMap dataset (Houtman et al. 2025) was used to help reflect the recovery of forests in the watershed from logging.

Table 3-6 provides the distribution of tree species within the Mattole River watershed The distribution of Douglas fir trees especially, plays a key role in the water balance of the watershed (Stubblefield et al. 2011; Stubblefield and Reddy 2022) and is illustrated in Figure 3-11. For the HRU development process, any NLCD land cover overlapping Douglas fir TreeMap cells are considered as "Forest".

This primarily shifts area from "Scrub" (11.3% of the watershed area to 7.0%) to "Forest" 71.3% to 76.1%).

Table 3-6. TreeMap 2022 distribution of tree species within the Mattole River watershed

TreeMap Class	Tree Species	Area (acres)	Area (%)
0	No Data	72,586	22.7%
201	Douglas fir	125,139	39.1%
202	Port Orford cedar	950	0.3%
221	Ponderosa pine	8	0.0%
224	Sugar pine	0	0.0%
225	Jeffrey pine	17	0.0%
241	Western white pine	39	0.0%
261	White fir	5,402	1.7%
281	Lodgepole pine	1	0.0%
301	Western hemlock	28	0.0%
341	Redwood	36,785	11.5%
361	Knobcone pine	0	0.0%
363	Bishop pine	4	0.0%
368	Miscellaneous western softwoods	0	0.0%
371	California mixed conifer	289	0.1%
722	Oregon ash	0	0.0%
911	Red alder	1,338	0.4%
912	Bigleaf maple	50	0.0%
921	Gray pine	133	0.0%
922	California black oak	1,217	0.4%
923	Oregon white oak	1,031	0.3%
924	Blue oak	237	0.1%
931	Coast live oak	178	0.1%
933	Canyon live oak	254	0.1%
934	Interior live oak	94	0.0%
935	California white oak (valley oak)	1	0.0%
941	Tanoak	47,062	14.7%
942	California laurel	26,512	8.3%
943	Giant chinkapin	4	0.0%
961	Pacific madrone	467	0.1%
962	Other hardwoods	219	0.1%
	Total	**320,046**	**100.0%**

Color Gradient: Lowest | Low | Medium | High | Highest

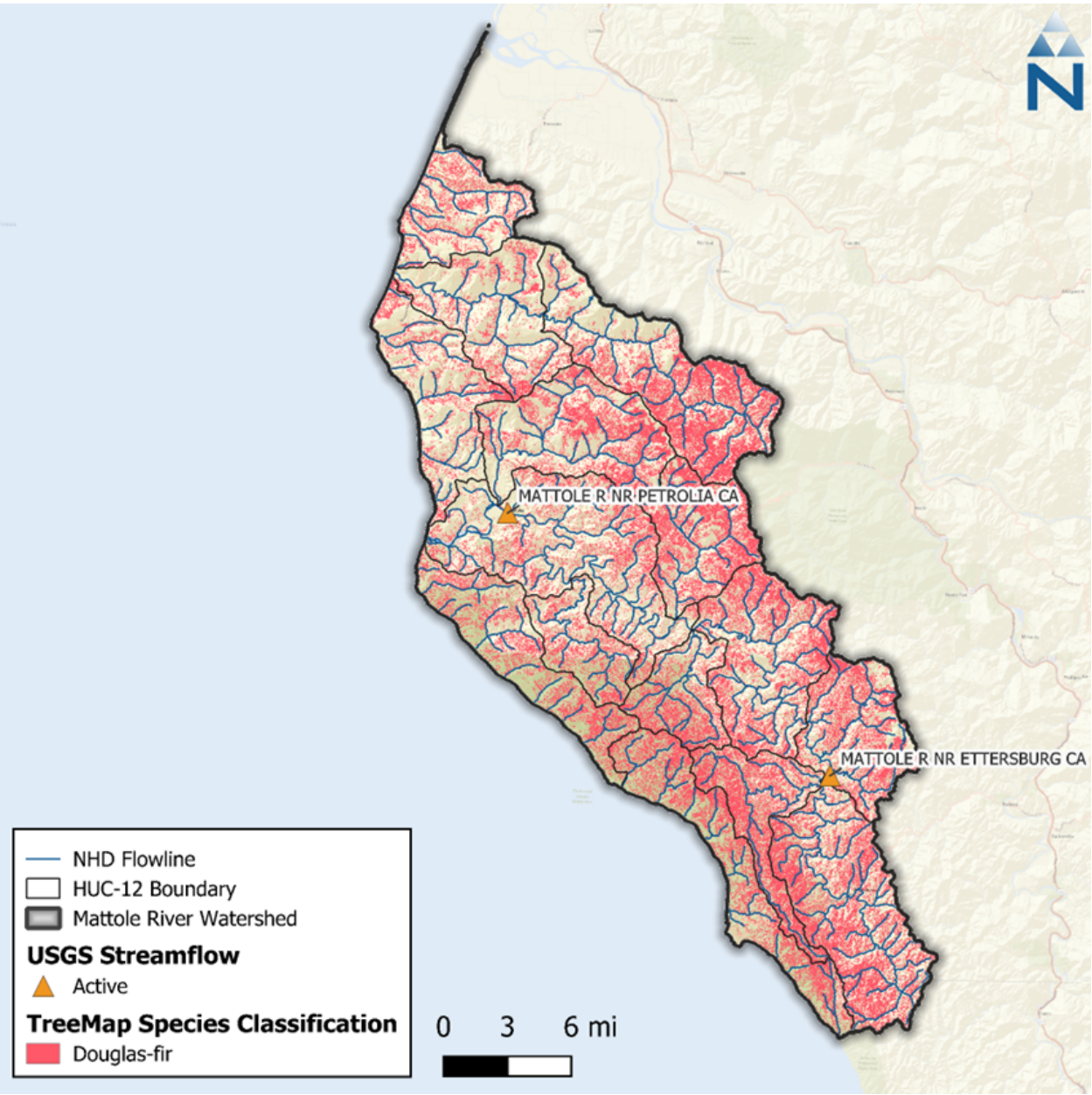

Figure 3-11. TreeMap 2022 distribution of Douglas fir within the Mattole River watershed.

3.6 HRU Consolidation

The five spatial datasets described above (land cover, cropland, impervious cover, soils, and slope) were spatially overlayed in GIS to derive a composite raster where each grid cell shows the combination of the values from the overlayed datasets. A zonal statistics operation is then performed in GIS to generate a summary table identifying unique grid cell values (i.e., HRUs) from the composite raster and corresponding areas across catchments. The combination of these datasets resulted in 132 potential HRUs. To balance model computational efficiency, the impervious HRUs were consolidated for soil and slope combinations to reduce the overall number of unique HRUs. This step was necessary to develop a model with a reasonable run time while maintaining the optimal model resolution to characterize hydrologic conditions adequately. The HRU refinement process involves analyzing the

percentage of the model area attributed to each unique HRU combination as shown in Table 3-7. The spatial distribution of mapped HRUs across the watershed is shown in Figure 3-12. Additionally, the impervious percentage is used to adjust and group developed land cover classes (Section 3.6.1) and agricultural areas located in catchments with surface water diversions for irrigation were assigned as irrigation HRUs (Section 5.1.2). The final 98 modeled HRU categories are described in Section 3.6.2.

Table 3-7. Percent land cover distribution by mapped HRU category for the Mattole River watershed

LULC	Total Area (%)	Soil Group (% LULC Area)				Slope (% LULC Area)		
		A	B	C	D	0-5	5-15	>15
Developed_Low_Intensity	0.3%	5.9%	50.7%	40.8%	2.6%	13.7%	29.3%	57.1%
Developed_Medium_Intensity	0.2%	6.5%	51.9%	38.7%	2.9%	18.4%	29.8%	51.9%
Developed_High_Intensity	0.0%	1.5%	63.5%	33.4%	1.5%	19.0%	26.0%	55.0%
Developed_Open_Space	3.1%	0.5%	64.7%	33.4%	1.4%	5.1%	17.8%	77.1%
Barren	0.8%	9.0%	65.2%	25.5%	0.3%	33.7%	22.4%	44.0%
Forest	76.1%	0.1%	72.5%	27.0%	0.5%	0.7%	3.9%	95.3%
Scrub	7.0%	0.4%	36.7%	60.9%	2.0%	2.2%	7.4%	90.4%
Grassland	3.5%	2.2%	38.2%	56.4%	3.3%	10.8%	16.1%	73.2%
Pasture	8.8%	1.0%	27.4%	68.2%	3.5%	8.9%	13.4%	77.7%
Agriculture	0.1%	13.6%	36.7%	46.7%	2.9%	19.5%	28.8%	51.6%
Water	0.1%	11.2%	74.5%	14.0%	0.3%	57.6%	36.2%	6.2%
Total	**100.0%**	**0.4%**	**64.4%**	**34.3%**	**1.0%**	**2.5%**	**6.2%**	**91.4%**

Color gradients indicate more Watershed Area and an increasing percentage of Soil and Slope, respectively.

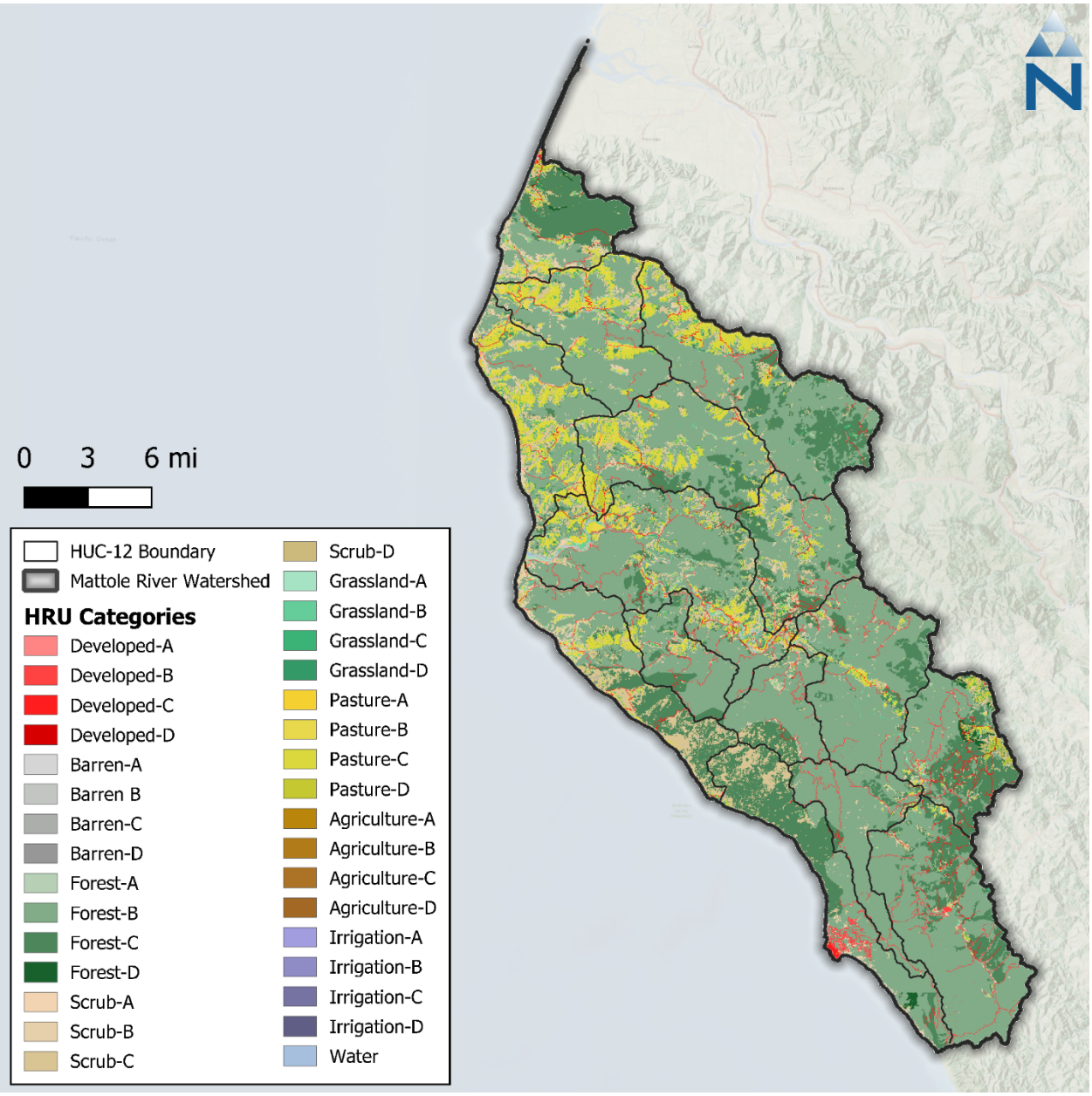

Figure 3-12. Mapped HRU categories within the Mattole River watershed. Note that slope categories are grouped for visual clarity.

3.6.1 Directly Connected Impervious Area

The HRU approach not only highlights the predominant composition of an area within the catchment but also provides additional texture and physical basis for parameterizing and representing natural processes. Within a given modeled catchment, HRU segments are modeled as being parallel to one another. Each HRU segment flows directly to the routing stream segment without any interaction with neighboring HRU segments. However, in the physical environment, the lines between impervious and pervious land are not as clearly distinguished—impervious land may flow downhill over pervious land on route to a storm drain or watercourse.

For modeling purposes, Effective Impervious Area (EIA) represents the portion of the total, or Mapped Impervious Area (MIA), that routes directly to the stream segments. It is derived as a function of the percent Directly Connected Impervious Area (DCIA), with other adjustments as needed to account for other structural and non-structural management practices in the flow network. Figure 3-13 illustrates the transitional sequence from MIA to DCIA. Impervious areas that are not connected to the drainage network can flow onto pervious surfaces, infiltrate, and become part of the pervious subsurface and overland flow. Because segments are modeled as being parallel to one another in LSPC, this process can be approximated using a conversion of a portion of impervious land to pervious land. On the open landscape, runoff from disconnected impervious surfaces can overwhelm the infiltration capacity of adjacent pervious surfaces during large rainfall/runoff events creating sheet flow over the landscape—therefore, the MIA→EIA translation is not actually a direct linear conversion. Finding the right balance between MIA and EIA can be an important part of the hydrology calibration effort.

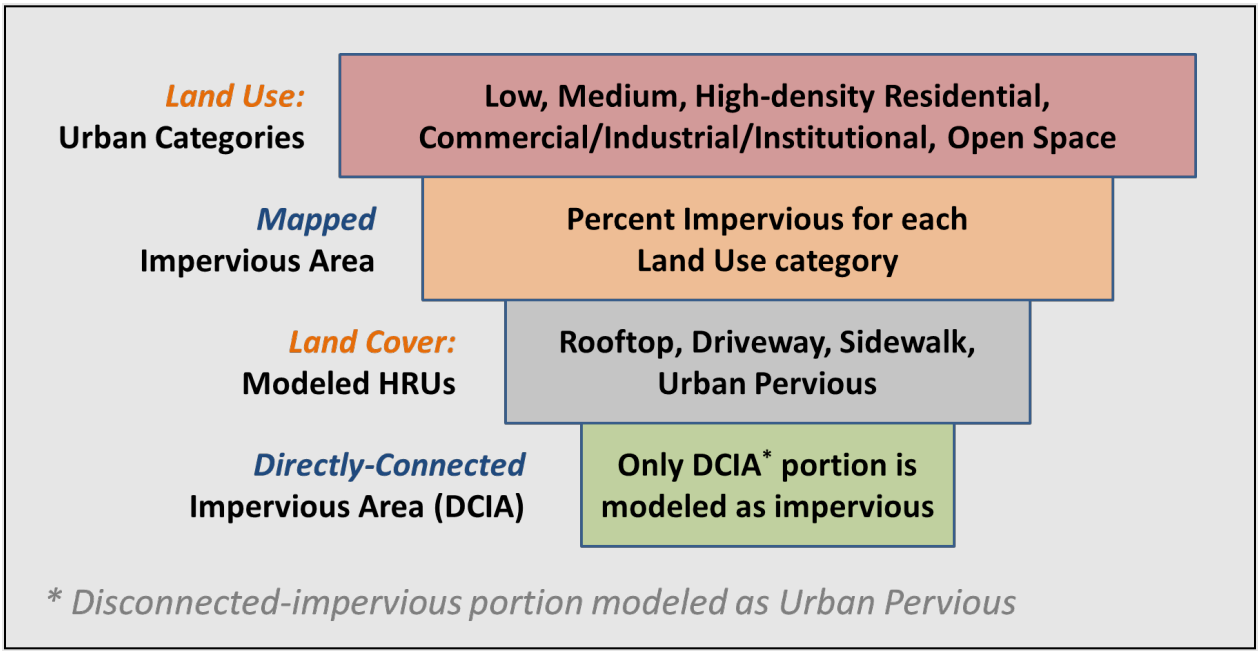

Figure 3-13. Generalized translation sequence from MIA to DCIA.

Empirical relationships like the Sutherland Equations (Sutherland 2000) presented in Figure 3-14 show a strong correlation between the *density* of developed areas and DCIA. The curve for high-density developed land trends closer to the line of equal value than the curve for less developed areas. Similarly, as the density of the mapped impervious area approaches 100%, the translation to DCIA also approaches 100%. An initial estimate of EIA is equal to MIA × DCIA. This empirical approximation can be further refined during model calibration to account for other flow disconnections resulting from structural or non-structural BMP practices or other inline hydraulic routing features.

For the Mattole River watershed, each developed land cover category was assigned a DCIA curve as shown in Table 3-8. The MIA, which is the impervious portion of each grid, was converted to EIA areas using these equations. Sutherland (2000) notes that areas with less than 1% MIA effectively behave like 100% pervious areas; therefore, EIA adjustments were only applicable to "Developed" areas. Table 3-9 is a summary of resampled MIA and calculated EIA by the land cover groups.

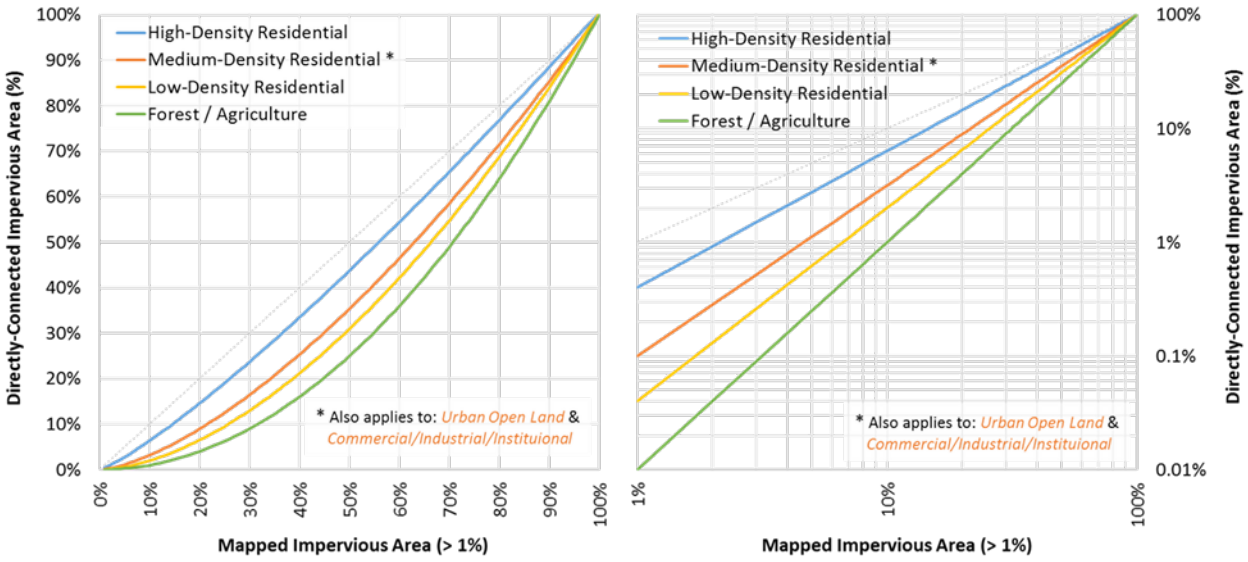

Figure 3-14. Mapped and directly connected impervious area relationships (Sutherland 2000).

Table 3-8. Assignment of DCIA curves by land cover category

Land Cover	MIA	EIA	EIA:MIA	Equation
High Density Developed	87.9%	86.1%	98.0%	$DCIA=0.4(MIA)^{1.2}$
Medium Density Developed	61.2%	48.0%	78.0%	$DCIA=0.1(MIA)^{1.5}$
Low Density Developed	31.6%	14.3%	45.0%	$DCIA=0.04(MIA)^{1.7}$
Open Space	4.3%	0.2%	5.0%	$DCIA=0.01(MIA)^{2.0}$
Undeveloped*	0.0%	0.0%	0.0%	NA

* Assume no DCIA (100% disconnection, EIA = 0)

Color Gradient: Lowest | Low | Medium | High | Highest

Table 3-9. Distribution of impervious area by grouped NLCD land cover class

Model Group	Area (acres)	Area (%)	Impervious (acre)		Impervious (%)	
			MIA	EIA	MIA	EIA
Developed_Low_Intensity	1,079.3	0.3%	341.4	154.5	31.6%	14.3%
Developed_Medium_Intensity	529.5	0.2%	324.0	253.9	61.2%	47.9%
Developed_High_Intensity	86.5	0.0%	76.1	74.5	87.9%	86.1%
Developed_Open_Space	9,989.7	3.1%	426.0	21.9	4.3%	0.2%
Barren	2,497.9	0.8%	0.0	0.0	0.0%	0.0%
Forest (Deciduous)	7,908.6	2.5%	0.0	0.0	0.0%	0.0%
Forest (Evergreen)	201,762.7	63.0%	0.0	0.0	0.0%	0.0%
Forest (Mixed)	18,115.5	5.7%	0.0	0.0	0.0%	0.0%
Scrub	36,287.6	11.3%	0.0	0.0	0.0%	0.0%
Grassland (Herbaceous)	10,644.9	3.3%	0.0	0.0	0.0%	0.0%
Pasture	28,417.3	8.9%	0.0	0.0	0.0%	0.0%
Agriculture	200.8	0.1%	0.0	0.0	0.0%	0.0%
Forest (Woody Wetlands)	530.2	0.2%	0.0	0.0	0.0%	0.0%
Grassland (Herbaceous Wetland)	1,603.9	0.5%	0.0	0.0	0.0%	0.0%
Water	391.9	0.1%	0.0	0.0	0.0%	0.0%
Total	**320,046.3**	**100.0%**	**1,167.5**	**504.8**	**--**	**--**

Color gradients indicate model groups with more Watershed Area and Imperviousness, respectively.

3.6.2 Modeled HRU Categories

The combinations of LULC, HSG, and slope represent the physical characteristics that influence hydrology. After accounting for DCIA, the four developed land cover classes were rolled up as either "Developed Impervious" or "Developed Pervious," stratified by HSG and slope. Agriculture HRUs (i.e., 4 HSGs × 3 slopes = 12 combinations) were further divided into irrigated and non-irrigated counterparts for a total of 24 HRUs. Altogether, a total of 98 HRU categories comprised the basic building blocks used in LSPC to represent hydrologic responses in the watershed. All the "Agricultural" HRU areas within catchments where streamflow was withdrawn for agricultural use were re-assigned to their "Irrigation" HRU counterparts. Irrigation was simulated for those HRUs as described in Section 5.1. The final HRU distribution in the watershed is shown in Table 3-10.

Table 3-10. Modeled HRU distribution within the Mattole River watershed

HRU ID	Land Use - Land Cover	HSG	Slope	Area (acres)	Area (%)
1000	Developed_Impervious	All	All	504.8	0.2%
2110	Developed_Pervious	A	Low	26.6	0.0%
2120	Developed_Pervious	A	Med	51.1	0.0%
2130	Developed_Pervious	A	High	43.3	0.0%
2210	Developed_Pervious	B	Low	399.7	0.1%
2220	Developed_Pervious	B	Med	1,331.4	0.4%
2230	Developed_Pervious	B	High	5,342.8	1.7%

Table 3-10. Modeled HRU distribution within the Mattole River watershed (continued)

HRU ID	Land Use - Land Cover	HSG	Slope	Area (acres)	Area (%)
2310	Developed_Pervious	C	Low	239.8	0.1%
2320	Developed_Pervious	C	Med	682.5	0.2%
2330	Developed_Pervious	C	High	2,895.1	0.9%
2410	Developed_Pervious	D	Low	20.8	0.0%
2420	Developed_Pervious	D	Med	59.5	0.0%
2430	Developed_Pervious	D	High	86.3	0.0%
3110	Barren	A	Low	125.2	0.0%
3120	Barren	A	Med	71.4	0.0%
3130	Barren	A	High	20.7	0.0%
3210	Barren	B	Low	517.1	0.2%
3220	Barren	B	Med	294.9	0.1%
3230	Barren	B	High	763.9	0.2%
3310	Barren	C	Low	169.2	0.1%
3320	Barren	C	Med	169.5	0.1%
3330	Barren	C	High	277.5	0.1%
3410	Barren	D	Low	2.9	0.0%
3420	Barren	D	Med	4.4	0.0%
3430	Barren	D	High	0.2	0.0%
4110	Forest	A	Low	85.2	0.0%
4120	Forest	A	Med	43.6	0.0%
4130	Forest	A	High	38.0	0.0%
4210	Forest	B	Low	1,262.5	0.4%
4220	Forest	B	Med	6,953.4	2.2%
4230	Forest	B	High	168,286.4	52.6%
4310	Forest	C	Low	444.1	0.1%
4320	Forest	C	Med	2,441.2	0.8%
4330	Forest	C	High	62,751.1	19.6%
4410	Forest	D	Low	15.6	0.0%
4420	Forest	D	Med	96.5	0.0%
4430	Forest	D	High	1,013.7	0.3%
5110	Scrub	A	Low	48.0	0.0%
5120	Scrub	A	Med	11.6	0.0%
5130	Scrub	A	High	21.8	0.0%
5210	Scrub	B	Low	241.5	0.1%
5220	Scrub	B	Med	1,025.0	0.3%
5230	Scrub	B	High	7,005.9	2.2%
5310	Scrub	C	Low	195.7	0.1%
5320	Scrub	C	Med	592.0	0.2%
5330	Scrub	C	High	12,963.6	4.1%

Table 3-10. Modeled HRU distribution within the Mattole River watershed (continued)

HRU ID	Land Use - Land Cover	HSG	Slope	Area (acres)	Area (%)
5410	Scrub	D	Low	9.3	0.0%
5420	Scrub	D	Med	50.9	0.0%
5430	Scrub	D	High	397.2	0.1%
6110	Grassland	A	Low	140.8	0.0%
6120	Grassland	A	Med	74.3	0.0%
6130	Grassland	A	High	33.8	0.0%
6210	Grassland	B	Low	692.5	0.2%
6220	Grassland	B	Med	1,102.0	0.3%
6230	Grassland	B	High	2,485.7	0.8%
6310	Grassland	C	Low	346.0	0.1%
6320	Grassland	C	Med	555.5	0.2%
6330	Grassland	C	High	5,420.6	1.7%
6410	Grassland	D	Low	27.8	0.0%
6420	Grassland	D	Med	71.6	0.0%
6430	Grassland	D	High	268.7	0.1%
7110	Pasture	A	Low	151.0	0.1%
7120	Pasture	A	Med	93.4	0.0%
7130	Pasture	A	High	36.0	0.0%
7210	Pasture	B	Low	1,193.8	0.4%
7220	Pasture	B	Med	2,151.2	0.7%
7230	Pasture	B	High	4,357.4	1.4%
7310	Pasture	C	Low	934.3	0.3%
7320	Pasture	C	Med	1,317.9	0.4%
7330	Pasture	C	High	16,938.4	5.3%
7410	Pasture	D	Low	231.1	0.1%
7420	Pasture	D	Med	205.9	0.1%
7430	Pasture	D	High	541.1	0.2%
8110	Agriculture	A	Low	5.6	0.0%
8120	Agriculture	A	Med	6.2	0.0%
8130	Agriculture	A	High	0.4	0.0%
8210	Agriculture	B	Low	3.1	0.0%
8220	Agriculture	B	Med	11.1	0.0%
8230	Agriculture	B	High	16.7	0.0%
8310	Agriculture	C	Low	1.1	0.0%
8320	Agriculture	C	Med	1.3	0.0%
8330	Agriculture	C	High	18.7	0.0%
8410	Agriculture	D	Low	0.0	0.0%
8420	Agriculture	D	Med	0.0	0.0%
8430	Agriculture	D	High	0.2	0.0%

Table 3-10. Modeled HRU distribution within the Mattole River watershed (continued)

HRU ID	Land Use - Land Cover	HSG	Slope	Area (acres)	Area (%)
9000	Water	All	All	391.9	0.1%
10110	Irrigation	A	Low	5.6	0.0%
10120	Irrigation	A	Med	7.8	0.0%
10130	Irrigation	A	High	0.2	0.0%
10210	Irrigation	B	Low	9.1	0.0%
10220	Irrigation	B	Med	16.2	0.0%
10230	Irrigation	B	High	13.1	0.0%
10310	Irrigation	C	Low	11.6	0.0%
10320	Irrigation	C	Med	8.9	0.0%
10330	Irrigation	C	High	46.7	0.0%
10410	Irrigation	D	Low	0.9	0.0%
10420	Irrigation	D	Med	2.9	0.0%
10430	Irrigation	D	High	1.6	0.0%
			Total	**320,046.3**	**100.0%**

Color Gradient: Lowest | Low | Med | High | Highest

4 CLIMATE FORCING INPUTS

The Mattole River watershed LSPC model uses hourly climate data forcing inputs to drive the hydrology module. In general, hydrologic models are highly dependent on the quantity and quality of meteorological input data (Quirmbach & Schultz 2002). Conventionally, meteorological boundary conditions for stormwater modeling rely on ground-based stations across an area; however, challenges arise when trying to associate point-sampled weather station data over complex and/or large terrain (Henn et al. 2018). Model representation of precipitation in regions with low station density is susceptible to distortion when using linearized downscaling methods (e.g., Thiessen polygons).

The hybrid approach supplements spatial and temporal gaps in observed meteorological data with gridded meteorological products from the Parameter-elevation Regressions on Independent Slopes Model (PRISM) and North American Land Data Assimilation System-2 (NLDAS). NLDAS and PRISM are Land Surface Model (LSM) datasets with 1/8th degree and 4-km spatial resolution, respectively, which are ideal for supplementing spatial gaps in the observed station network as well as patching missing or erroneous temporal gaps in the observed time series data. The use of a hybrid approach that blends ground-based stations with remotely sensed precipitation products, i.e., increasing the rainfall gauge density over the watershed, has been shown to improve the representation of rainfall and increase forecast accuracy more than using ground-based stations alone (Kim et al. 2018; Looper & Vieux 2012; Xia, Mitchell, Ek, Cosgrove, et al. 2012; Xia, Mitchell, Ek, Sheffield, et al. 2012). This approach has been applied for large watershed-scale modeling applications in Los Angeles County (LACFCD 2020).

Potential evapotranspiration (PET) is another critical forcing input for hydrology simulation. Section 4.2 describes how PET was derived for this modeling effort.

4.1 Precipitation

Figure 4-1 presents a summary of the hybrid approach to blend observed precipitation with gridded meteorological products. Observed data and gridded products were first processed in parallel (1) to identify the highest quality gauge data and (2) to merge gridded products to produce continuous hourly time series. Next, gridded products were used to fill spatial and temporal gaps in the observed precipitation coverage. The final coverage shown in Figure 4-2 comprises the highest quality observed time series, supplemented by gridded products only where spatial and temporal gaps occurred in the observed coverage. The parallel processing of observed and gridded precipitation is presented in Section 4.1.1. Section 4.1.2 describes how those outputs were synthesized into the model's final set of precipitation time series.

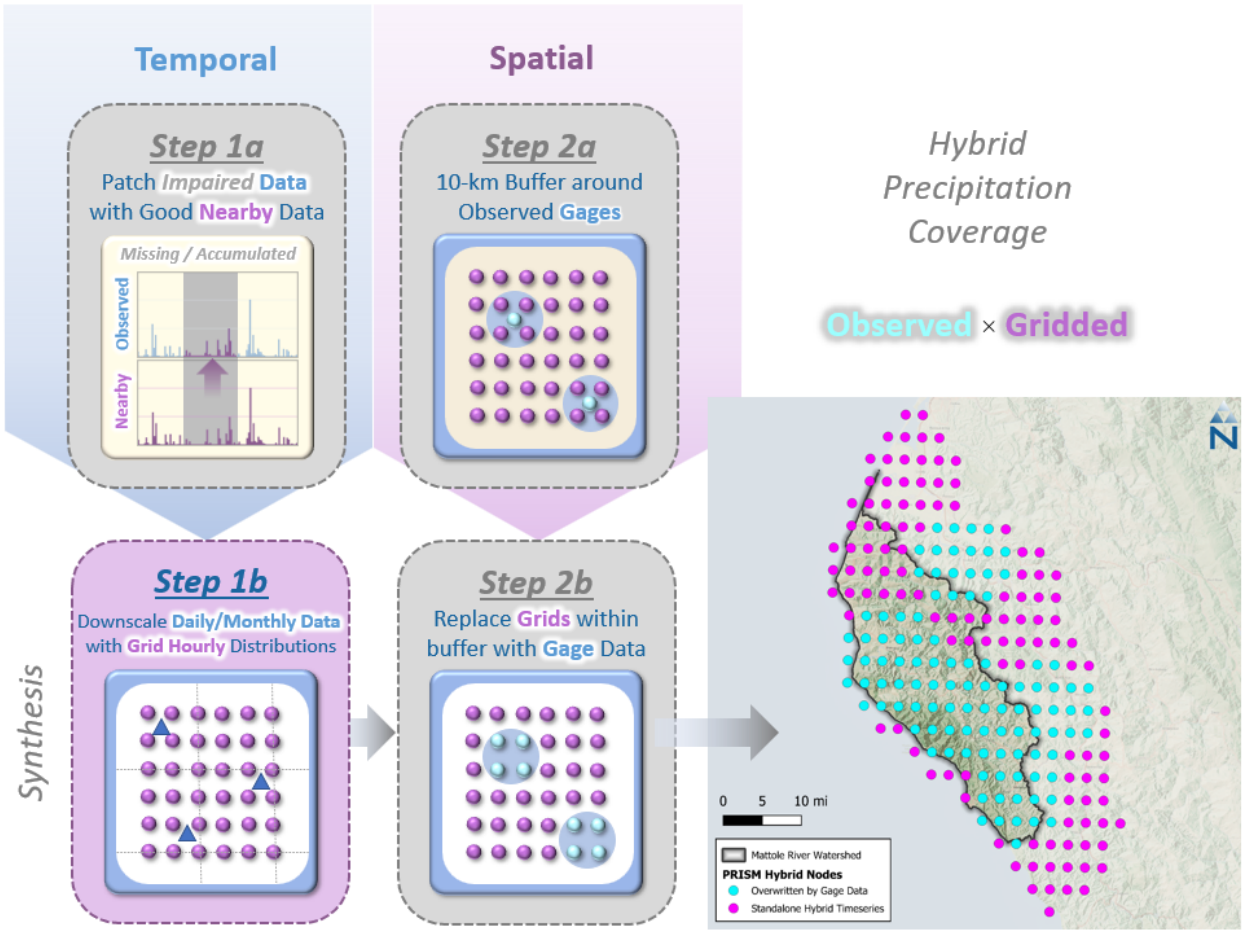

Figure 4-1. Hybrid approach to blend observed precipitation with gridded meteorological products.

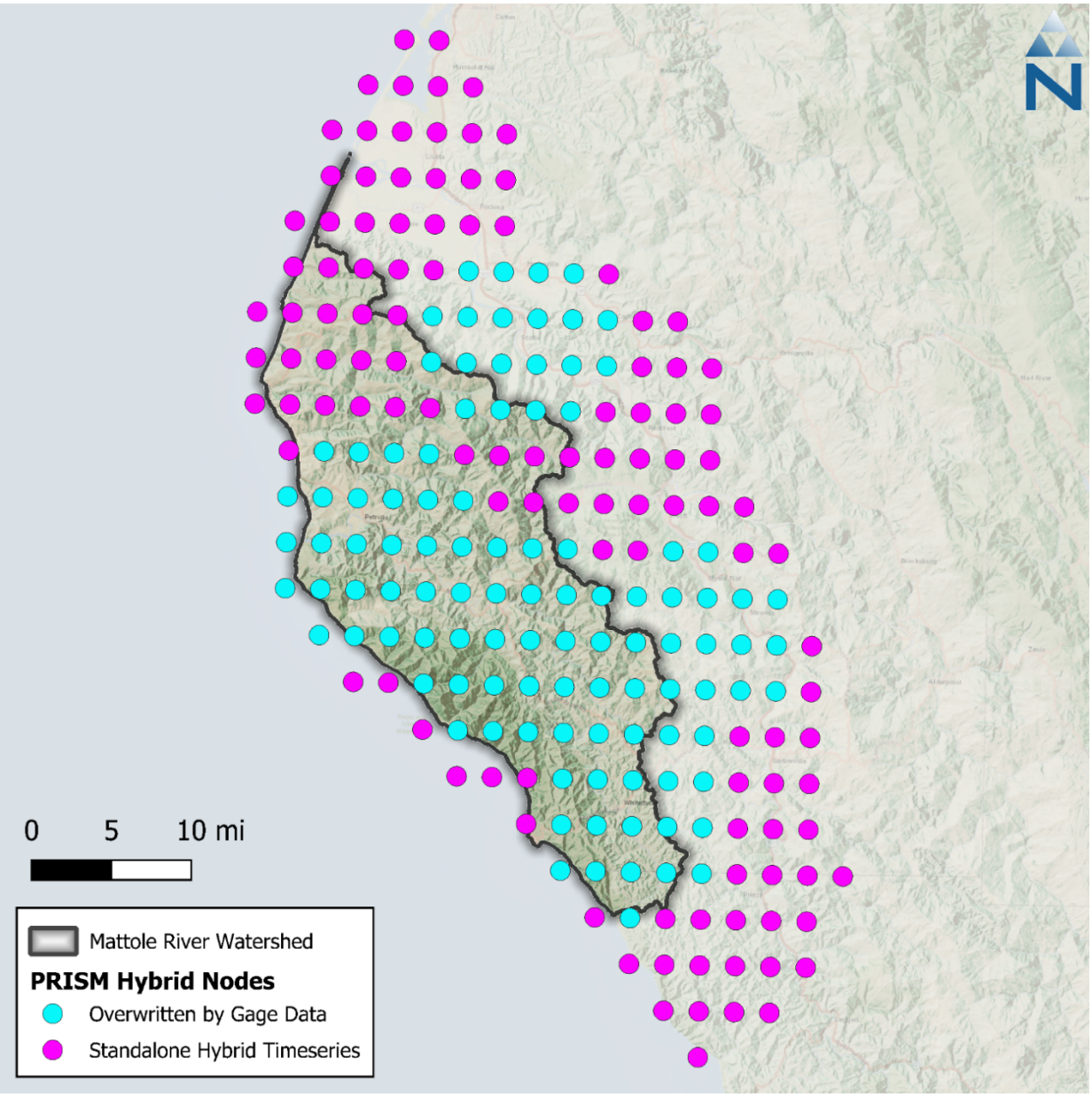

Figure 4-2. Spatial coverage of PRISM nodes by hybrid data source.

4.1.1 Parallel Processing of Observed Data and Gridded Products

Observations from 9 precipitation gauges, summarized in Table 4-1, were processed for use in the hybrid precipitation time series. These stations report daily precipitation totals, which were disaggregated to hourly based on the distribution of the nearest NLDAS grid cell, while maintaining observed daily totals Six of the gauges are from the Global Historical Climatology Network Daily (GHCND) database which is operated by the National Ocean and Atmospheric Association (NOAA). Three additional stations from the California Data Exchange Center (CDEC) and the Remote Automated Weather Stations (RAWS) were also used. The relationship between annual average total precipitation and elevation for these stations is shown in Figure 4-3. The Mattole River work plan had additional precipitation gauges listed, however those stations were dropped from further use as either duplicates or were outside of the 10km buffer used to create hybrid time series.

Table 4-1. Precipitation stations used to develop hybrid precipitation time series

Agency	Station ID[1]	Name	Start Date	End Date	Lat.	Long.	Elevation (meters)	Data Coverage (%)[2]
NOAA - GHCN	GHCND:US1CAHM0091	ETTERSBURG 2.8 N, CA US	12/18/2019	Present	40.17447	-123.99	501.1	100%
	GHCND:US1CAHM0070	HONEYDEW 3.2 SSE, CA US	6/30/2016	Present	40.2002	-124.105	425.2	95%
	GHCND:US1CAHM0014	MIRANDA 4.1 SW, CA US	12/12/2008	Present	40.20927	-123.894	164.3	93%
	GHCND:US1CAHM0073	PETROLIA 0.6 SSE, CA US	9/1/2016	Present	40.31716	-124.282	28	99%
	GHCND:US1CAHM0066	WHITETHORN 1.7 NNW, CA US	1/20/2016	Present	40.0447	-123.959	294.7	85%
	GHCND:USC00048045	SCOTIA, CA US	1/1/1926	Present	40.4833	-124.104	41.5	99%
CDEC	CSM	COOSKIE MOUNTAIN	10/1/2005	Present	40.258	-124.25	899.2	- -
	HNY	HONEYDEW	1/1/1987	Present	40.2375	-124.132	112.8	- -
RAWS	COO	COOSKIE MOUNTAIN, CA	05/23/1985	Present	40.2569	-124.266	897.6	--

1. Stations presented have at least 90% data coverage.
2. NOAA data coverage as reported.

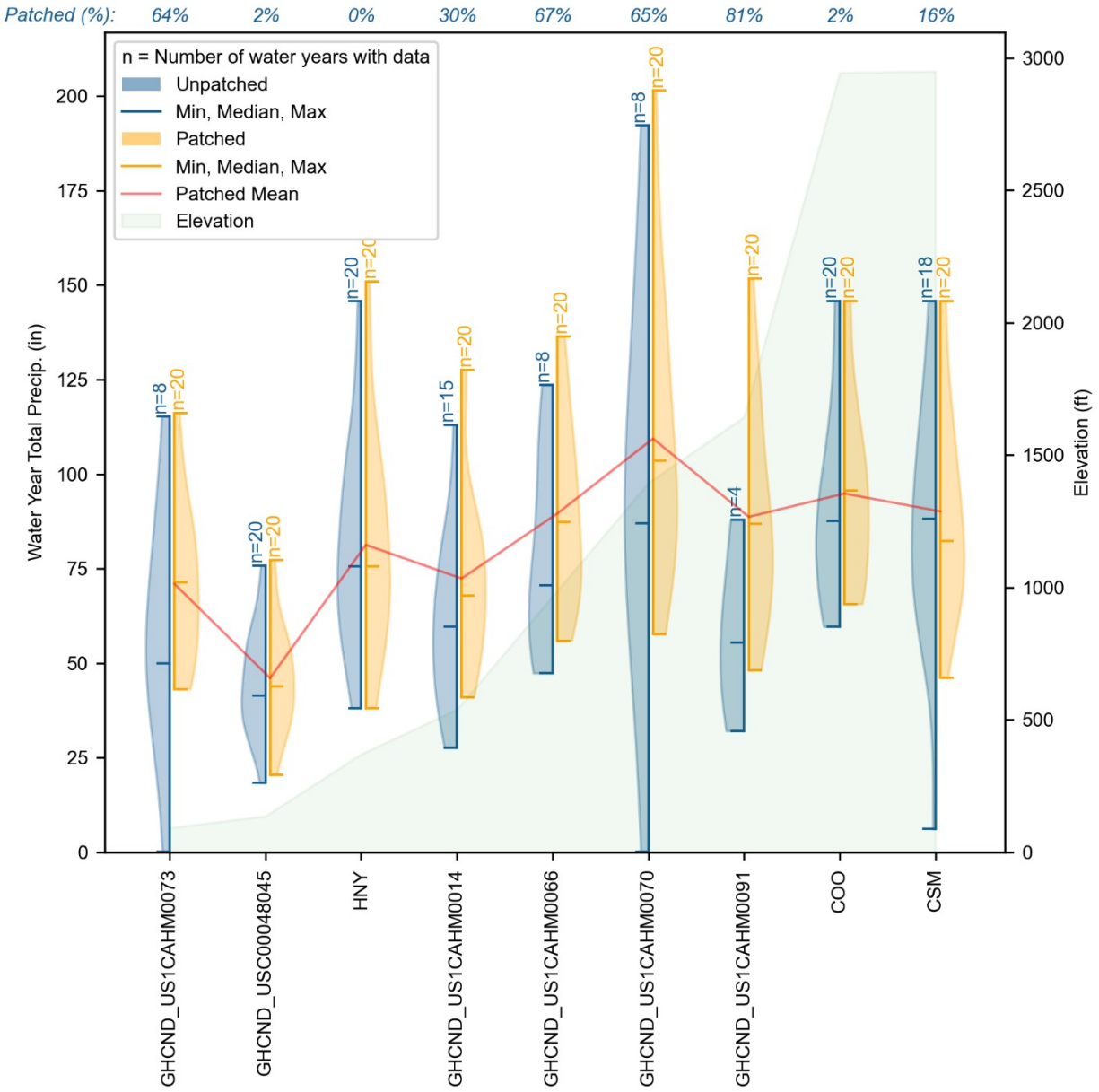

Figure 4-3. Water year precipitation totals and elevation of selected precipitation stations for 2004 - 2023.

The gridded meteorological products were processed in parallel with the observed data and used to patch spatial and temporal gaps in the observed data record. PRISM monthly precipitation time series data are available at a 4-km spatial resolution across the conterminous United States (Daly et al. 1994, 1997; Gibson et al. 2002). PRISM combines point data and spatial datasets (primarily DEMs) via statistical methods to generate estimates of annual, monthly, and event-based precipitation in a gridded format from as early as 1961 (Daly et al. 2000). PRISM has undergone several iterations of refinement, extensive peer review, and performance validation through case study applications.

NLDAS is a quality-controlled meteorological dataset designed specifically to support continuous simulation modeling activities (Cosgrove et al. 2003; Mitchell et al. 2004). NLDAS provides hourly predictions of meteorological data at a 1/8th degree spatial resolution for North America (approximately 13.8-kilometer intervals), with retrospective simulations beginning in January 1979. For this model, hourly NLDAS precipitation distributions were mapped to the nearest PRISM grid

cell and used to disaggregate the monthly PRISM totals to hourly—the resulting set of gridded precipitation time series reflects monthly PRISM totals that have hourly distributions from the nearest NLDAS grid. Using monthly PRISM totals with hourly NLDAS, as opposed to daily PRISM totals, eliminates the need to estimate distributions for occasional but rare instances where an hourly distribution does not coincide with a daily total.

4.1.2 Synthesis of Observed Data and Gridded Products

Where available, observed precipitation data were preferentially selected over gridded data where data quantity and quality were adequate. Impaired intervals are gaps in the observed record flagged as missing, deleted, or accumulated rainfall. Gridded time series are used to patch impaired intervals as follows. First, a 10-km buffer was created around each of the observed gauges that were prescreened for quality. Next, the 10-km gauge buffer was intersected with the PRISM grid layer. The time series at any grid falling within the buffer is ultimately overridden by the associated observed gauge time series, except for impaired intervals, where the gridded data are retained to patch those temporal impairments. Consequently, most of the observed data at a PRISM grid location will be identical to a neighboring grid within a 10-km buffer of the gauge but will have slightly different PRISM time series for impaired intervals.

After the creation of the hybrid precipitation time series, each catchment is assigned a time series based on the Thiessen polygon its centroid falls within. Figure 4-4 illustrates the final assignment of gauge-based or LSM-based hybrid time series by catchment. Figure 4-5 shows the distribution of monthly total precipitation across all hybrid time series within the watershed and Figure 4-6 illustrates the spatial distribution of annual average precipitation from the hybrid time series by catchment.

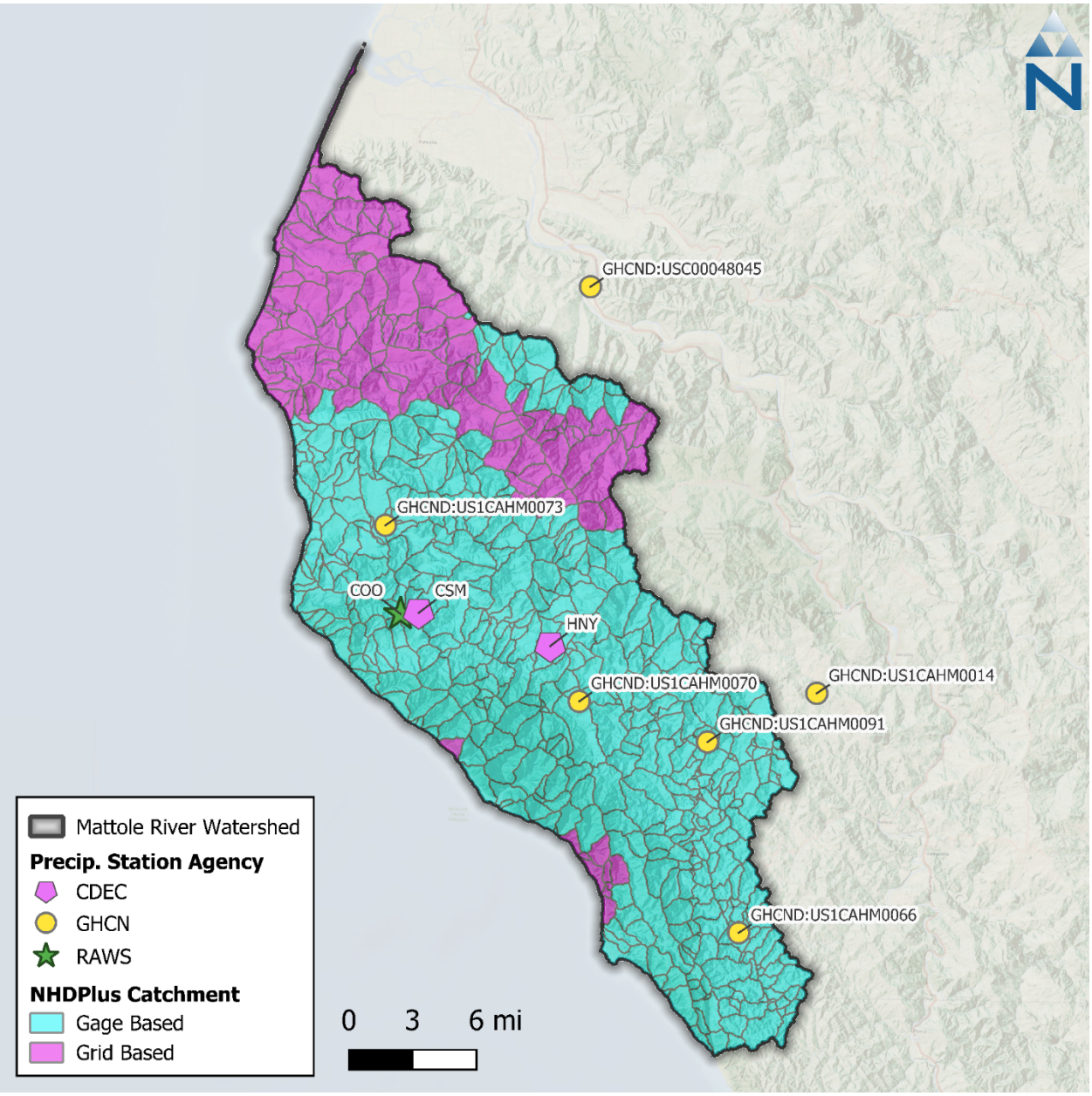

Figure 4-4. Spatial coverage of precipitation time series by catchment.

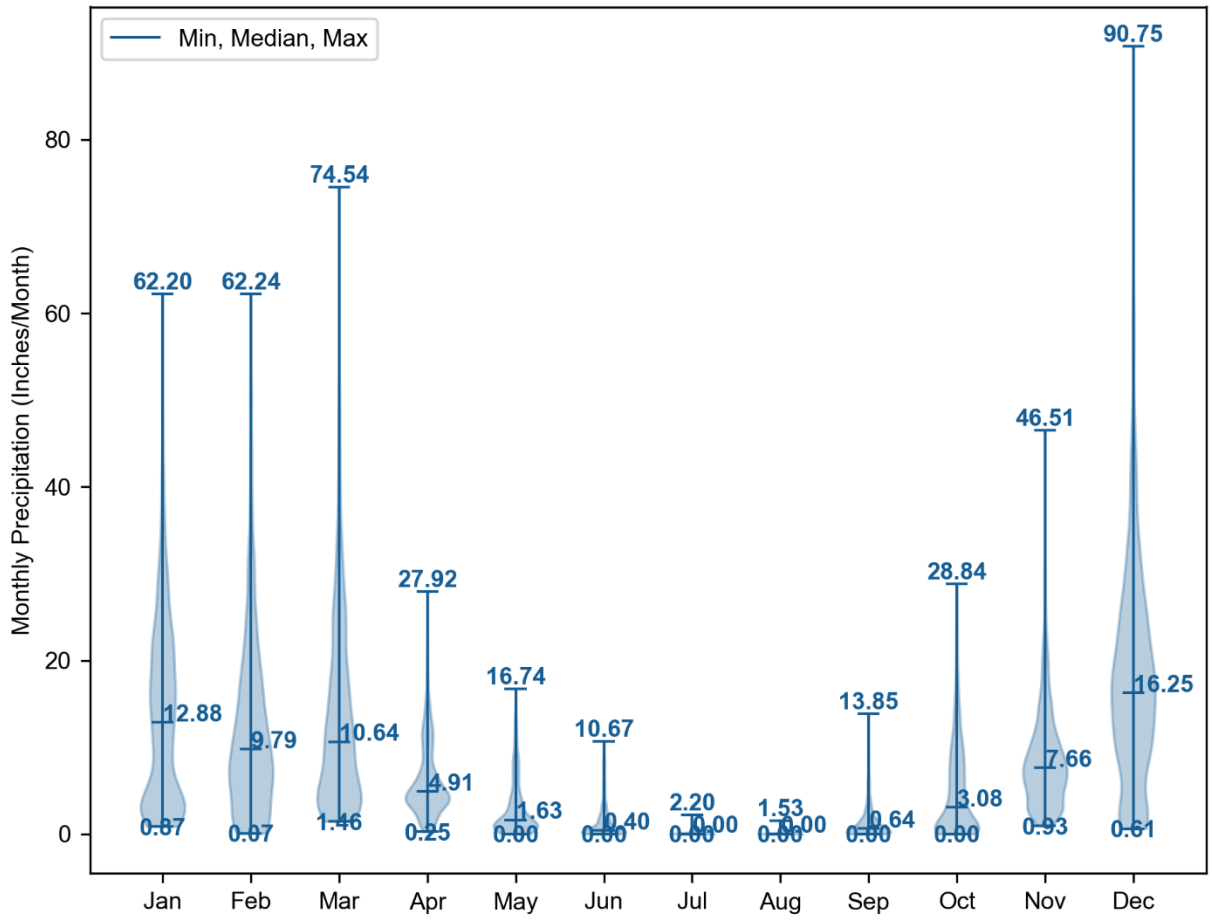

Figure 4-5. Distribution of monthly total precipitation across all hybrid time series within the Mattole River watershed for Water Years 2004-2023.

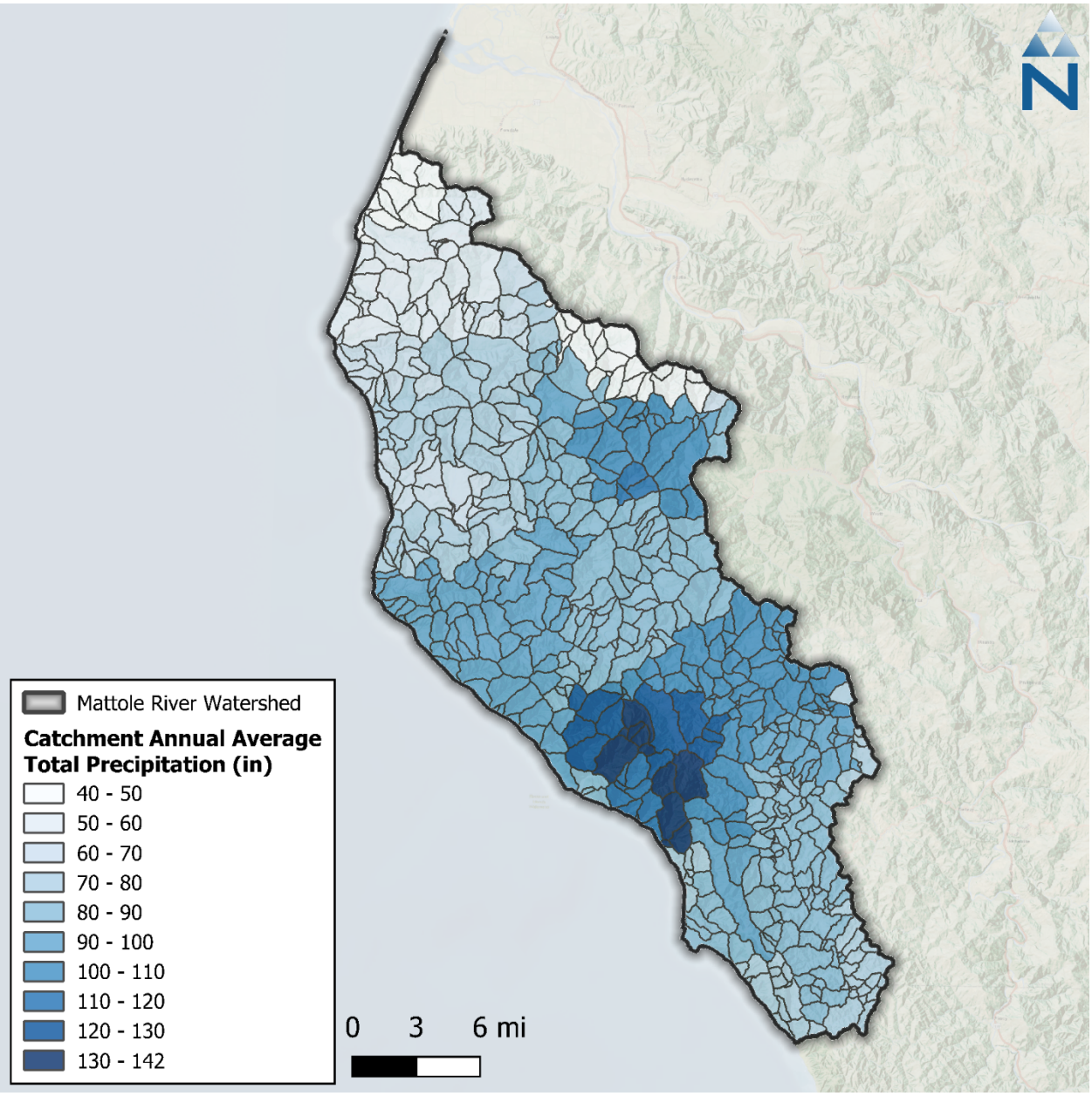

Figure 4-6. Annual average hybrid precipitation totals by catchment from Water Years 2004-2023.

4.2 Potential Evapotranspiration

In addition to precipitation, potential evapotranspiration forcing input time series were created and assigned to each catchment. Daily total reference evapotranspiration (ET_o) from the California Irrigation Management Information System (CIMIS) Spatial dataset was downscaled to hourly using the NLDAS hourly solar radiation. CIMIS Spatial expresses daily ET_o estimates calculated at a statewide 2-km spatial resolution using the American Society of Civil Engineers version of the Penman-Monteith equation (ASCE-PM). This product provides a consistent spatial estimate of ET_o that is California-specific, implicitly captures macro-scale spatial variability and orographic influences, is available from 2004 through the Present, and is routinely updated. Within each catchment, actual ET is calculated for each Hydrologic Response Unit (HRU) during the model simulation as a function of parameters representing differences in vegetation (type, height, and density) and soil conditions.

Figure 4-7 shows the distribution of monthly total ET_o across all grid points within the watershed. Figure 4-8 shows the spatial distribution of CIMIS annual average total ET_o across the watershed.

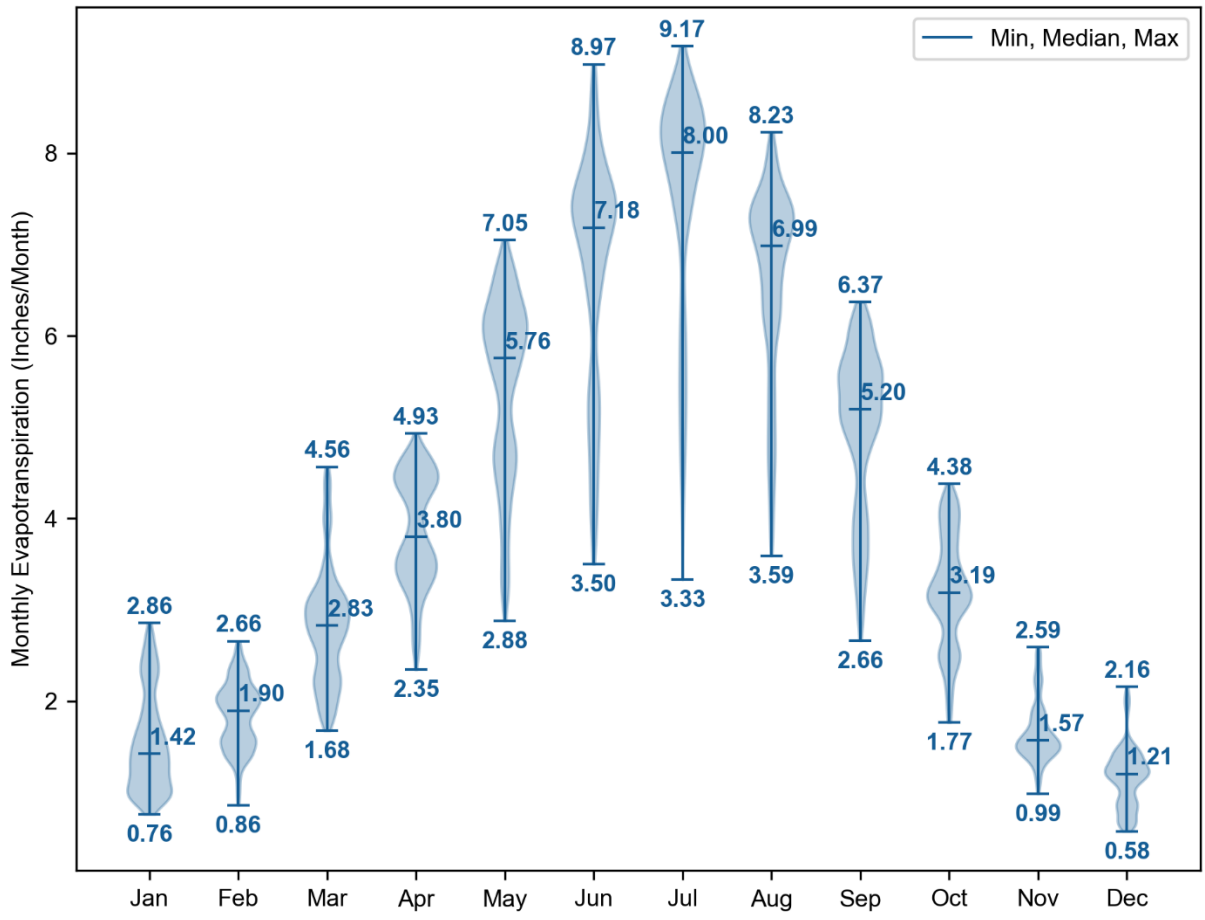

Figure 4-7. Distribution of monthly total ET_o across all CIMIS spatial grid points within the Mattole River watershed from WY 2004-2023.

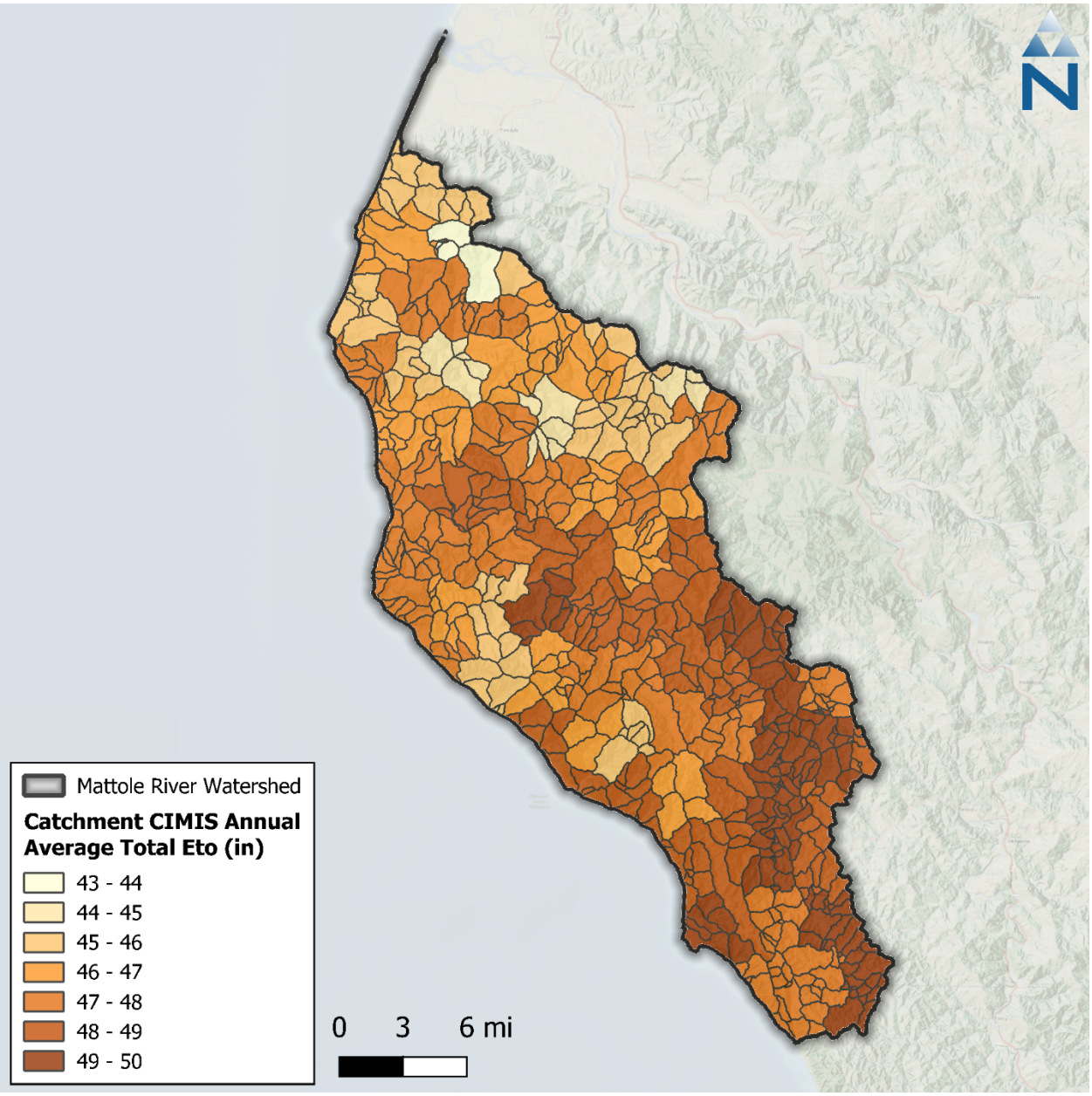

Figure 4-8. CIMIS annual average total ET_o by catchment within the Mattole River watershed.

5 SURFACE WATER WITHDRAWALS

Datasets related to water rights, points of diversion (PODs), and water use were identified through the Water Board's eWRIMS database. These data were used to represent diversions and withdrawals in the watershed model. Monthly data from 579 active water rights within the Mattole River watershed from 2017 to 2023 were received from the Board's Supply and Demand Unit staff. Of these, 542 had reported withdrawals; surface water withdrawals from these active water rights occur from 610 PODs which are mapped in Figure 5-1. By count, Irrigation accounts for more than half (57%) of the water usage, while Domestic (27%), Other (15%), and Municipal (0.1%) make up the remainder (Figure 5-2). Here, the 'Other' category groups dust control, fire protection, stock-watering, irrigation and

domestic municipality, and fish and wildlife preservation and enhancement primary uses. By volume however, the usage is roughly evenly split between Irrigation (30%), Municipal (27%), Domestic (22%), and Other (20%).

For the non-irrigated water demand, the received monthly data in acre-feet are summed by catchment and then converted to a flow rate for withdrawal from the appropriate catchment's modeled reach segment. Irrigation demand is similarly converted from monthly volume into a withdrawal rate by application number. These water demand data are added to the LSPC model as surface water withdrawals from the appropriate reach segments based on the following considerations.

- Diversions were classified based on primary usage (irrigation, municipal, industrial, recreational, etc.) as well as by allocation type (direct and storage).
- During simulations, diverted streamflow was routed out of the system to represent the different usages (i.e., irrigation).
- For instances where PODs in different catchments share the same application/permit number, water demand was proportionally distributed based on the magnitude of upstream drainage area.

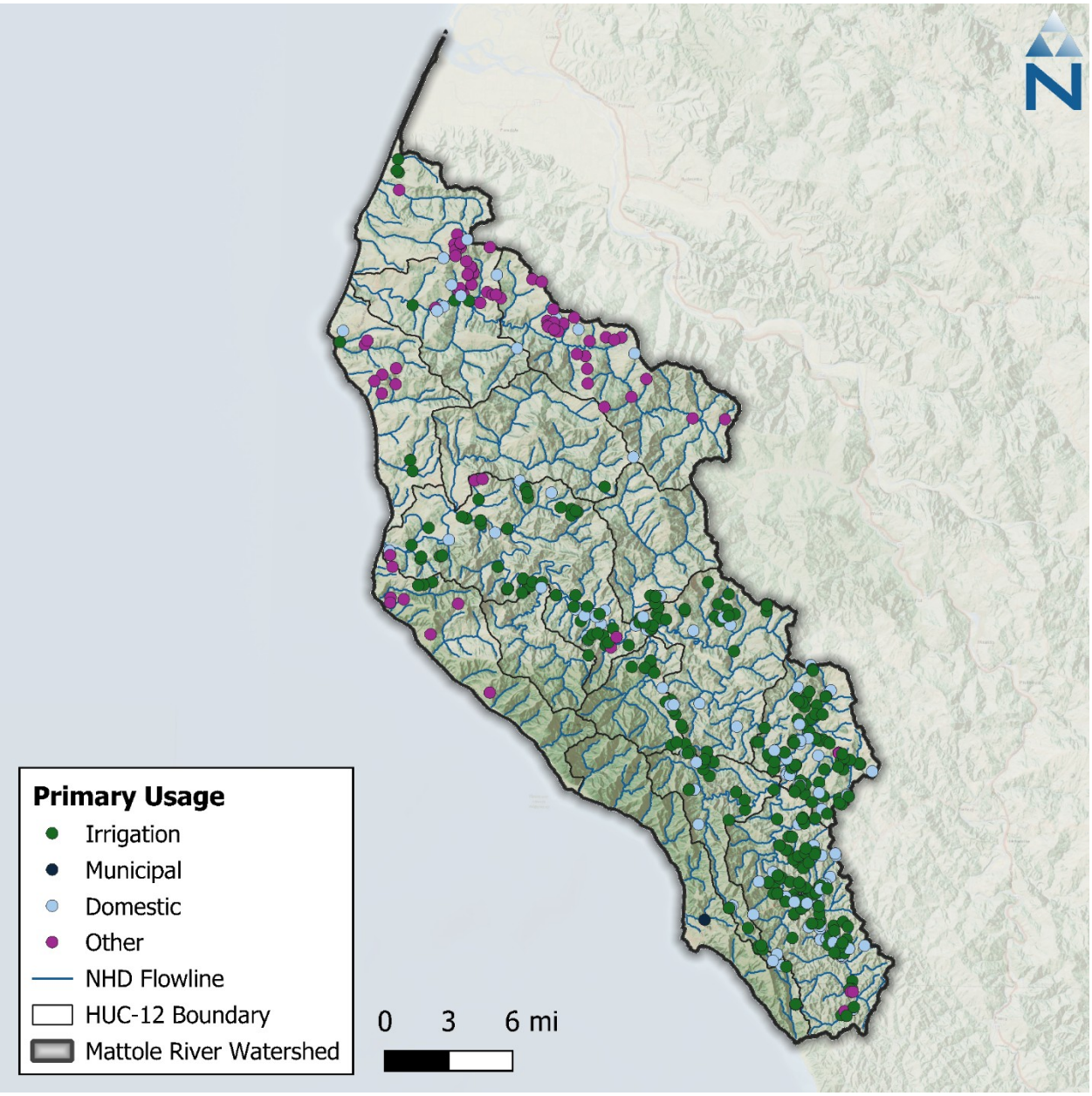

Figure 5-1. Points of diversion within the Mattole River watershed.

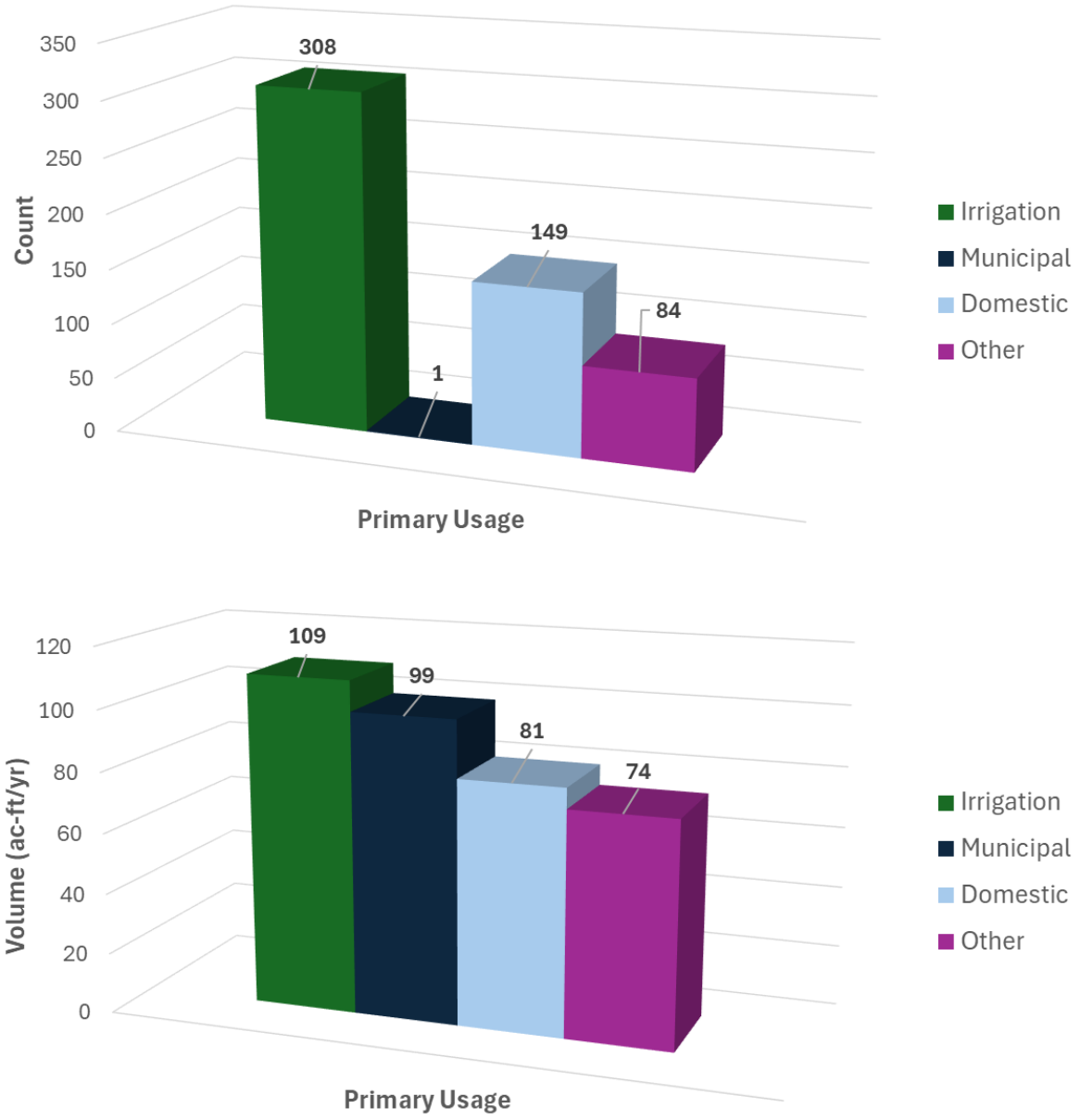

Figure 5-2. Primary water usage for points of diversion within the Mattole River watershed.

5.1 Irrigation

The LSPC irrigation module is designed to streamline the spatial and temporal representation of water demand, irrigation application, and associated return flows. In practice, irrigation demand is estimated as the deficit of precipitation from the product of a crop-specific evaporative coefficient (ET_c) and reference evapotranspiration (ET_0). This LSPC configuration uses a similar approach but instead works backwards to estimate the monthly crop coefficients for agricultural HRUs by using observed irrigation demand and climate data. Those crop coefficients are then used with observed climate data to calculate irrigation application rates during LSPC simulations. The equation used to calculate monthly evaporative crop coefficients for agricultural HRUs is shown as Equation 2:

$$V_{irr} = (PET \times ET_c - PREC) \times A_{irr} \quad \text{Equation 2}$$

where (V_{irr}) is the volume of irrigation demand in acre-feet, (A_{irr}) is the cropland being irrigated in acres, (PET) is the potential evapotranspiration depth in feet, ET_c is the crop-specific evaporative coefficient, and (PREC) is the observed precipitation depth in feet. As mentioned above, irrigation demand was inferred from stream diversion records for each catchment. Because the exact location of irrigated vs. non-irrigated parcels was unknown, it was assumed that agricultural land located in catchments immediately draining to reach segments with irrigation PODs were irrigated, as well as adjacent catchments.

The process for representing irrigation in the Mattole River watershed is summarized by the following steps:

1. Estimate irrigation demand.
2. Define irrigated hydrologic response units.
3. Calculate crop evaporative coefficients.

5.1.1 Estimation of Irrigation Demand

Irrigation demand was inferred from eWRIMS stream diversion data for records between 2017 and 2023. For each LSPC catchment, the total monthly irrigation demand was estimated as the sum of all irrigation-associated stream diversions. As mentioned above, stream diversions were either directly used for the application or routed to a storage facility for later use. Due to data limitations, it was unknown exactly when and how stored streamflow was used for irrigation; however, because direct diversion is higher during the growing season and generally follows PET, it was assumed that irrigation of stored water would also follow a similar pattern that scales in proportion to evaporative demand, which is higher during the warmer and drier growing season. Figure 5-3 shows average monthly diversion volumes vs. potential evapotranspiration.

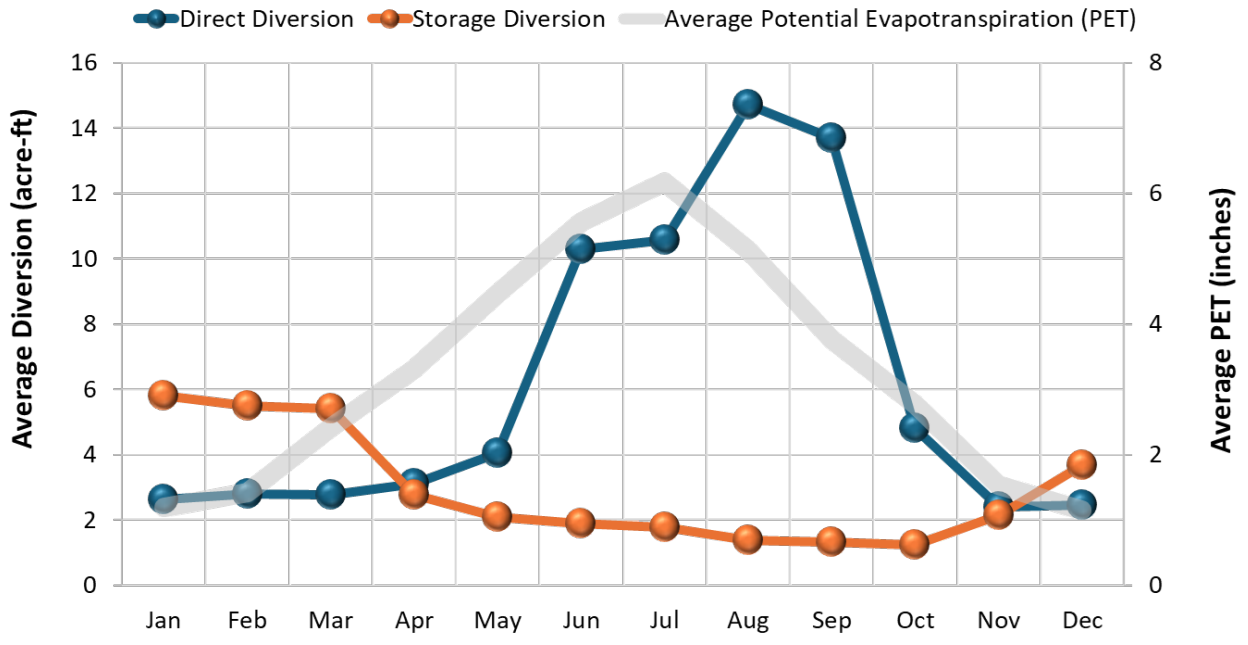

Figure 5-3. Total reported direct and storage diversions vs. average potential evapotranspiration.

5.1.2 Defining Irrigated Hydrologic Response Units

The LSPC model simulates irrigation on a unit-area basis. Agricultural HRUs were partitioned into irrigated and non-irrigated HRU counterparts, as previously described in Section 3.6.2. Because the exact location of irrigated vs. non-irrigated parcels was unknown, it was assumed that 100% of agricultural land located in catchments with irrigation PODs and immediately adjacent catchments was irrigated; 99 out of the 630 catchments were irrigated.

As shown in Figure 5-4, the sum of all croplands, pasture, and grassland areas represents 12.4% of the watershed and could potentially be irrigated. Of that area, 42% is within the catchments selected for irrigation. The "Irrigated" area - where the modeled unit-area response is applied - is 125 acres, which is less than 0.1% of the Mattole River watershed, as shown in Figure 5-5. For the unit-area model representation, it was assumed that 50 percent of irrigation water was applied as sprinkler and 50 percent as flood (or drip) irrigation. These are common practices in the nearby Navarro River and Russian River watersheds (McGourty et al. 2020). Sprinkler irrigation enters the model at the same layer as precipitation, making it subject to interception storage and associated evaporation. Flood irrigation enters the model below interception storage and is only subject to surface ponding and infiltration.

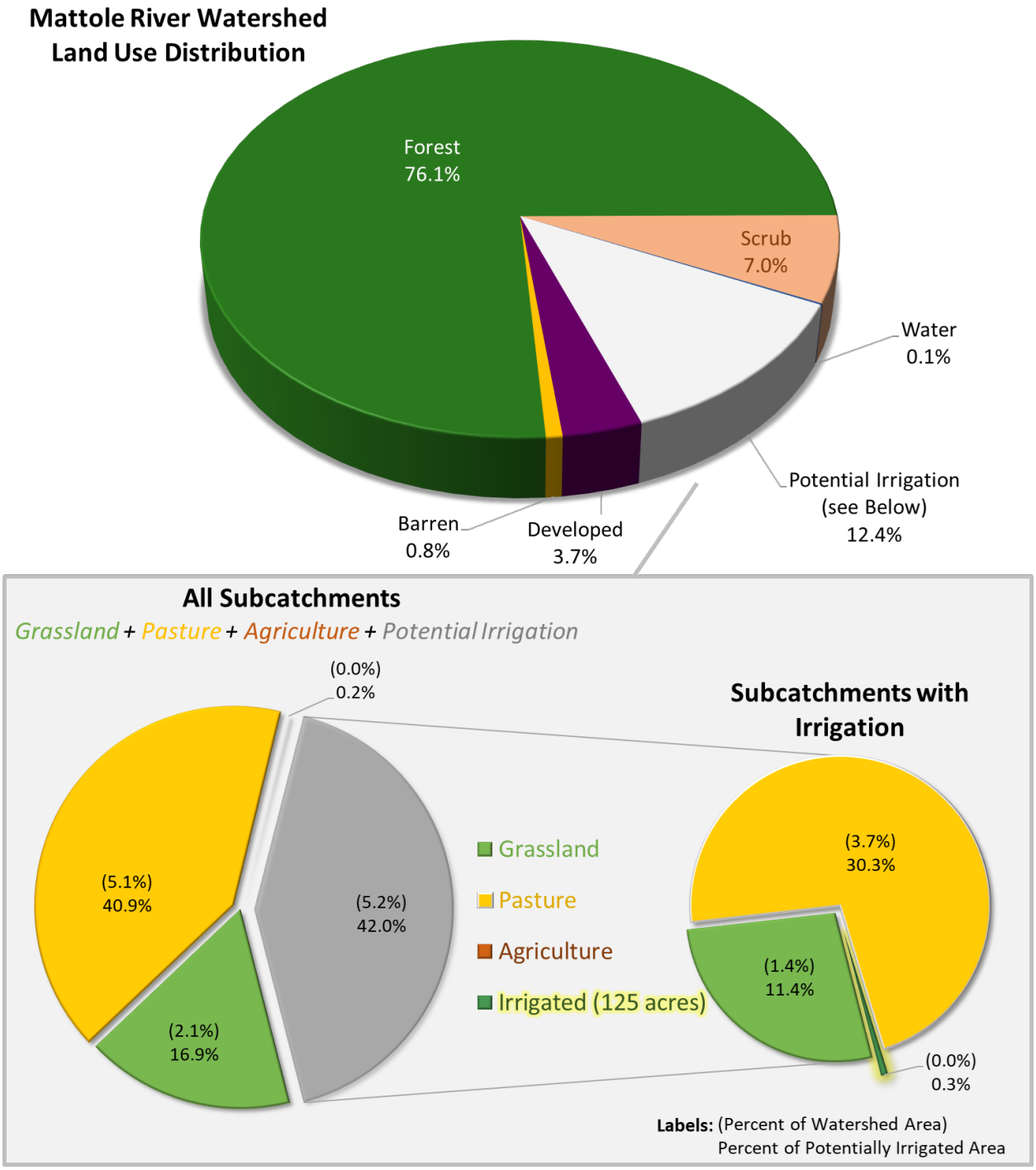

Figure 5-4. Irrigated area as a subset of the Mattole River watershed.

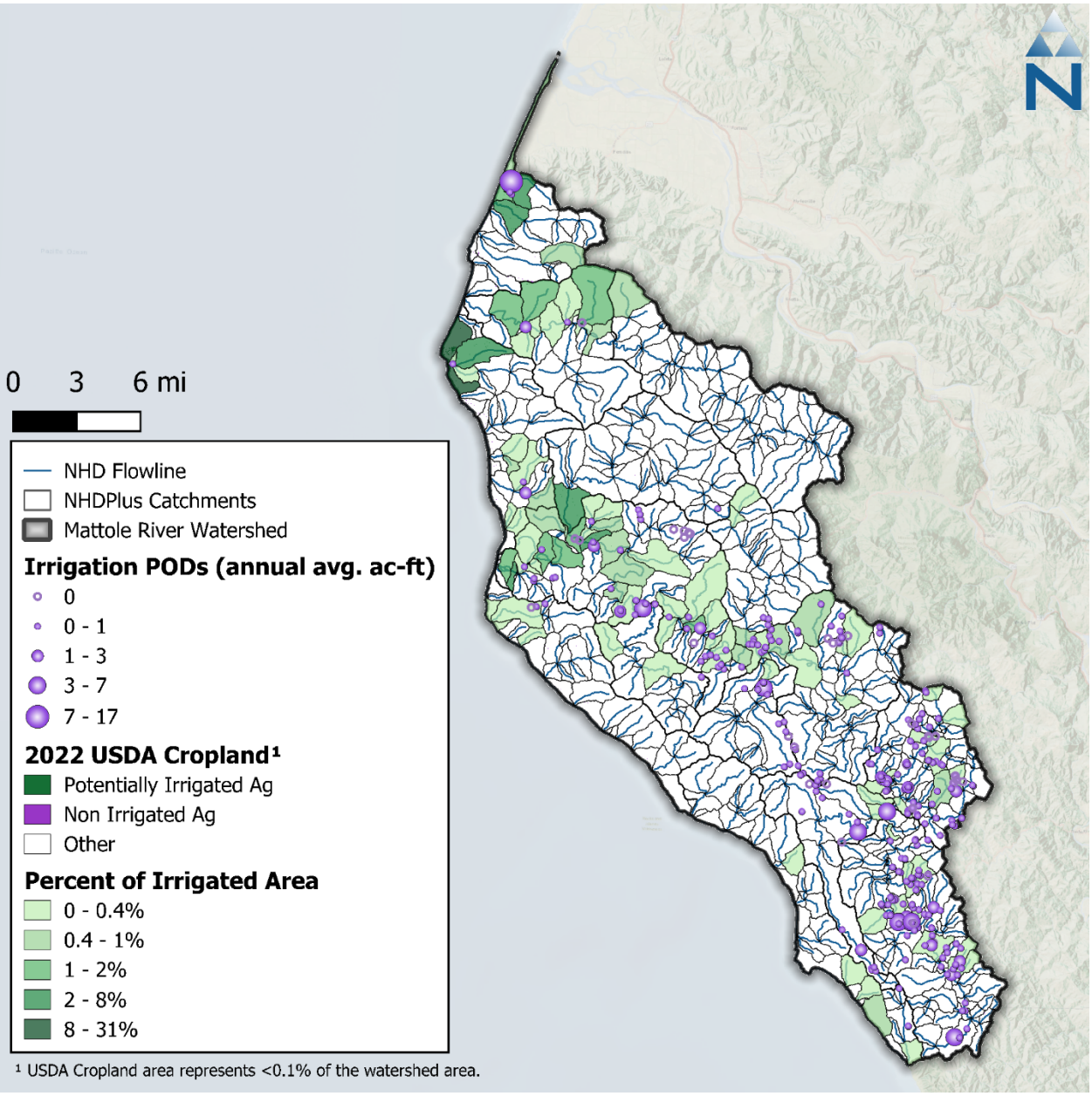

Figure 5-5. Irrigated and non-irrigated agriculture areas within the Mattole River watershed.

5.1.3 Calculation of Crop Evaporative Coefficients

Crop evaporative coefficients (ET_c) are used to adjust reference evapotranspiration rates to better represent an evaporative demand for a specific vegetation type. In the absence of high-resolution irrigation data, this crop-specific evaporative demand can be used with observed precipitation and PET data to predict irrigation demand. For this LSPC model instance, distinct crop types were not represented in hydrologic response units; therefore, one value of crop evaporative coefficient per calendar month was used to represent all irrigated areas. Storage occurs in the wetter winter/spring months. Direct diversion is higher during the growing season and closely follows PET.

The coefficients used in the model were derived by optimizing ET_C in Equation 2 using Microsoft Excel solver to match total irrigation demand volume (V_{irr}) with the total withdrawal volume for

irrigation use. Initial estimates for these coefficients are provided in Table 5-1. Storage diversion and management were not explicitly modeled. By using these coefficients, it was assumed that the same total water diverted for irrigation (storage + direct diversion) was eventually irrigated in proportion to monthly potential evapotranspiration. However, these estimates are subject to change during streamflow calibration to improve the water balance.

Table 5-1. Estimated crop evaporative coefficients (ET_c) by month

Jan	Feb	Mar	Apr	May	Jun	Jul	Aug	Sep	Oct	Nov	Dec
0.717	0.169	0.134	0.180	0.342	0.473	0.555	0.566	0.537	0.551	0.440	0.587

6 Observed Water Balance

A water balance analysis was conducted using the primary observed data to explore the hydrological behavior of the Mattole River watershed. For this analysis, precipitation (as described in Section 4.1) is assumed to be the primary source of water and potential evapotranspiration (as described in Section 4.2) and streamflow are the primary sinks. Streamflow is retrieved from two USGS stations: the Mattole River near Petrolia (USGS 11469000) and the Mattole River near Ettersburg (USGS 11468900). These stations are detailed in Table 6-1 and shown in Figure 6-1. The Ettersburg station is nested within the drainage area of the Petrolia station and represents nearly one-third of its drainage area (29%).

The water balance components are spatially and temporally aggregated over each station's drainage area for the period from October 2003 through September 2023. The water year total volumes for this period are shown in Table 6-2 and Table 6-3 for the Ettersburg and Petrolia stations, respectively. These tables include the percentile ranking of each WY by precipitation total, which helps illustrate the long-term pattern of wet and dry years. Because PET is based on the CIMIS reference ET, these tables also include an estimated actual ET value, which is calculated as the difference between precipitation and streamflow; note that this value can include other unknown storages and losses. For the Ettersburg and Petrolia stations, streamflow makes up between 68% and 63% of outflow on average, while estimated ET and other storages/losses account for the remainder. These values are reasonable given the relatively wet conditions in the drainages for these stations (see Figure 4-6).

Monthly average water balances for both the Ettersburg (Figure 6-2) and Petrolia (Figure 6-3) stations were also created to illustrate the intra-annual hydrological patterns. These charts are normalized by drainage area to allow consistent comparison in terms of depth. Both show the expected seasonal pattern of high precipitation and streamflow in the wet season (October – April) and PET peaking in the dry season (May – September).

Table 6-1. Summary of streamflow stations with observations available after 2000

Agency	Station Description	Station ID	Drainage Area (mi^2)	Start Date	End Date	Gauge Active?
USGS	MATTOLE R NR PETROLIA CA	11469000	245	10/01/1988	Present	Yes
	MATTOLE R NR ETTERSBURG CA	11468900	70.9	06/22/2001	Present	Yes

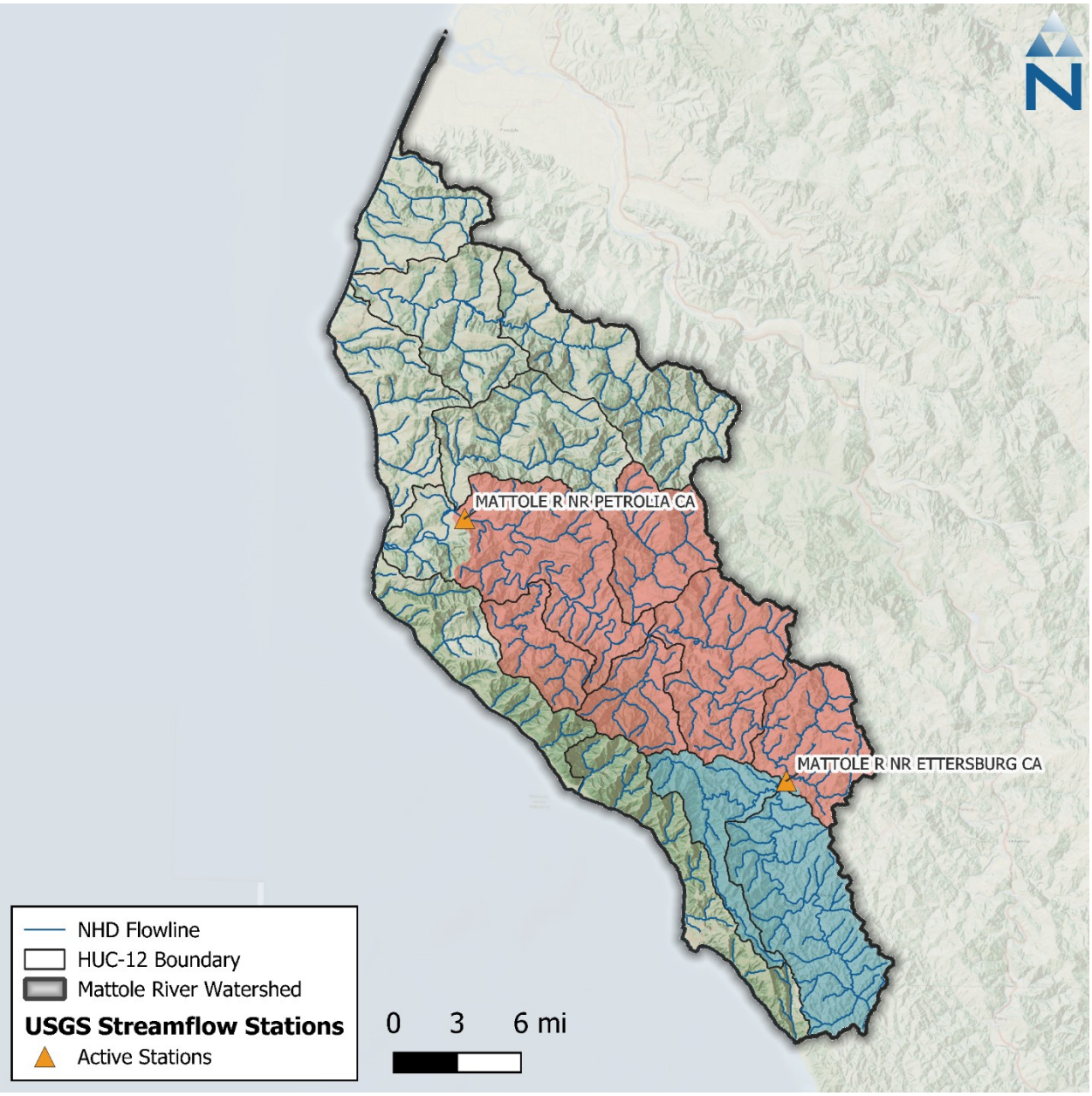

Figure 6-1. USGS streamflow stations in the Mattole River watershed with drainage areas highlighted.

Table 6-2. Water year total volumes for observed water budget components at the MATTOLE R NR ETTERSBURG CA (11468900) station

Water Year	Precipitation Percentile Rank	Total Volume (ac-ft)				Est. ET (% PET)
		Precipitation	PET[1]	Streamflow	Est. ET & Other Losses[2]	
2004	53%	351,264	194,488	248,307	102,957	53%
2005	47%	333,364	175,427	216,968	116,396	66%
2006	95%	518,718	187,228	427,098	91,620	49%
2007	26%	278,275	200,620	204,297	73,978	37%
2008	32%	281,334	200,458	165,901	115,433	58%
2009	16%	266,893	208,295	173,434	93,459	45%
2010	79%	432,271	178,260	254,637	177,635	100%
2011	89%	469,933	176,584	297,967	171,966	97%
2012	63%	368,904	186,013	256,789	112,115	60%
2013	58%	360,894	197,354	163,663	197,232	100%
2014	11%	238,487	212,138	125,678	112,808	53%
2015	37%	283,616	206,686	179,578	104,038	50%
2016	74%	424,185	189,044	302,271	121,914	64%
2017	100%	564,812	173,415	465,028	99,784	58%
2018	42%	297,776	182,880	219,079	78,697	43%
2019	84%	443,623	189,687	381,348	62,275	33%
2020	0%	209,199	148,686	115,945	93,255	63%
2021	5%	210,765	159,494	114,636	96,129	60%
2022	21%	268,395	146,663	150,482	117,913	80%
2023	68%	373,777	155,459	251,725	122,052	79%
Average	--	**348,824**	**183,444**	**235,742**	**113,083**	**62%**
In/Out (%)	--	**100%**	--	**68%**	**32%**	--

1. Potential Evapotranspiration (PET) is based on the CIMIS reference ET, as described in Section 4.2.
2. Estimated ET is calculated as Precipitation minus Streamflow and represents an approximate actual ET plus any other storages or losses.

Color Gradient: Lowest | Low | Medium | High | Highest

Table 6-3. Water year total volumes for observed water budget components at the MATTOLE R NR PETROLIA CA (11469000) station

Water Year	Precipitation Percentile Rank	Total Volume (ac-ft)				Est. ET (% PET)
		Precipitation	PET[1]	Streamflow	Est. ET & Other Losses[2]	
2004	63%	1,195,420	674,967	830,525	364,895	54%
2005	53%	1,158,000	611,113	800,205	357,796	59%
2006	95%	1,830,085	654,076	1,632,988	197,098	30%
2007	32%	952,974	698,498	693,412	259,562	37%
2008	42%	977,104	695,659	626,748	350,356	50%
2009	21%	913,756	725,053	608,952	304,804	42%
2010	84%	1,485,690	622,275	873,007	612,683	98%
2011	79%	1,474,341	615,728	877,769	596,572	97%
2012	58%	1,178,827	647,470	688,123	490,704	76%
2013	47%	1,115,290	689,331	548,235	567,055	82%
2014	0%	674,190	741,719	311,330	362,860	49%
2015	37%	960,603	721,404	508,034	452,570	63%
2016	74%	1,428,181	656,788	877,854	550,326	84%
2017	100%	1,986,865	600,575	1,416,649	570,216	95%
2018	26%	950,736	636,415	491,418	459,318	72%
2019	89%	1,489,440	649,021	925,084	564,356	87%
2020	5%	675,274	485,714	349,124	326,150	67%
2021	11%	696,788	509,385	400,217	296,571	58%
2022	16%	839,169	478,636	427,150	412,020	86%
2023	68%	1,252,609	522,163	821,243	431,367	83%
Average	--	**1,161,767**	**631,800**	**735,403**	**426,364**	**68%**
In/Out (%)	--	**100%**	--	**63%**	**37%**	--

1. Potential Evapotranspiration (PET) is based on the CIMIS reference ET, as described in Section 4.2.
2. Estimated ET is calculated as Precipitation minus Streamflow and represents an approximate actual ET plus any other storages or losses.

Color Gradient: Lowest | Low | Medium | High | Highest

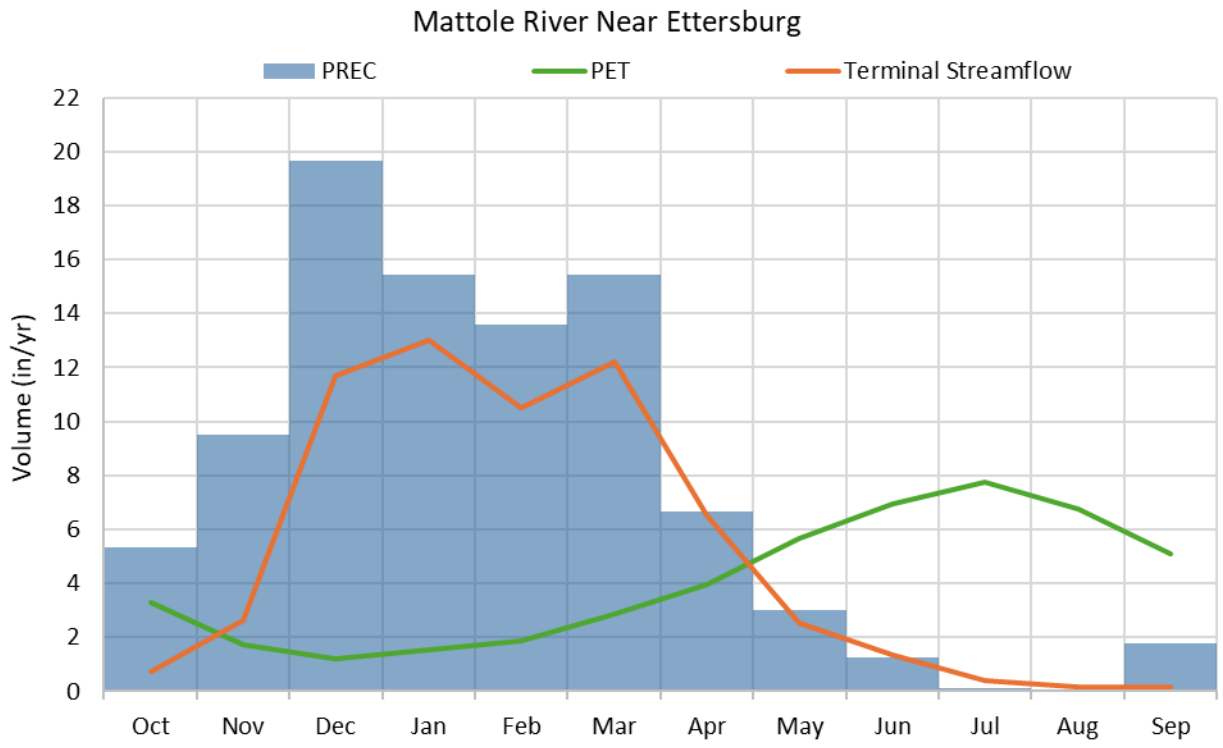

Figure 6-2. Monthly observed area-normalized average depths for the modeling period (water years 2004 -2023) at the MATTOLE R NR ETTERSBURG CA (11468900) station.

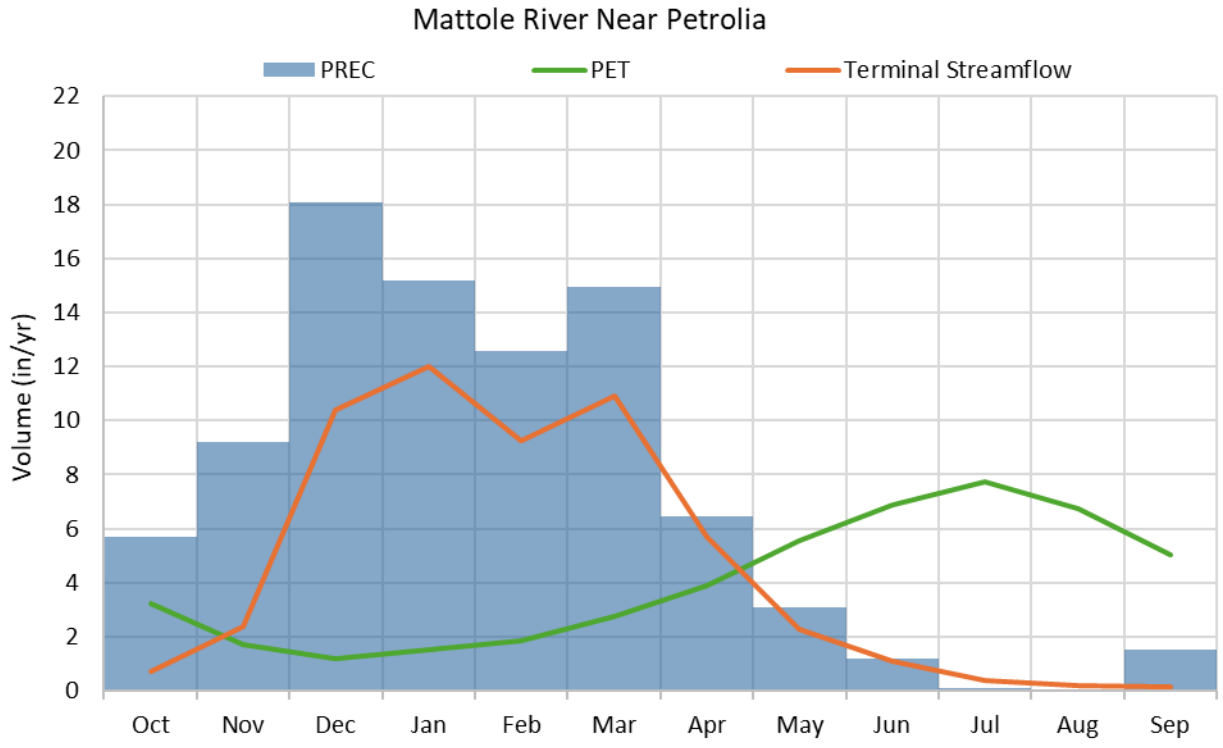

Figure 6-3. Monthly observed area-normalized average depths for the modeling period (water years 2004 -2023) at the MATTOLE R NR PETROLIA CA (11469000) station.

7 MODEL CALIBRATION

The goal of the hydrology model calibration is to adjust model parameters to improve predictive performance based on comparisons to observed data. The desired outcome of the calibration process is a set of modeling parameters that characterize existing conditions for all processes in LSPC that vary by HRU (as described in Section 3), reach group, and process-based parameters group. The model development approach prioritizes model configuration over calibration by investigating and expressing known physical characteristics of the watershed wherever possible and practical, and only leaving responses that cannot be explained by physical characteristics to calibration of model parameters. The resulting model is parameterized in such a way that variability trends in the observed data are replicated relative to hydrological conditions (e.g., wet and dry streamflow conditions and rainfall magnitude). The resulting calibrated parameters are consistent by HRU with responses varying as a function of HRU distribution and weather variability, which minimizes spatial biases and reduces the possibility of over tuning during model calibration. A robustly calibrated model can then serve as the starting point for future watershed-specific applications and investigations and management scenarios.

Figure 7-1 shows how the model configuration and calibration components are layered in the model. LSPC makes clear distinctions between inputs that are physical characteristics and process parameters. The term "parameters" refers to the rates and constants used to represent physical processes in the model. All other model inputs previously described such as weather data, HRU distribution, and the length and slope of overland flow for individual HRUs are generally considered physical characteristics of the watershed because they can be directly measured, assigned, or reasonably estimated from available spatial and temporal data sources. Those components are generally set during model configuration and are not varied during model calibration unless new information is received that justifies a systemwide change to those components.

Developing modeling parameters begins with specifying one set of parameters systemwide. The Mattole River model comprises 98 possible HRUs per catchment and 145 unique combinations of meteorological boundary conditions (i.e., unique combinations of precipitation time series and potential evapotranspiration time series). As described in Section 3.4.1, LSUR and SLSUR are uniquely computed by HRU and catchment combinations; therefore, the initial degrees of freedom of modeled responses are already quite broad. Consequently, using one parameter group, the model represents 181,395 unique non-zero area HRU × meteorological responses over the model domain of 630 catchments. Wherever model responses diverge from observed data in ways that the modeling parameters cannot explain, further investigation may warrant introducing a new parameter group or reach group to add more degrees of freedom to the range of model parameters. This methodical calibration sequence can also help to identify areas where additional data collection may be warranted to better characterize the physical system.

Figure 7-2 shows the model calibration sequence, a top-down data approach that began with the extensive model configuration and quality control process previously described in Section 2 through Section 5. The sequence begins with climate-forcing data, followed by edge-of-stream land hydrology and water budget estimates and representation of the stream routing network. This sequencing minimizes the propagation of uncertainty and error by distinguishing physical characteristics of the watershed that can be measured and configured from process-based parameters, which are rates and constants that can be estimated within a reasonable range of variability by HRU.

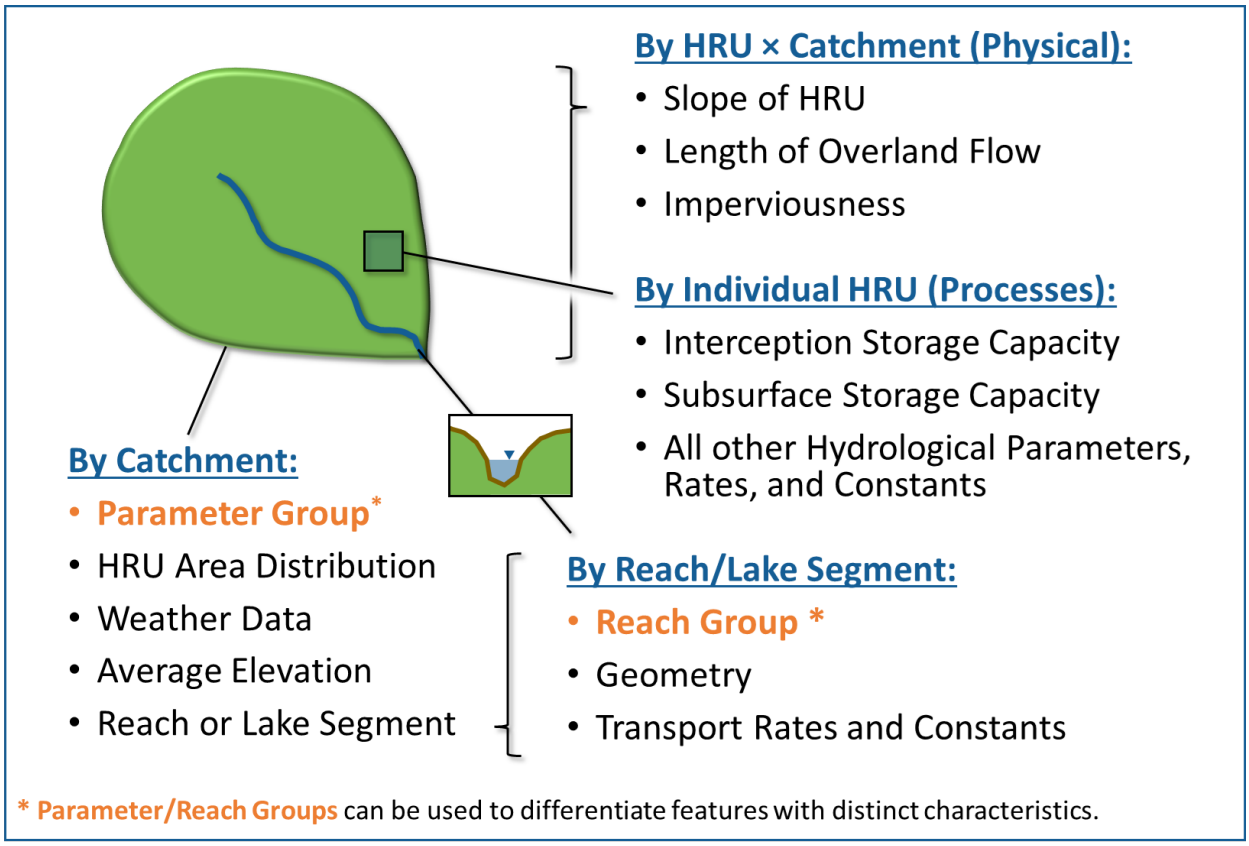

Figure 7-1. LSPC model configuration and calibration components.

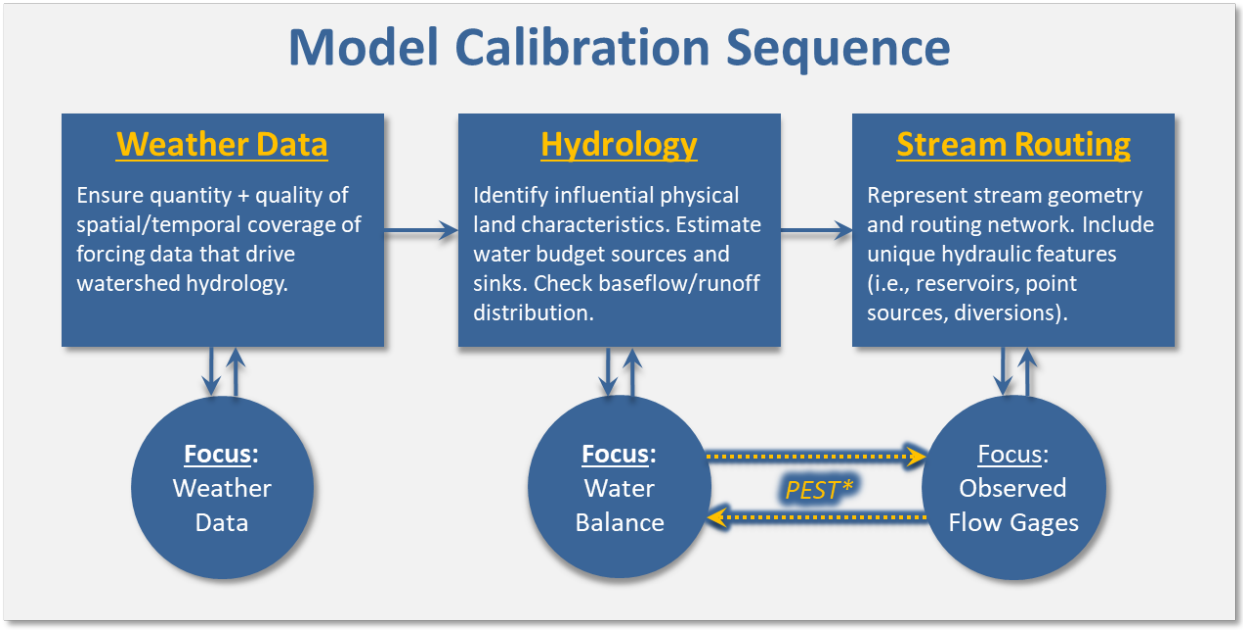

Figure 7-2. Top-down calibration sequence for hydrology model calibration.

Twenty water years of meteorological forcing data between October 2003 and September 2023 were processed to drive the Mattole River watershed model. Reported consumptive use data were available for the most recent 7 among those 20 years, water years 2017 through 2023; therefore, those years were selected for model calibration and Parameter Estimation (PEST) with 2017 used as a model spin up period—that process is further described in Section 7.2. As shown in Figure 7-3, the 6-year calibration period included a range of moderately wet (2019) to very dry years (2020, 2021). The 13 water years prior to the calibration period (water years 2005 through 2017) were selected for independent model validation at both USGS stations (Petrolia and Ettersburg).

Calibration of hydrology parameters was carried out in two phases. First, PEST was used to estimate selected parameters for the Mattole River near Ettersburg USGS station (11468900) because it has a high-quality data record (see Figure 6-1 and Table 6-1 for details). This station is near the headwaters of the watershed, which allows for faster model run times compared to the larger Mattole River near Petrolia USGS station (11469000), and is largely representative of the HRU distributions throughout the watershed, as shown in Table 7-1 and Table 7-2. The second phase of calibration applied the PEST estimated parameters model-wide; additional adjustments to model configuration and calibration were then performed to balance performance across the two USGS stations.

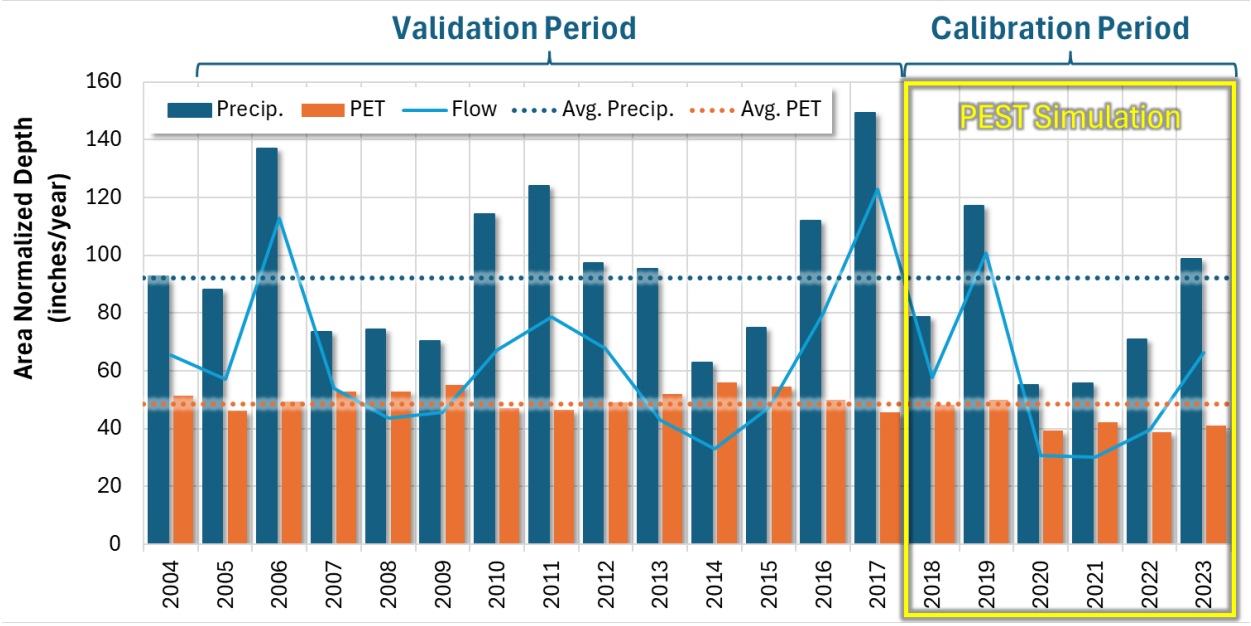

Figure 7-3. Annual average precipitation, potential evapotranspiration (PET), and streamflow between water years 2004 – 2023, along with PEST simulation and hydrology calibration periods for the Mattole River near Ettersburg USGS station (11468900) drainage area.

Table 7-1. HRU distribution for the Mattole River near Ettersburg station

Mattole River near Ettersburg Land Cover	LC (%)	Area by HSG (%)					Area by Slope (%)			
		Imp/Water	A	B	C	D	Imp/Water	Low	Med	High
Developed Impervious	0.1%	0.1%	--	--	--	--	0.1%	--	--	--
Developed Pervious	4.8%	--	--	3.4%	1.3%	--	--	0.3%	1.0%	3.5%
Barren	--	--	--	--	--	--	--	--	--	--
Forest	92.1%	--	--	76.0%	16.1%	--	--	1.2%	5.4%	85.4%
Scrub	1.5%	--	--	0.8%	0.7%	--	--	0.1%	0.3%	1.1%
Grassland	0.8%	--	--	0.5%	0.3%	--	--	0.1%	0.2%	0.5%
Pasture	0.7%	--	--	0.4%	0.3%	--	--	0.1%	0.1%	0.5%
Agriculture	0.0%	--	--	0.0%	--	--	--	--	--	0.0%
Water	0.0%	0.0%	--	--	--	--	0.0%	--	--	--
Irrigation	0.0%	--	--	0.0%	0.0%	--	--	--	0.0%	0.0%
Total (%)	**100.0%**	**0.1%**	**0.0%**	**81.1%**	**18.8%**	**0.0%**	**0.1%**	**1.8%**	**7.1%**	**91.0%**
Total (ac)	**45,448.0**	**63.0**	**0.0**	**36,853.7**	**8,531.3**	**0.0**	**63.0**	**812.3**	**3217.2**	**41,355.5**

Color gradients indicate more Watershed Area and an increasing percentage of Soil and Slope, respectively.

Table 7-2. HRU distribution for the Mattole River near Petrolia station, excluding the nested Ettersburg station drainage area

Mattole River near Petrolia (Below Ettersburg) Land Cover	LC (%)	Area by HSG (%)					Area by Slope (%)			
		Imp/Water	A	B	C	D	Imp/Water	Low	Med	High
Developed Impervious	0.1%	0.1%	--	--	--	--	0.1%	--	--	--
Developed Pervious	3.9%	--	0.0%	2.4%	1.4%	0.1%	--	0.2%	0.6%	3.0%
Barren	0.4%	--	0.0%	0.3%	0.1%	--	--	0.2%	0.1%	0.1%
Forest	81.3%	--	0.0%	61.4%	19.2%	0.7%	--	0.5%	3.0%	77.8%
Scrub	5.5%	--	0.0%	1.9%	3.2%	0.4%	--	0.2%	0.5%	4.9%
Grassland	3.4%	--	0.0%	1.3%	1.8%	0.3%	--	0.4%	0.5%	2.4%
Pasture	5.3%	--	0.0%	1.3%	3.5%	0.6%	--	0.9%	0.7%	3.8%
Agriculture	0.0%	--	--	0.0%	0.0%	0.0%	--	--	--	0.0%
Water	0.0%	0.0%	--	--	--	--	0.0%	--	--	--
Irrigation	0.0%	--	--	0.0%	0.0%	0.0%	--	0.0%	0.0%	0.0%
Total (%)	**100.0%**	**0.2%**	**0.1%**	**68.6%**	**29.2%**	**2.0%**	**0.2%**	**2.3%**	**5.5%**	**92.0%**
Total (ac)	**112,083.2**	**168.7**	**85.9**	**76,884.6**	**32,729.8**	**2,214.2**	**168.7**	**2,630.2**	**6,202.3**	**103,082.1**

Color gradients indicate more Watershed Area and an increasing percentage of Soil and Slope, respectively.

7.1 Calibration Assessment and Metrics

A combination of visual assessments and computed numerical evaluation metrics were used to assess model performance during calibration. Model performance was assessed using graphical comparisons of simulated vs. observed data (e.g., time-series plots, flow duration curves, etc.), quantitative metrics, and qualitative thresholds recommended by Moriasi et al. (2015) and Duda et al. (2012), which are considered highly conservative. Moriasi et al. (2007 and 2015) assign narrative grades for hydrology and water quality modeling to the percent bias (PBIAS), the ratio of the root-mean-square error to the standard deviation of measured data (RSR), and the Nash-Sutcliffe model efficiency (NSE). These metrics are defined as follows:

- The percent bias (PBIAS) quantifies systematic overprediction or underprediction of observations. Positive values of PBIAS reflect a bias towards underestimation, while negative values reflect a bias towards overestimation. Low magnitude values of PBIAS indicate better fit, with a value of 0 being zero net difference between modeled and observed.
- The ratio of the root-mean-square error to the standard deviation of measured data (RSR) provides a measure of error based on the root-mean-square error (RMSE), which indicates error results in the same units as the simulated and observed data but normalized based on the standard deviation of observed data. Values for RSR can be greater than or equal to 0, with a value of 0 indicating perfect fit. Moriasi et al. (2007) provides narrative grades for RSR.
- The Nash-Sutcliffe efficiency (NSE) is a normalized statistic that determines the relative magnitude of the residual variance compared to the measured data variance (Nash and Sutcliffe, 1970). NSE indicates how well the plot of observed versus simulated data fits the 1:1 line. Values for NSE can range between -∞ and 1, with NSE = 1 indicating a perfect fit.

Other metrics were computed and used to assess calibrated model performance, including the Kling-Gupta Efficiency (KGE). This metric can provide additional or complementary information on model performance to the three metrics listed above and is defined as follows:

- The Kling-Gupta Efficiency (KGE) metric is based on the Euclidean Distance between an idealized reference point and a sample's bias, standard deviation, and correlation within a three-dimensional space (Gupta et al. 2009). KGE attempts to address documented shortcomings of NSE, but the two metrics are not directly comparable. A KGE value of 1 indicates perfect fit, with agreement worsening for values less than 1. Knoben et al. (2019) have suggested a KGE value > - 0.41 as a benchmark that indicates a model has more predictive skill than using the mean observed flow. Qualitative thresholds for KGE have been used by Kouchi et al. (2017).

Both simulated time series and observed data were binned into subsets of time to highlight seasonal performance and different flow conditions. Hydrograph separation was also performed to assess stormwater runoff vs. baseflow periods to isolate model performance on stormflows and low flows. Table 7-3 is a summary of performance metrics that will be used to evaluate the hydrology calibration. As shown in the table, "All Conditions" (i.e., annual interval) for R-squared and NSE is the primary condition typically evaluated during model calibration. For sub-annual intervals, the pattern established in the literature for PBIAS/RME when going from "All Conditions" to sub-annual intervals is to shift the qualitative assessment by one category (e.g., use the "good" range for "very good", "satisfactory" for "good", and so on). This pattern was followed for RSR and NSE qualitative assessments of sub-annual intervals.

Using hydrograph separation to classify baseflow and stormflow provides a more reliable method for assessing low-flow model performance than using the lowest 50% of flows, a metric widely used in hydrology model calibration as a convenient indicator of low-flow model performance. There are several key reasons for this:

1. **Improved Representation of Low-Flow Conditions:** The lowest 50% of flows include not only baseflow but also portions of stormflow as the hydrograph rises and falls. This can mask the true low-flow or baseflow behavior of the system, as the transitions from baseflow to stormflow can have very different physical and hydrological drivers. By using hydrograph separation, baseflow, which is primarily driven by groundwater contributions, can be isolated from storm flows, which are influenced by rainfall (Smakhtin 2001). This provides a clearer, more consistent metric for assessing low-flow conditions during model calibration and performance evaluation.
2. **Reduction in Variability of Metrics:** Because the rising and falling limbs of the hydrograph are affected by factors such as precipitation intensity, antecedent moisture conditions, and catchment characteristics, including portions of these limbs in the low-flow metric can lead to high variability in model performance metrics. This variability can obscure the modeler's ability to accurately assess low-flow performance. Hydrograph separation, on the other hand, offers a cleaner classification, resulting in lower variability and a more stable and reliable assessment of baseflow model performance.
3. **Better Calibration for Baseflow-Driven Processes:** In many hydrological studies, low flows are important for understanding groundwater-surface water interactions, sustaining streamflow during dry periods, and supporting aquatic habitats. Hydrograph separation allows for the explicit calibration of baseflow processes, providing a better assessment of groundwater dynamics and groundwater-fed contributions to the stream network. Without separating baseflow and stormflow, calibration based on a statistic like the lowest 50% of flows may inadvertently skew model performance assessment because a percentile-based statistic can indiscriminately include portions of stormflow recessions, rather than isolating actual sustained low flows.
4. **Alignment with Process-Based Hydrology:** Hydrograph separation aligns with a process-based understanding of hydrology, where distinct processes govern baseflow and stormflow. This approach respects the inherent differences in generation mechanisms: baseflow is usually a slower, more consistent groundwater-driven process, while stormflow is a quicker response to precipitation events. This distinction is essential for accurately simulating hydrological systems and ensuring model results that are realistic and representative of different flow conditions. Models that capture these distinct flow components are better suited for making predictions about changes in land use, climate, or other factors affecting baseflow and stormflow differently.
5. **Widely Accepted in Hydrological Modeling:** Hydrograph separation techniques are well-established and widely used in hydrological research and practice, offering a consistent framework for distinguishing between baseflow and stormflow (Arnold et al. 1995; Nathan and McMahon 1990). Techniques like those used in the United States Geological Survey (USGS) Hydrograph SEParation (HySEP) methodology provide different options for empirically parsing baseflow time series from storm flows (Sloto and Crouse 1996). The sliding interval method was used to separate both observed and simulated hydrographs at a daily timestep. This provides a consistent approach for the rollup and comparison of hydrograph components. This method is robust because they can be directly applicable to time series data as a function of the upstream drainage area.

Table 7-3. Summary of qualitative thresholds for performance metrics used to evaluate hydrology calibration

Performance Metric	Hydrological Condition	Performance Threshold for Hydrology Simulation			
		Very Good	Good	Fair	Poor
Percent Bias (PBIAS)	All Conditions [1]	<5%	5% - 10%	10% - 15%	>15%
	Seasonal Flows [2]	<10%	10% - 15%	15% - 25%	>25%
	Highest 10% of Daily Flow Rates [3]				
	Days Categorized as Storm Flow [4]				
	Days Categorized as Baseflow [4]				
RMSE – Std Dev Ratio (RSR)	All Conditions [1]	≤0.50	0.50 - 0.60	0.60 - 0.70	>0.70
	Seasonal Flows [2]	≤0.60	0.60 - 0.70	0.70 - 0.80	>0.80
Nash-Sutcliffe Efficiency (NSE)	All Conditions [1]	>0.80	0.70 - 0.80	0.50 - 0.70	≤0.50
	Seasonal Flows [2]	>0.70	0.50 - 0.70	0.40 - 0.50	≤0.40
Kling-Gupta Efficiency (KGE)	Monthly Aggregated [5]	≥0.90	0.90 - 0.75	0.75 - 0. 50	<0.50

1. All Flows considers all daily time steps in the model time series.
2. Seasonal Flows consider daily flows during a predefined, seasonal period (e.g., Wet Season and Dry Season). The Wet Season includes the months of October through April. The Dry Season includes the months of May through September.
3. Highest 10% of Flows considers the top 10% of daily flows by magnitude as determined from the observed flow duration curve.
4. Baseflows and Storm flows were determined from analyzing the daily model time series by applying the USGS hydrograph separation approach (Sloto and Crouse 1996).
5. KGE evaluated using thresholds for monthly aggregated time series (Kouchi et al. 2017).

7.2 Parameter Estimation

The model-independent Parameter ESTimation tool (PEST) is a powerful tool used for model parameter estimation, sensitivity analysis, and uncertainty analysis (Doherty 2015). It automates adjusting a specific set of model parameters within a reasonably constrained range of variability, with the objective of minimizing the differences between observed and simulated data. PEST seeks to minimize the sum of Squared Errors (SSE) across all specified observations that can be customized as needed to evaluate complete flow time series or other temporal categorizations such as flow duration intervals, monthly volumes, wet and dry periods, etc. A supervised PEST simulation helps to ensure that recommended outcomes are realistic and representative of the natural system being modeled. PEST is versatile and can be integrated with a wide range of environmental and hydrological models, including LSPC.

Sections 2 through 5 above describe model configuration and quality control methods used to represent physical characteristics of the watershed that are either directly measurable or can be reasonably estimated from available spatial or temporal data. On the other hand, parameters associated with subsurface hydrology represent one of the areas of uncertainty in the model where

optimization of model parameters can improve performance. PEST was used in conjunction with model parameterization guidance documentation (BASINS Technical Note 6 [EPA 2000]) to vary five parameters associated with subsurface hydrology: the infiltration index parameter (INFILT), the lower zone nominal storage parameter (LZSN), the upper zone nominal storage parameter (UZSN), the active groundwater recession coefficient (AGWRC), and the interflow recession coefficient (IRC).

The infiltration index parameter (INFILT) is one of the parameters optimized by PEST. Within a given hydrological soil group, TN6 guidance suggests that INFILT typically varies within minimum and maximum values shown in Table 7-4. Some model parameters are codependent. For example, TN6 recommends that the upper zone nominal storage parameter (UZSN) should first be estimated as a percentage of the lower zone nominal storage parameter (LZSN), taking into consideration other physical characteristics such as slope, vegetation cover, and depression storage, and then calibrated. Table 7-5 shows recommended initial values for UZSN as a percentage of LZSN and other physical characteristics. The active groundwater recession coefficient (AGWRC), the ratio of current groundwater discharge to that of the previous day, was the fourth parameter optimized by PEST. TN6 notes that "the overall watershed recession rate is a complex function of watershed conditions, including climate, topography, soils, and land use" that can be estimated from observed time series, and then adjusted during calibration (EPA 2000). Interflow recession coefficient (IRC), the ratio of the current daily interflow discharge to the interflow discharge on the previous day, affects the rate that interflow is discharged from storage and, therefore, the shape of the hydrograph receding limb after storm events. Model guidance and previous experience suggest that these parameters are both uncertain and very sensitive; therefore, using PEST to explore their impact and optimize performance is worthwhile and beneficial.

Table 7-4. Typical ranges by hydrological soil group for the infiltration index model parameter, INFILT

Hydrological Soil Group	INFILT Typical Ranges (in./hr)		Runoff Potential
	Low	High	
A	0.40	1.00	Low
B	0.10	0.40	Moderate
C	0.05	0.10	Moderate to High
D	0.01	0.05	High

Source: BASINS Technical Note 6 (EPA 2000)

Table 7-5. Recommended initial values for upper zone nominal storage (UZSN) as a percentage of lower zone nominal storage (LZSN) and other physical characteristics

Slope	Vegetation Cover	Depression Storage	UZSN (% of LZSN)
Very Mild	Heavy/Forest	High	14%
Moderate	Moderate	Moderate	8%
Steep	Moderate	Moderate	6%

Source: BASINS Technical Note 6 (EPA 2000)

PEST could have optimized model parameters at the HRU level (up to 97 possible degrees of freedom per parameter for previous HRUs); however, to better manage the search space, those degrees of freedom were constrained to 12 combinations of hydrological soil group (4 types) × slope (3 categories). Figure 7-4 is a schematic of HRU-level LSPC hydrology parameters with the six PEST-optimized parameters and process pathways highlighted. Table 7-6 shows the minimum and maximum parameter value ranges used to constrain PEST optimization by hydrological soil group

and slope. Table 7-7 shows the initial and final PEST-optimized estimates for subsurface process parameters, summarized by hydrological soil group and slope—the data bars show the relative magnitude of the initial and estimated parameter value within the PEST min/max range (a full cell indicates the maximum value while an empty cell indicates the minimum value). Note that initial parameter values were based on final calibrated values from the nearby Navarro River watershed model (SWRCB 2025), with the exception of the slope-based boundaries for UZSN and the initial INFILT values, which were adjusted toward the upper bound to increase baseflow as part of the iterative PEST configuration workflow.

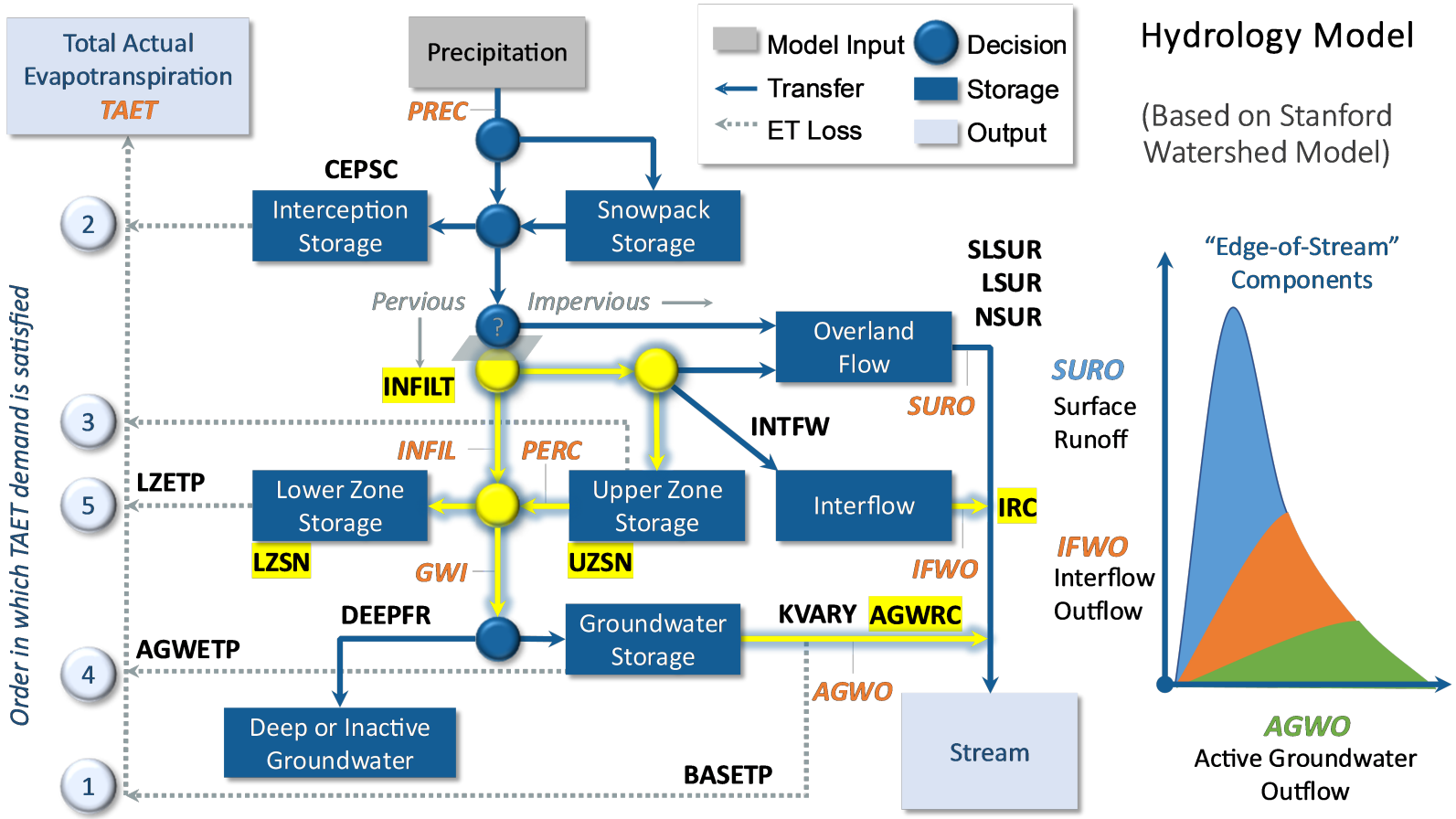

PEST: LSPC parameters and process optimized by Parameter Estimation (PEST) during hydrology calibration.

Figure 7-4. HRU-level LSPC hydrology parameters with PEST-optimized parameters and process pathways highlighted.

Table 7-6. Minimum and maximum parameter value ranges used to constrain PEST optimization, by hydrological soil group and slope

HSG	Slope	Area (ac)	Area (%)	LZSN		INFILT		AGWRC		UZSN (% LZSN)		IRC	
				Min	Max	Min	Max	Min	Max	Min	Max	Min	Max
A	Low	0.0	0.0%	2	15	0.4	1	0.85	0.999	10	17	0.3	0.85
A	Med	0.0	0.0%	2	15	0.4	1	0.85	0.999	6	12	0.3	0.85
A	High	0.0	0.0%	2	15	0.4	1	0.85	0.999	4	8	0.3	0.85
B	Low	687.3	1.5%	2	15	0.1	0.4	0.85	0.999	10	17	0.3	0.85
B	Med	2,457.8	5.4%	2	15	0.1	0.4	0.85	0.999	6	12	0.3	0.85
B	High	33,708.7	74.3%	2	15	0.1	0.4	0.85	0.999	4	8	0.3	0.85
C	Low	125.0	0.3%	2	15	0.05	0.1	0.85	0.999	10	17	0.3	0.85
C	Med	759.4	1.7%	2	15	0.05	0.1	0.85	0.999	6	12	0.3	0.85
C	High	7,646.8	16.8%	2	15	0.05	0.1	0.85	0.999	4	8	0.3	0.85
D	Low	0.0	0.0%	2	15	0.001	0.05	0.85	0.999	10	17	0.3	0.85
D	Med	0.0	0.0%	2	15	0.001	0.05	0.85	0.999	6	12	0.3	0.85
D	High	0.0	0.0%	2	15	0.001	0.05	0.85	0.999	4	8	0.3	0.85
PEST Subtotal[1]		**45,385.0**	**99.9%**	--	--	--	--	--	--	--	--	--	--

1. PEST subtotal based on area draining to the Mattole River near Ettersburg, CA USGS station (11468900).

Color Gradient: Lowest | Low | Med | High | Highest

Table 7-7. Initial and final PEST optimized estimates for subsurface process parameters, summarized by hydrological soil group and slope for the Mattole River near Ettersburg, CA USGS station (11468900)

HSG	Slope	Area (ac)	Area (%)	LZSN		INFILT[1]		AGWRC		UZSN (% LZSN)[2]		UZSN		IRC	
				Initial	Estimated	Initial	Estimated	Initial	Estimated	Initial	Estimated	Initial	Estimated	Initial	Estimated
A	Low	0.0	0.0%	10.18	10.18	0.990	0.990	0.85	0.850	14.00	14.00	1.43	1.43	0.65	0.65
A	Med	0.0	0.0%	10.18	10.18	0.990	0.990	0.85	0.850	8.00	8.00	0.81	0.81	0.65	0.65
A	High	0.0	0.0%	10.18	10.18	0.990	0.990	0.85	0.850	6.00	6.00	0.61	0.61	0.65	0.65
B	Low	687.3	1.5%	12.50	7.76	0.390	0.183	0.95	0.937	14.00	8.69	1.75	0.67	0.58	0.47
B	Med	2,457.8	5.4%	12.50	7.76	0.390	0.183	0.95	0.937	8.00	4.97	1.00	0.39	0.58	0.47
B	High	33,708.7	74.3%	12.50	7.76	0.390	0.183	0.95	0.937	6.00	3.73	0.75	0.29	0.58	0.47
C	Low	125.0	0.3%	15.00	10.95	0.099	0.100	0.97	0.987	14.00	10.22	2.10	1.12	0.57	0.48
C	Med	759.4	1.7%	15.00	10.95	0.099	0.100	0.97	0.987	8.00	5.84	1.20	0.64	0.57	0.48
C	High	7,646.8	16.8%	15.00	10.95	0.099	0.100	0.97	0.987	6.00	4.38	0.90	0.48	0.57	0.48
D	Low	0.0	0.0%	15.00	15.00	0.050	0.049	0.85	0.850	14.00	14.00	2.10	2.10	0.35	0.35
D	Med	0.0	0.0%	15.00	15.00	0.050	0.049	0.85	0.850	8.00	8.00	1.20	1.20	0.35	0.35
D	High	0.0	0.0%	15.00	15.00	0.050	0.049	0.85	0.850	6.00	6.00	0.90	0.90	0.35	0.35
PEST Subtotal		**45,385.0**	**99.9%**	–	–	–	–	–	–	–	–	–	–	–	–

1. Note that the initial INFILT values were updated towards the upper bound compared to the values adopted from the Navarro River watershed model to increase baseflow.
2. Note that the UZSN ranges were updated compared to the initial values adopted from the Navarro River watershed model.

Data Bars Show the relative magnitude of the parameter values within the PEST min/max ranges (See Table 7-6).

Color Gradient: Lowest | Low | Med | High | Highest

7.2.1 Additional Parameter Calibration

The second phase of calibration included applying the PEST estimated parameters model-wide, evaluating initial model performance, and then making additional parameter adjustments as needed. As illustrated by the flow duration curve (FDC) in Figure 7-5, the PEST estimated parameter values provide a high degree of correspondence between simulated and observed flow at the Ettersburg station during the calibration period. Using these parameters for the larger Petrolia drainage area, however, resulted in consistent overprediction of flows across the FDC (Figure 7-6). Therefore, several additional parameters were fine-tuned to achieve an acceptable calibration at the Petrolia station while maintaining performance at the Ettersburg station.

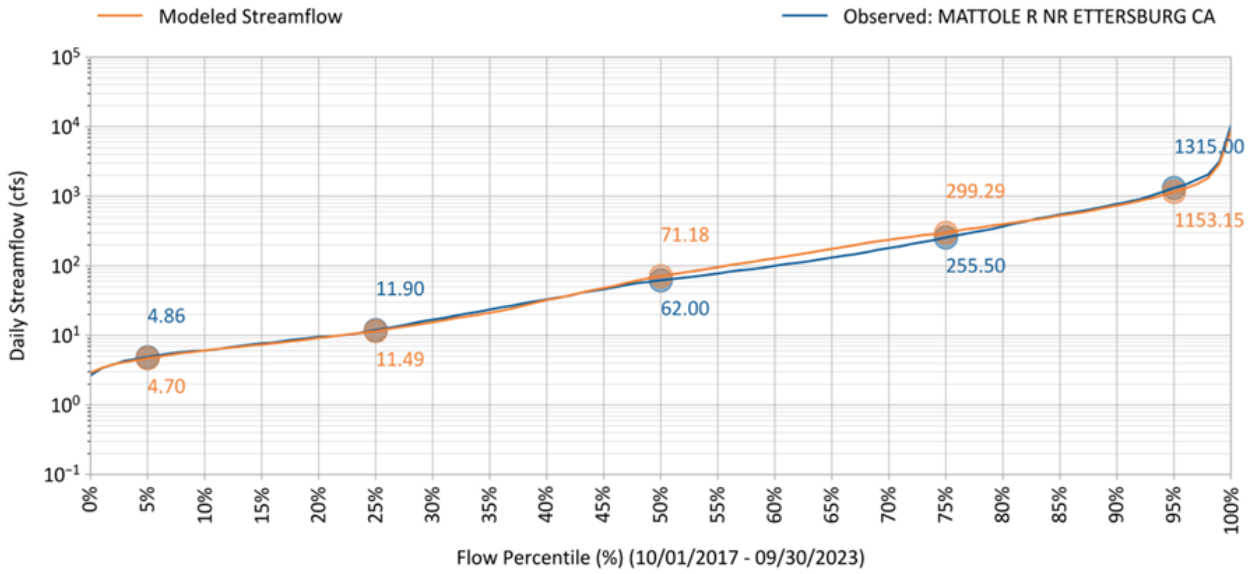

Figure 7-5. Simulated vs. observed flow duration curve from the calibration period for the MATTOLE R NR ETTERSBURG CA (11468900) using PEST estimated parameter values.

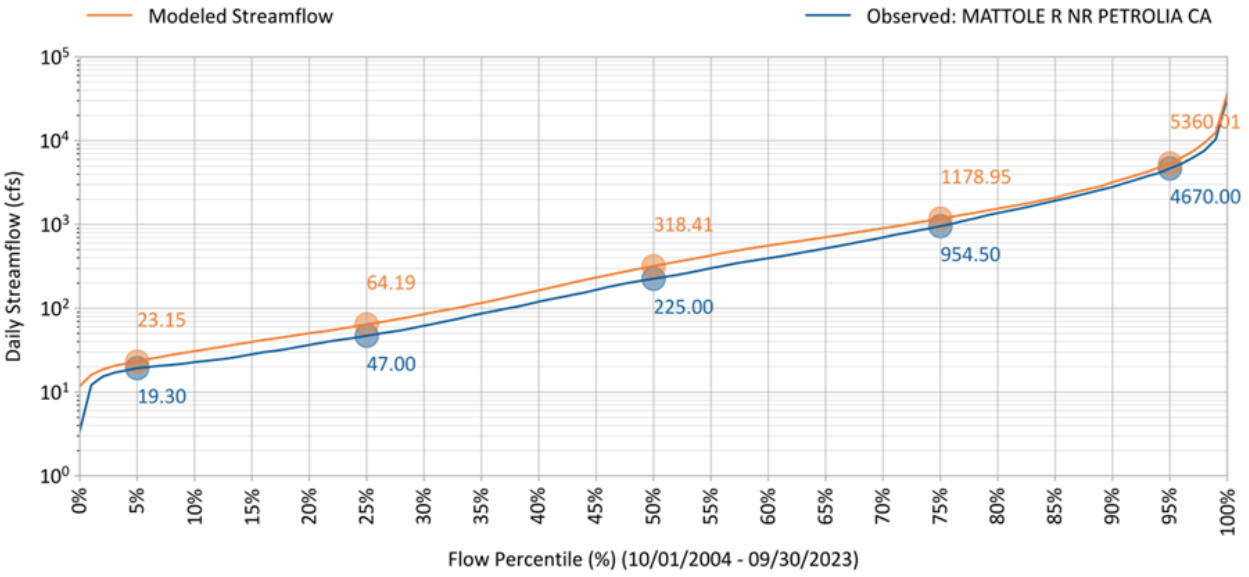

Figure 7-6. Simulated vs. observed flow duration curve from the entire modeling period for the MATTOLE R NR PETROLIA CA (11469000) using PEST estimated parameter values from the Ettersburg station.

After applying the PEST estimated parameters, the differences in model performance between the Ettersburg and Petrolia stations suggested that there was too much water in the system between the two stations. Therefore, forest HRU parameters were further calibrated, ET from riparian vegetation was configured in the model, and the lower zone soil moisture storage and ET were adjusted. The assigned precipitation stations were also reviewed to check for rainfall biases. The main objective behind these model refinements was to reduce the simulated flow volumes and increase the simulated ET at the Petrolia station. The rationale for these adjusted parameters is described below.

1. **Reconfiguration of precipitation stations near Honeydew**: Precipitation forcing inputs, which can be highly variable even over short distances, represent the baseline of available water to the hydrology model, and play a large role in the ability of the model to accurately represent observed streamflow. Associated gauge assignments were evaluated as a contributing factor to the difference in flow simulation performance between the Ettersburg and Petrolia stations. Within the Petrolia area downstream of Ettersburg, there are two precipitation stations within 3 miles of each other near Honeydew, CA: GHCND US1CAHM0070 and CDEC HNY. As seen in Figure 4-3, this GHCN station has the highest annual precipitation totals in the watershed, with some years near 200in and approximately 50in greater than the nearby HNY station. While this GHCN station is at a higher elevation than the HNY station, and may be particularly influenced by the strong orographic effect of the King Range mountains, its records start in July 2016 (Table 4-1). Because using that gauge may have introduced a higher precipitation bias for disproportionately more of the drainage area, catchments within the Petrolia drainage area that were originally assigned to the GHCN station were reassigned to the HNY station, which has a period of record covering the entire model period. This change reduced the annual precipitation volume within the Petrolia drainage area by 66,600 ac-ft (5.4%) on average and represented a lower, more representative baseline for further parameter refinements.
2. **Reconfiguration of Forest HRU area**: As discussed in Section 3.5.3, the distribution of Douglas-fir was used to better capture the footprint of forests within the watershed as a snapshot of recovery from extensive logging from the 1950s and 1960s. As shown in Table 7-8, the Ettersburg drainage area, which was predominately forest, only saw an increase of 1.2% when Douglas fir area was introduced. On the other hand, for the Petrolia drainage area below Ettersburg, forest area increased by 6.3% with the inclusion of Douglas fir (Table 7-9). This is primarily due to the conversion of grassland (-9%) and scrub (-44%) to forest. Adding Douglas fir increased the percentage of forest in the Petrolia drainage area from 76.5% to 81.3%. This in turn increased interception and ET opportunity, consistent with the objectives of water balance refinement.

Table 7-8. Change in land use / land cover HRU groups for NLCD with and without Douglas fir forest for the Ettersburg drainage area

LULC Group	NLCD (acres)	NLCD (%)	NLCD + Douglas Fir (acres)	NLCD + Douglas Fir (%)	Change (%)
Developed_Low_Intensity	107.9	0.2%	107.9	0.2%	0.0%
Developed_Medium_Intensity	64.0	0.1%	64.0	0.1%	0.0%
Developed_High_Intensity	11.8	0.0%	11.8	0.0%	0.0%
Developed_Open_Space	2,047.4	4.5%	2,047.4	4.5%	0.0%
Developed_Impervious	0.0	0.0%	0.0	0.0%	--
Developed_Pervious	0.0	0.0%	0.0	0.0%	--
Barren	0.0	0.0%	0.0	0.0%	--
Forest	41,338.8	91.0%	41,851.9	92.1%	1.2%
Scrub	1,138.4	2.5%	689.6	1.5%	-39.4%
Grassland	408.3	0.9%	348.9	0.8%	-14.5%
Pasture	324.5	0.7%	320.5	0.7%	-1.2%
Agriculture	3.8	0.0%	2.9	0.0%	-23.5%
Water	3.1	0.0%	3.1	0.0%	0.0%
Total	**45,448.0**	**100.0%**	**45,448.0**	**100.0%**	**--**

Table 7-9. Change in land use / land cover HRU groups for NLCD with and without Douglas fir forest for the Petrolia drainage area, excluding the nested Ettersburg station drainage area

LULC Group	NLCD (acres)	NLCD (%)	NLCD + Douglas Fir (acres)	NLCD + Douglas Fir (%)	Change (%)
Developed_Low_Intensity	363.2	0.3%	363.2	0.3%	0.0%
Developed_Medium_Intensity	173.0	0.2%	173.0	0.2%	0.0%
Developed_High_Intensity	28.7	0.0%	28.7	0.0%	0.0%
Developed_Open_Space	3,933.5	3.5%	3,932.6	3.5%	0.0%
Developed_Impervious	0.0	0.0%	0.0	0.0%	--
Developed_Pervious	0.0	0.0%	0.0	0.0%	--
Barren	489.3	0.4%	481.9	0.4%	-1.5%
Forest	85,708.4	76.5%	91,110.4	81.3%	6.3%
Scrub	11,164.6	10.0%	6,219.9	5.5%	-44.3%
Grassland	4,140.5	3.7%	3,758.7	3.4%	-9.2%
Pasture	6,049.1	5.4%	5,983.1	5.3%	-1.1%
Agriculture	28.9	0.0%	27.8	0.0%	-3.8%
Water	4.0	0.0%	4.0	0.0%	0.0%
Total	**112,083.2**	**100.0%**	**112,083.2**	**100.0%**	--

Change (%): -100% | No Change | 100%

Drainage Area (%): Lowest | Low | Med | High | Highest

3. **Lower and Upper Zone Nominal Soil Moisture Storage (LZSN and UZSN)**: LZSN, which represents the primary soil moisture storage and root zone of the soil profile, was increased for HSG-B and C by 2in from the PEST estimated values of 7.76 and 10.95, respectively. USZN was correspondingly updated for these soil groups to maintain the UZSN:LZSN ratios shown in Table 7-7. These changes allow for additional storage of water in the upper and lower soil zones and, therefore, additional ET opportunities.
4. **Forest interception and ET**: The Mattole River watershed is known to have higher than typical forest density due to industrial logging and fire suppression practices which have led to higher forest ET volumes that contribute to lower dry season flows (California State Coastal Conservancy 2018; Stubblefield et al. 2011; Stubblefield and Reddy 2022). To better represent these conditions, Forest HRUs were updated to use an increased Interception Storage Capacity (CEPSC) value and monthly Lower Zone Evapotranspiration Index (LZETP) values. CEPSC — which controls the amount of rainfall which is retained by vegetation, never reaches the land surface, and is eventually evaporated — was increased from 0.15in to 0.3in. LZETP controls ET from the lower soil zone and is primarily a function of vegetation (see Table 7-10). Monthly values of LZETP were developed by scaling against the monthly average PET for the Ettersburg drainage area, as shown in Figure 7-7.

Table 7-10. Typical ranges for lower zone evapotranspiration parameter, LZETP

Land Use/Land Cover	Typical LZETP (coefficient): Low	Typical LZETP (coefficient): High
Forest	0.60	0.80
Grassland	0.40	0.60
Row crops	0.50	0.70
Barren	0.10	0.40
Wetlands	0.60	0.90

Source: BASINS Technical Note 6 (EPA 2000)

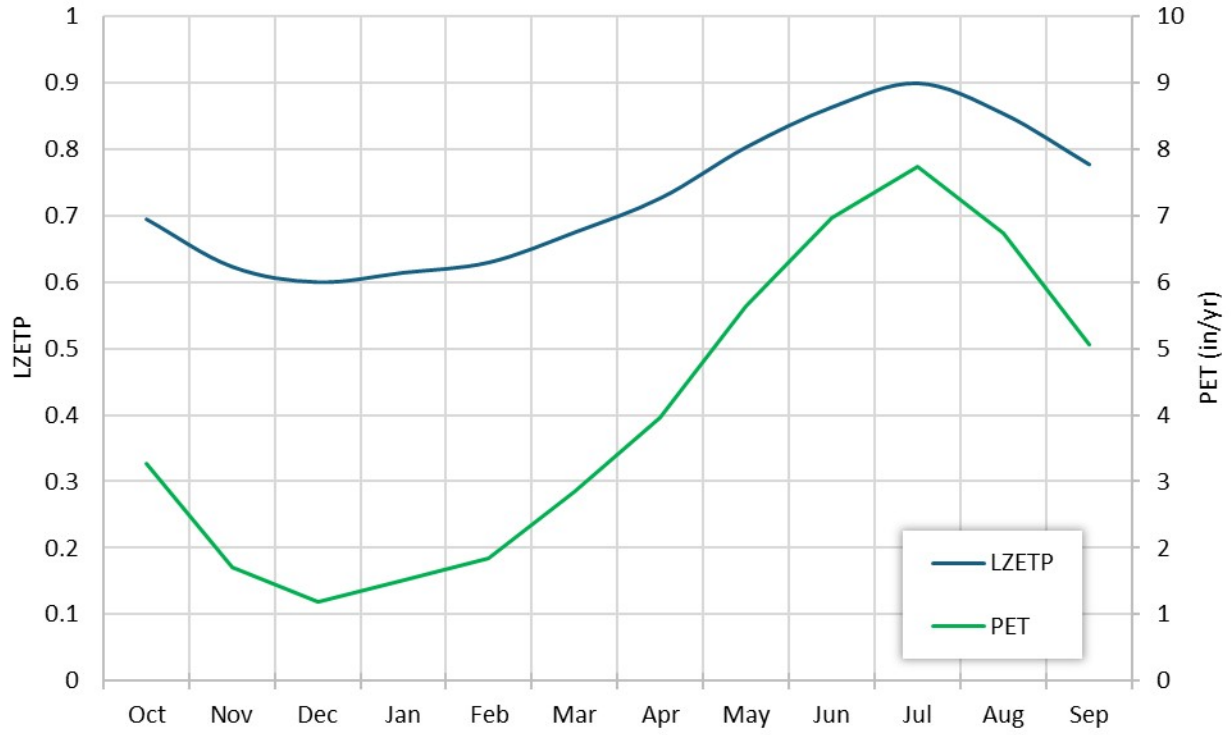

Figure 7-7. Monthly LZETP for Forest HRUs and monthly average PET for the Ettersburg drainage area.

5. **Riparian Evapotranspiration (Riparian ET)**: Riparian ET was estimated to represent the ET losses from riparian corridors. Examination of the NLCD land cover data indicated that the Petrolia drainage area had a higher percentage of wetlands (over 1,000 ac or 0.9%) where riparian ET is expected to be high compared to the 0.2% of wetland area in the Ettersburg drainage area (Table 7-11). Wetlands are not explicitly represented by an HRU; therefore, riparian ET was proportionally configured for stream segments in catchments with NLCD wetland area. In these catchments, it was assumed that wetlands are always along the edge of the stream segment. Riparian width (RIPWID) and fraction of Riparian Cover (RIPCOV) were back-calculated from wetland area and stream length (LEN) using this equation: wetland area = LEN×RIPWID×RIPCOV with RIPCOV ranging from 0-1. The total wetland area in the Mattole River watershed was 2,460 acres, of which 2,292 was converted into riparian areas. Riparian ET was not applied for the remaining 168 acres because they were in smaller catchments with no simulated stream segment. Figure 7 8 is a distribution plot of wetland area along modeled stream length, which was used to model riparian ET. About 40% of total stream length had nearby wetland area ranging from 0.2 acres to 112 acres.

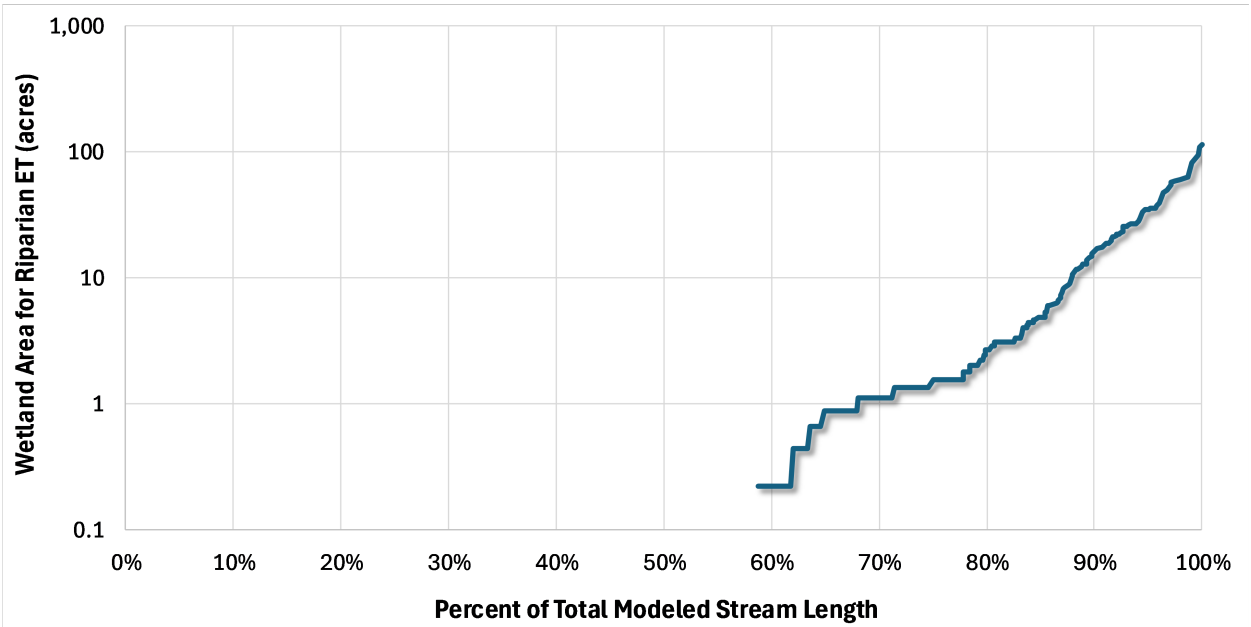

Figure 7-8. Distribution of wetland area along modeled stream length used for riparian ET.

Table 7-11. Comparison of NLCD wetland classes between the Ettersburg and Petrolia drainage areas

Drainage Area Name	Woody Wetlands (acres)	Emergent Herbaceous Wetlands (acres)	Total Wetlands (acres)	Drainage Area (%)
Ettersburg	52.3	41.1	93.4	0.2%
Petrolia (excluding Ettersburg)	177.9	848.9	1,026.8	0.9%

7.3 Calibration Results

Using the final calibrated parameters, the model was run for water years 2018 through 2023 and calibration performance was evaluated. Note that all results presented below exclude observed flows < 1 cfs, where there may be more uncertainty in gauge readings.

7.3.1 Upstream – Mattole River near Ettersburg

Because model parameters were adjusted to balance performance at both the Ettersburg and Petrolia stations (which had overprediction), flows at Ettersburg for the calibration period are slightly underpredicted. As shown in Table 7-12, performance across the calibration period was "Good" for PBIAS with simulated flow volumes underpredicted by 9%. Much of this underprediction is driven by underprediction of the highest 10% of flows ("Fair") and stormflows ("Fair"), which predominately occur during the wet season ("Good"). PBIAS during the dry season and for baseflow, which are especially important given the purposes of this model, were "Very Good" with slight underprediction of 1% and 2%, respectively. RSR and NSE performance was "Very Good" to "Good" across the entire calibration period and seasons. KGE (calculated with monthly flow values) was "Good" across the entire calibration period and wet season and "Very Good" for the dry season. These metric values indicate the model is performing reasonably well at capturing the observed volume (PBIAS) and trends in wet and dry season flow (RSR, NSE, KGE) for this specific time period and drainage area.

Table 7-13 is a summary of model calibration performance metrics computed using monthly time series, as recommended by Moriasi et al. (2015). As expected, PBIAS is not impacted by the time step change, however, RSR and NSE both show notable improvement in performance compared to using daily average time series.

Table 7-12. Summary of daily calibration performance metrics for MATTOLE R NR ETTERSBURG CA (11468900)

Hydrology Monitoring Locations	Performance Metrics (10/01/2017 - 09/30/2023)														
	PBIAS						RSR			NSE			KGE[1]		
	All	Wet Season	Dry Season	>10th %ile Flows	Storm Flows	Baseflow	All	Wet Season	Dry Season	All	Wet Season	Dry Season	All	Wet Season	Dry Season
MATTOLE R NR ETTERSBURG CA	9.4%	10.2%	1.0%	18.5%	15.9%	2.2%	0.41	0.43	0.6	0.83	0.81	0.64	0.83	0.82	0.97

[1] Monthly, as specified in Table 7-3.

Table 7-13. Summary of calibration performance metrics using monthly total volume at MATTOLE R NR ETTERSBURG CA (11468900)

Calibration Metrics for Monthly Flow (10/01/2017 - 09/30/2023)	Hydrological Condition		
	All (n = 72)	Wet Season (n = 42)	Dry Season (n = 30)
Percent Bias (PBIAS)	9.4%	10.2%	1.0%
Nash-Sutcliffe Efficiency (NSE)	0.95	0.94	0.98
RMSE-Std-Dev. Ratio (RSR)	0.21	0.25	0.14
Kling–Gupta Efficiency (KGE)	0.83	0.82	0.97

Very Good Good Fair Poor
\- Overpredicts + Underpredicts

Examination of daily and normalized monthly streamflow (Figure 7-9 and Figure 7-10, respectively) shows that, as indicated by the metrics, the most extreme peaks are underestimated, but general rising/falling patterns in the hydrographs are well captured. Figure 7-11 and Figure 7-12 present the interquartile ranges and averages, respectively, of monthly normalized flow—both show a high degree of correspondence between observed and simulated values and illustrate the wet season underprediction. The highest flows at the beginning of the Wet season (especially January and December) show the most underprediction, but the spring flows at the end of the Wet season and dry season flows are well matched. The FDC shown in Figure 7-13 indicates that observed flow regime trends are generally well matched by the model. Below the 50th percentile, modeled flows are slightly lower than observed, which is conservative for the purposes of the model; it should be noted that

modeled and observed FDCs are calculated independently, and flows of the same percentile do not necessarily occur at the same time.

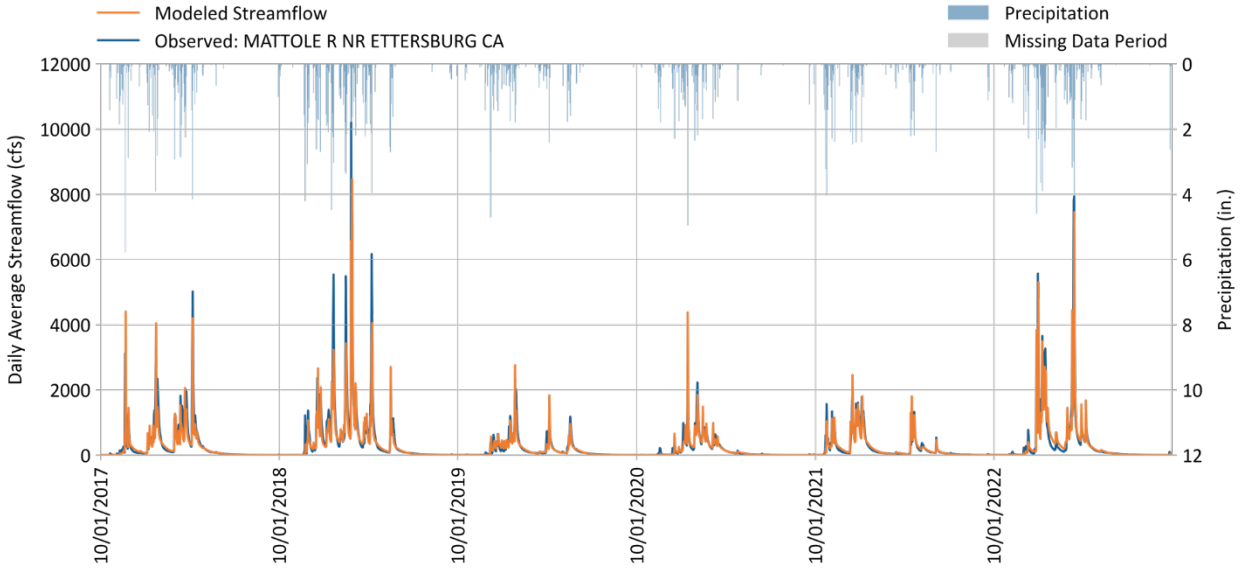

Figure 7-9. Daily simulated vs. observed streamflow for MATTOLE R NR ETTERSBURG CA (11468900).

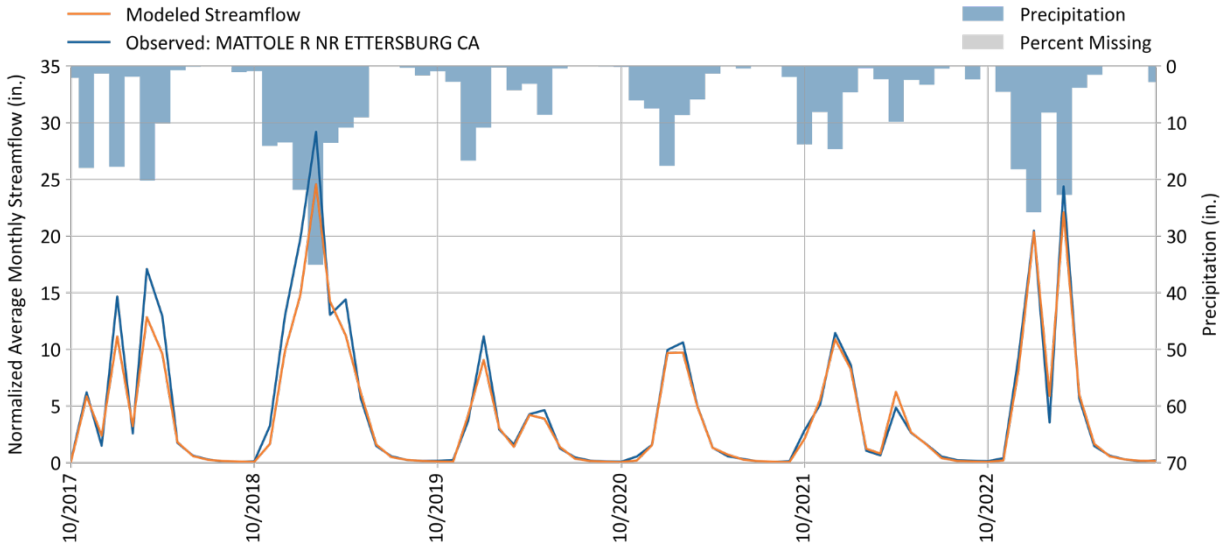

Figure 7-10. Monthly simulated vs. observed streamflow for MATTOLE R NR ETTERSBURG CA (11468900).

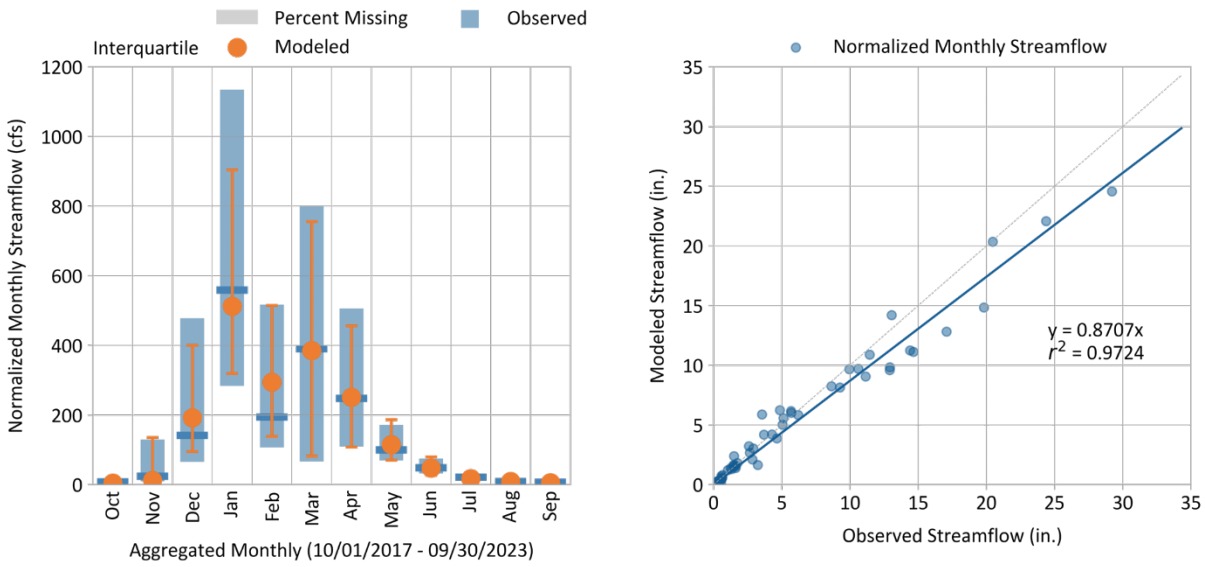

Figure 7-11. Monthly normalized simulated vs. observed streamflow for MATTOLE R NR ETTERSBURG CA (11468900).

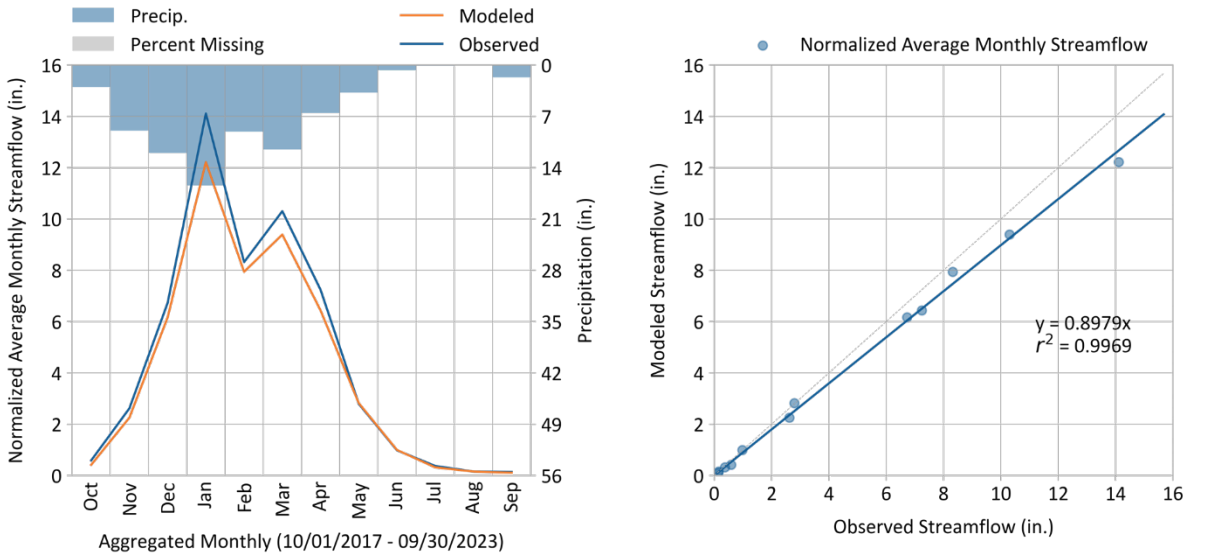

Figure 7-12. Average monthly simulated vs. observed streamflow for MATTOLE R NR ETTERSBURG CA (11468900).

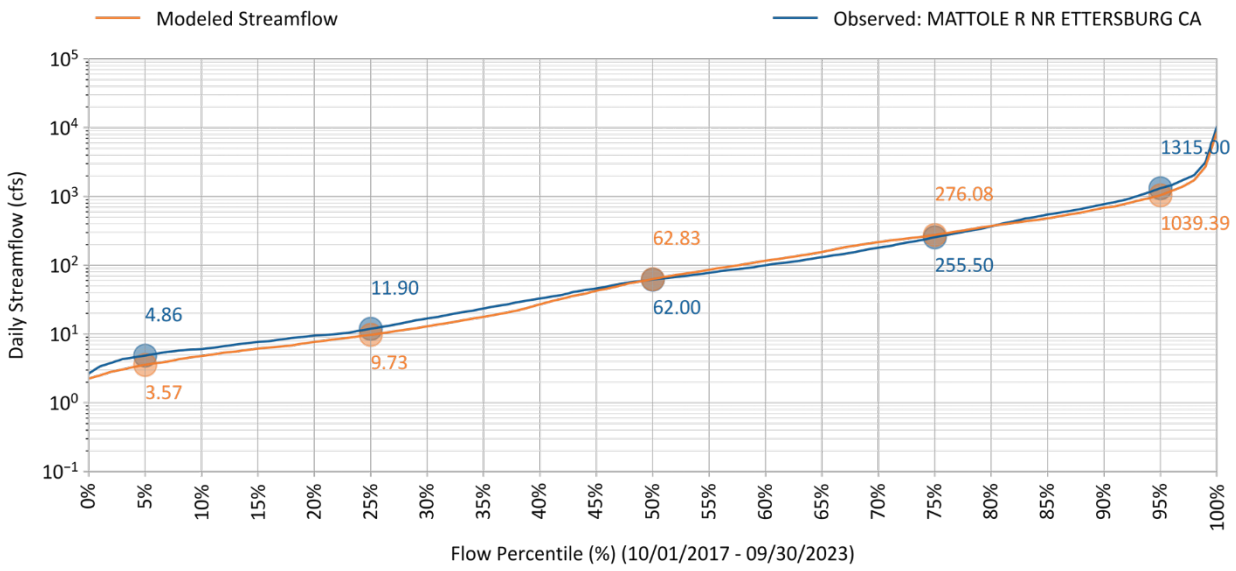

Figure 7-13. Simulated vs. observed flow duration curve for MATTOLE R NR ETTERSBURG CA (11468900).

PBIAS, NSE, and RSR performance values by season and flow regime are shown in Table 7-14, Table 7-15, and Table 7-16, respectively; the count of values used to calculate each of these metrics is provided in Table 7-17. The "Days Categorized as Baseflow" metric, which is derived from hydrograph separation, consistently shows "Very Good" model performance across all conditions and all metrics. The other metrics are consistent with the performance discussed above, with intentional underprediction of wet-weather flows to balance satisfactory performance across all flow regimes at the larger Petrolia station downstream. Wet and dry season daily hydrographs for water year 2021 are provided in Figure 7-14 and Figure 7-15 respectively, to illustrate model performance during drought conditions (5th percentile total yearly precipitation based on the water year 2005-2023 period as shown in Table 6-2).

Table 7-14. Simulated vs. observed daily streamflow PBIAS at MATTOLE R NR ETTERSBURG CA (11468900)

Calibration Metrics *(10/01/2017 - 09/30/2023)*	Percent Bias (PBIAS)		
	All Seasons	Wet Season	Dry Season
All Conditions	9.4%	10.2%	1.0%
Highest 10% of Daily Flow Rates	18.5%	18.8%	3.4%
Days Categorized as Storm Flow	15.9%	16.6%	-0.5%
Days Categorized as Baseflow	2.2%	2.3%	1.7%

Table 7-15. Simulated vs. observed daily streamflow NSE at MATTOLE R NR ETTERSBURG CA (11468900)

Calibration Metrics *(10/01/2017 - 09/30/2023)*	Nash-Sutcliffe Efficiency (NSE)		
	All Seasons	Wet Season	Dry Season
All Conditions	0.83	0.81	0.64
Highest 10% of Daily Flow Rates	0.61	0.62	-26.46
Days Categorized as Storm Flow	0.78	0.77	0.45
Days Categorized as Baseflow	0.91	0.9	0.89

Table 7-16. Simulated vs. observed daily streamflow RSR at MATTOLE R NR ETTERSBURG CA (11468900)

Calibration Metrics *(10/01/2017 - 09/30/2023)*	RMSE-Std-Dev. Ratio (RSR)		
	All Seasons	Wet Season	Dry Season
All Conditions	0.41	0.43	0.6
Highest 10% of Daily Flow Rates	0.62	0.62	5.24
Days Categorized as Storm Flow	0.46	0.48	0.74
Days Categorized as Baseflow	0.29	0.31	0.34

Very Good Good Fair Poor
\- Overpredicts + Underpredicts

Table 7-17. Count of values used to calculate daily calibration metrics at MATTOLE R NR ETTERSBURG CA (11468900)

Calibration Metrics *(10/01/2017 - 09/30/2023)*	Data Count		
	All Seasons	Wet Season	Dry Season
All Conditions	2191	1273	918
Highest 10% of Daily Flow Rates	219	211	8
Days Categorized as Storm Flow	710	509	201
Days Categorized as Baseflow	1481	764	717

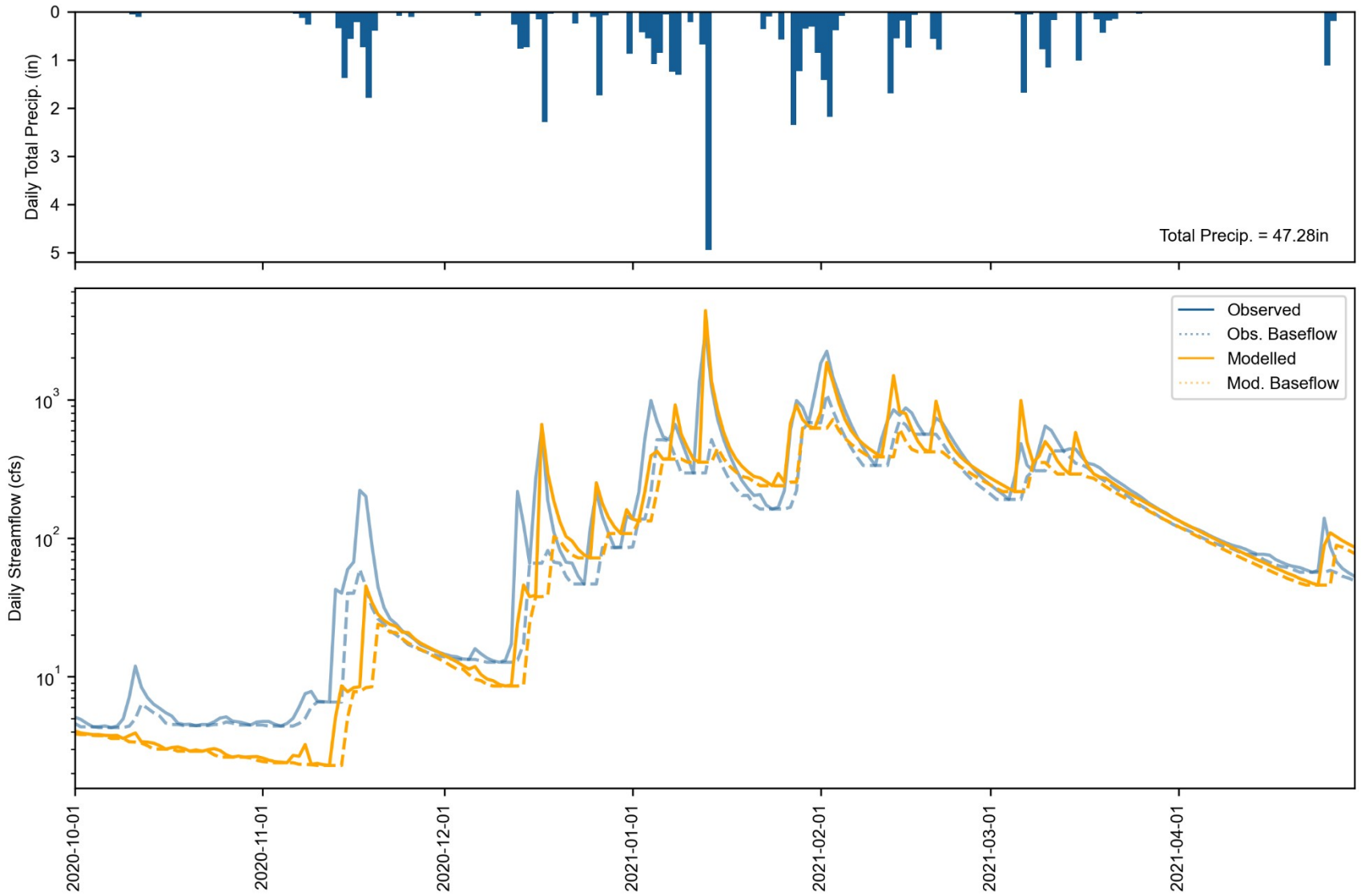

Figure 7-14. Water Year 2021 Wet season daily total precipitation (top) and streamflow (bottom) at MATTOLE R NR ETTERSBURG CA (11468900). Observed and simulated baseflow are calculated with HYSEP.

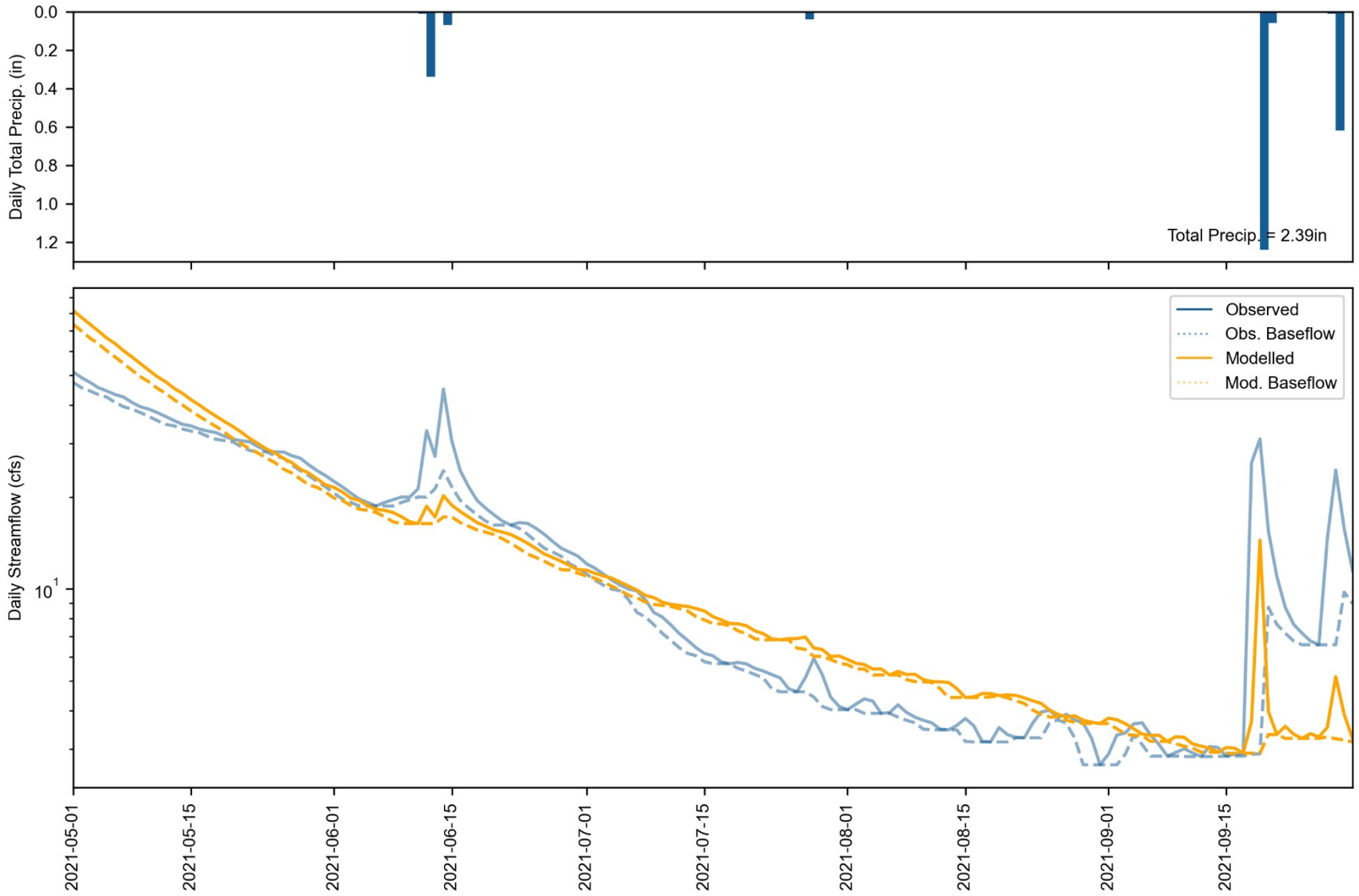

Figure 7-15. Water Year 2021 Dry season daily total precipitation (top) and streamflow (bottom) at MATTOLE R NR ETTERSBURG CA (11468900). Observed and simulated baseflow are calculated with HYSEP.

7.3.2 Downstream – Mattole River near Petrolia

In contrast to the Ettersburg station, flows at the Petrolia station for the calibration period are somewhat overpredicted. As shown in Table 7-18, model performance across the calibration period was "Very Good" for PBIAS with simulated flow volumes overpredicted by 4.5%. Much of this is driven by overprediction of dry season stormflows, as further detailed in Table 7-20, which represent a relatively small portion of total flow volume. Overall, PBIAS for baseflow was "Very Good" with slight overprediction of 5.6%. RSR and NSE performance was "Very Good" across the entire calibration period and the wet season and "Good" during the dry season. KGE (calculated with monthly flow values) was also "Very Good" across the entire calibration period and wet season and "Fair" for the dry season.

Table 7-19 is a summary of model calibration performance metrics computed using monthly time series, as recommended by Moriasi et al. (2015). As expected, PBIAS is not impacted by the time step change, however, RSR and NSE both show notable improvement in performance compared to using daily average time series.

Table 7-18. Summary of daily calibration performance metrics for MATTOLE R NR PETROLIA CA (11469000)

Hydrology Monitoring Locations	Performance Metrics (10/01/2017 - 09/30/2023)														
	PBIAS						RSR			NSE			KGE[1]		
	All	Wet Season	Dry Season	>10th %ile Flows	Storm Flows	Baseflow	All	Wet Season	Dry Season	All	Wet Season	Dry Season	All	Wet Season	Dry Season
MATTOLE R NR PETROLIA CA	-4.5%	-2.7%	-24.7%	2.7%	-3.7%	-5.6%	0.27	0.28	0.61	0.93	0.92	0.62	0.94	0.94	0.61

[1] Monthly, as specified in Table 7-3.

Table 7-19. Summary of calibration performance metrics using monthly total volume at MATTOLE R NR PETROLIA CA (11469000)

Calibration Metrics for Monthly Flow (10/01/2017 - 09/30/2023)	Hydrological Condition		
	All (n = 72)	Wet Season (n = 42)	Dry Season (n = 30)
Percent Bias (PBIAS)	-4.5%	-2.7%	-24.7%
Nash-Sutcliffe Efficiency (NSE)	0.98	0.97	0.76
RMSE-Std-Dev. Ratio (RSR)	0.16	0.17	0.49
Kling–Gupta Efficiency (KGE)	0.94	0.94	0.61

Very Good Good Fair Poor
\- Overpredicts + Underpredicts

Examination of daily and normalized monthly streamflow (Figure 7-16 and Figure 7-17, respectively) shows that, as indicated by the metrics, peak flows and the general rising/falling patterns in the hydrographs are well captured. Figure 7-18 and Figure 7-19 present the interquartile ranges and averages, respectively, of monthly normalized flow—both show a high degree of correspondence between observed and simulated values and illustrate the slight overprediction of spring flows that carries into the dry season. The FDC shown in Figure 7-20 indicates that observed flow regime trends are generally well matched by the model. Below the 10th percentile, modeled flows are slightly lower than observed; it should be noted that modeled and observed FDCs are calculated independently, and flows of the same percentile do not necessarily occur at the same time.

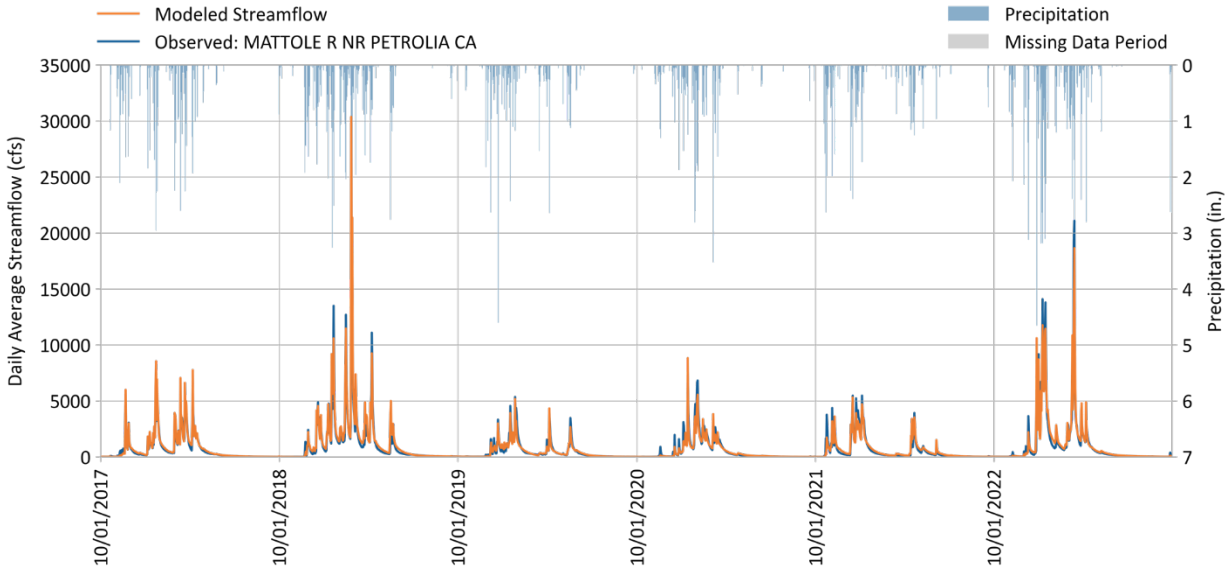

Figure 7-16. Daily simulated vs. observed streamflow for MATTOLE R NR PETROLIA CA (11469000).

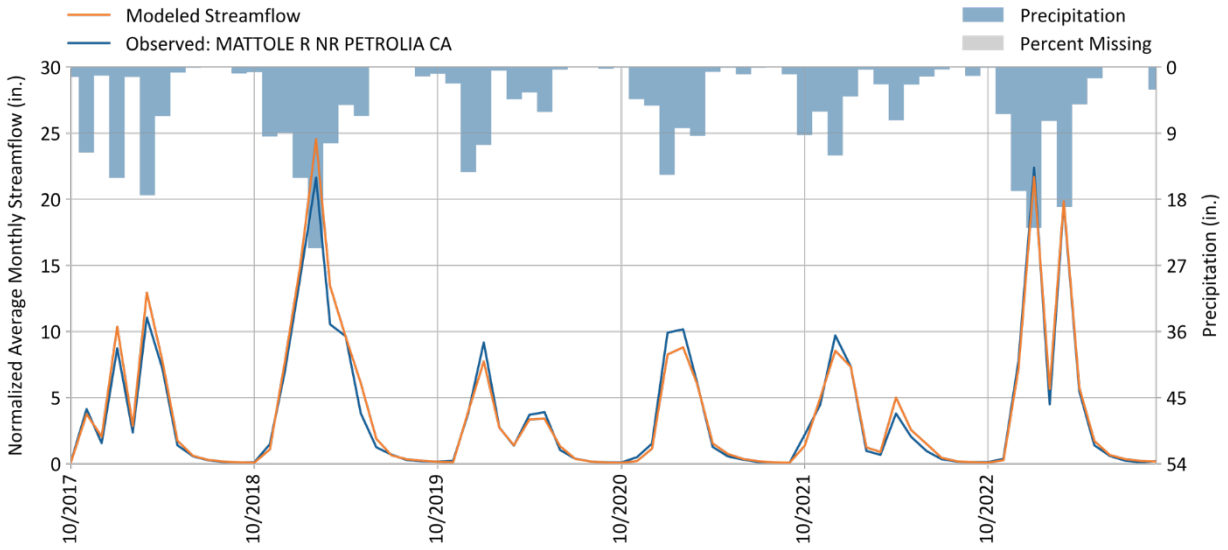

Figure 7-17. Monthly simulated vs. observed streamflow for MATTOLE R NR PETROLIA CA (11469000).

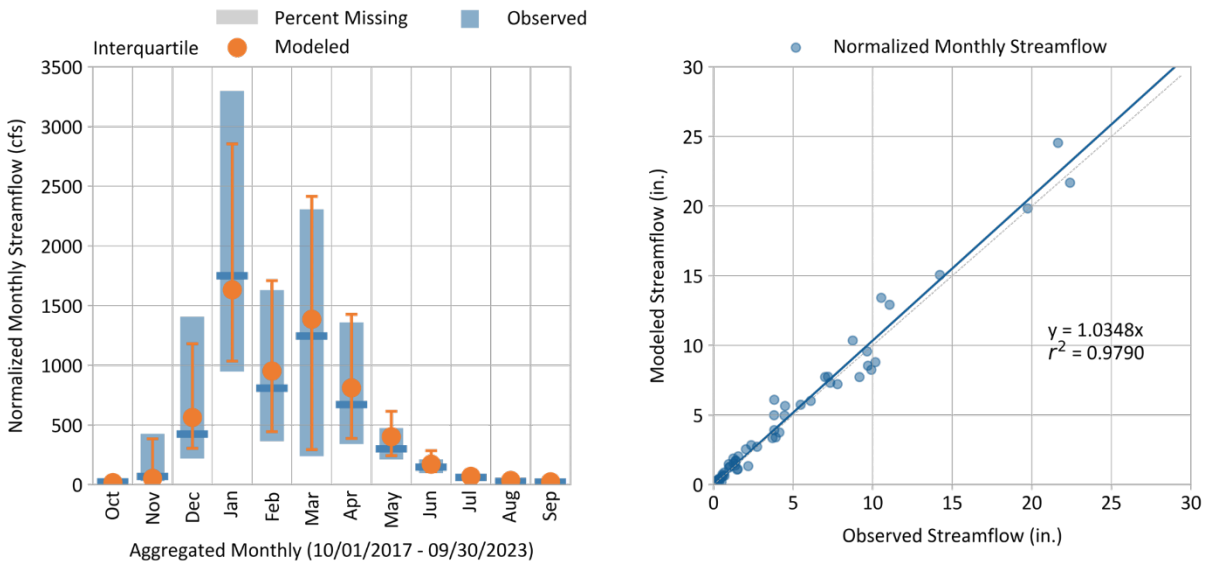

Figure 7-18. Monthly normalized simulated vs. observed streamflow for MATTOLE R NR PETROLIA CA (11469000).

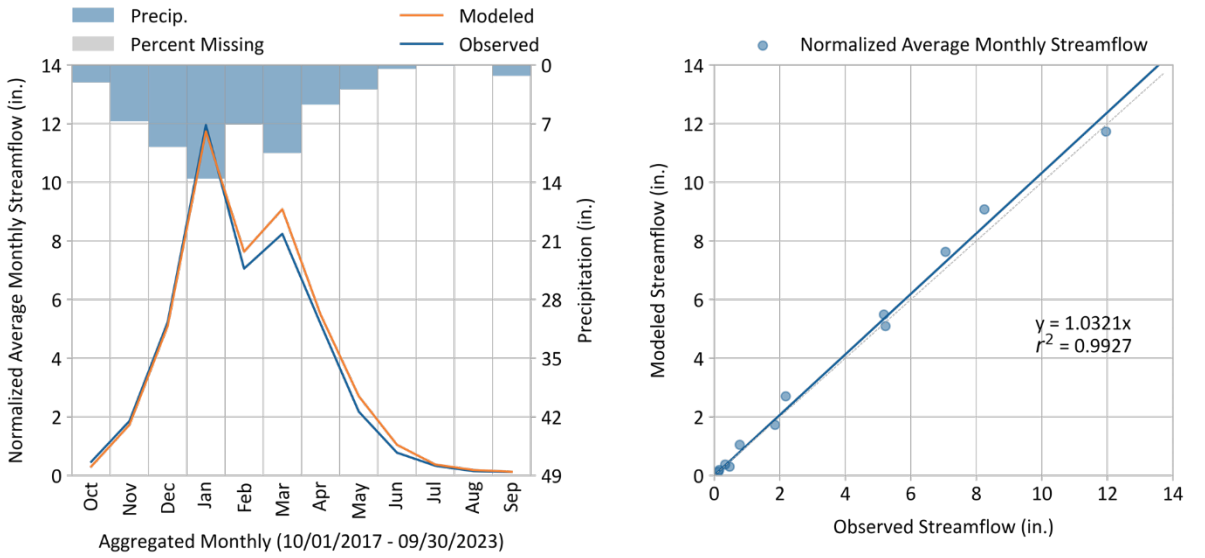

Figure 7-19. Average monthly simulated vs. observed streamflow for MATTOLE R NR PETROLIA CA (11469000).

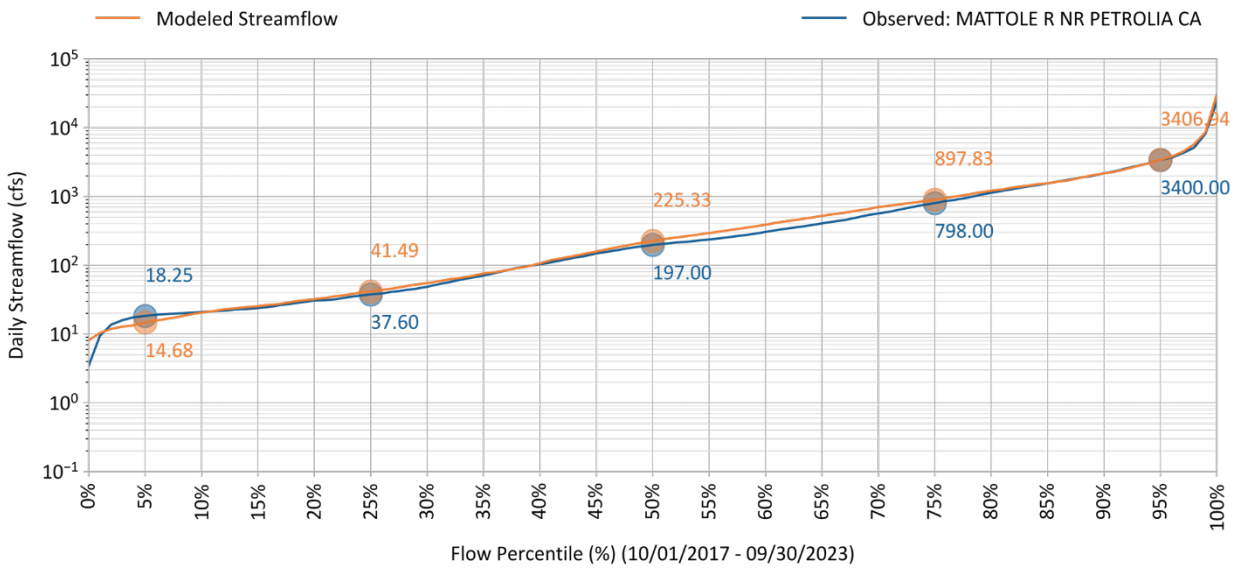

Figure 7-20. Simulated vs. observed flow duration curve for MATTOLE R NR PETROLIA CA (11469000).

PBIAS, NSE, and RSR performance values by season and flow regime are shown in Table 7-14, Table 7-15, and Table 7-16, respectively; the count of values used to calculate each of these metrics is provided in Table 7-23. The "Days Categorized as Baseflow" metric, which is derived from hydrograph separation, consistently shows "Very Good" model performance across all conditions and all metrics, with the exception of "Fair" dry season PBIAS. The other metrics are consistent with the performance discussed above, with "Very Good" performance under most conditions except as discussed for the dry season and further examined below.

Wet and dry season daily hydrographs for water year 2021 are provided in Figure 7-14 and Figure 7-15 respectively, to illustrate model performance during drought conditions. Examination of these plots, along with the performance metric values, helps highlight some important observations regarding hydrologic behavior at this station:

1. There may be connections to the groundwater system that are providing relatively consistent sustained baseflows even at the beginning of the wet season. This can be seen in the constant and slightly increasing October flows in Figure 7-14. As shown in Figure 7-23, there are many springs in this portion of the watershed, possibly due in part to the high precipitation on the King Range, and streams that are potentially gaining flow from groundwater. Data was not immediately identified to quantify these features except for their location, so these conditions are not explicitly represented in the model.
2. There may be withdrawals or other losses of water that are not currently represented. For example, in mid-August through mid-September in Figure 7-15, observed flow has rapid declines and then recovers even though there is little to no rainfall. This maybe indicative of surface water diversions being turned on and off; the surface water withdrawal data however, does not provide the temporal resolution needed to capture intra-monthly withdrawal timing. Additionally, examination of well completion reports (DWR 2025) shows that the number of wells drilled within the Petrolia drainage area below Ettersburg has been increasing since 2012 and was highest for 2016 – 2018 (see Figure 7-24 and Figure 7-25). The majority of these wells were listed for domestic (55%) and irrigation use (37%). While the number of wells drilled does not provide an estimate of actual increases in pumping, it does illustrate increased demand for water that is not represented in the model and may be impacting hydrologic behavior.

Table 7-20. Simulated vs. observed daily streamflow PBIAS at MATTOLE R NR PETROLIA CA (11469000)

Calibration Metrics *(10/01/2017 - 09/30/2023)*	Percent Bias (PBIAS)		
	All Seasons	Wet Season	Dry Season
All Conditions	-4.5%	-2.7%	-24.7%
Highest 10% of Daily Flow Rates	2.7%	2.5%	14.0%
Days Categorized as Storm Flow	-3.7%	-2.7%	-26.0%
Days Categorized as Baseflow	-5.6%	-2.8%	-24.1%

Table 7-21. Simulated vs. observed daily streamflow NSE at MATTOLE R NR PETROLIA CA (11469000)

Calibration Metrics *(10/01/2017 - 09/30/2023)*	Nash-Sutcliffe Efficiency (NSE)		
	All Seasons	Wet Season	Dry Season
All Conditions	0.93	0.92	0.62
Highest 10% of Daily Flow Rates	0.86	0.86	-1.15
Days Categorized as Storm Flow	0.9	0.9	0.46
Days Categorized as Baseflow	0.97	0.97	0.86

Table 7-22. Simulated vs. observed daily streamflow RSR at MATTOLE R NR PETROLIA CA (11469000)

Calibration Metrics *(10/01/2017 - 09/30/2023)*	RMSE-Std-Dev. Ratio (RSR)		
	All Seasons	Wet Season	Dry Season
All Conditions	0.27	0.28	0.61
Highest 10% of Daily Flow Rates	0.38	0.38	1.46
Days Categorized as Storm Flow	0.32	0.32	0.73
Days Categorized as Baseflow	0.18	0.18	0.37

Very Good Good Fair Poor
\- Overpredicts + Underpredicts

Table 7-23. Count of values used to calculate daily calibration metrics at MATTOLE R NR PETROLIA CA (11469000)

Calibration Metrics *(10/01/2017 - 09/30/2023)*	Data Count		
	All Seasons	Wet Season	Dry Season
All Conditions	2191	1273	918
Highest 10% of Daily Flow Rates	218	213	5
Days Categorized as Storm Flow	805	597	208
Days Categorized as Baseflow	1386	676	710

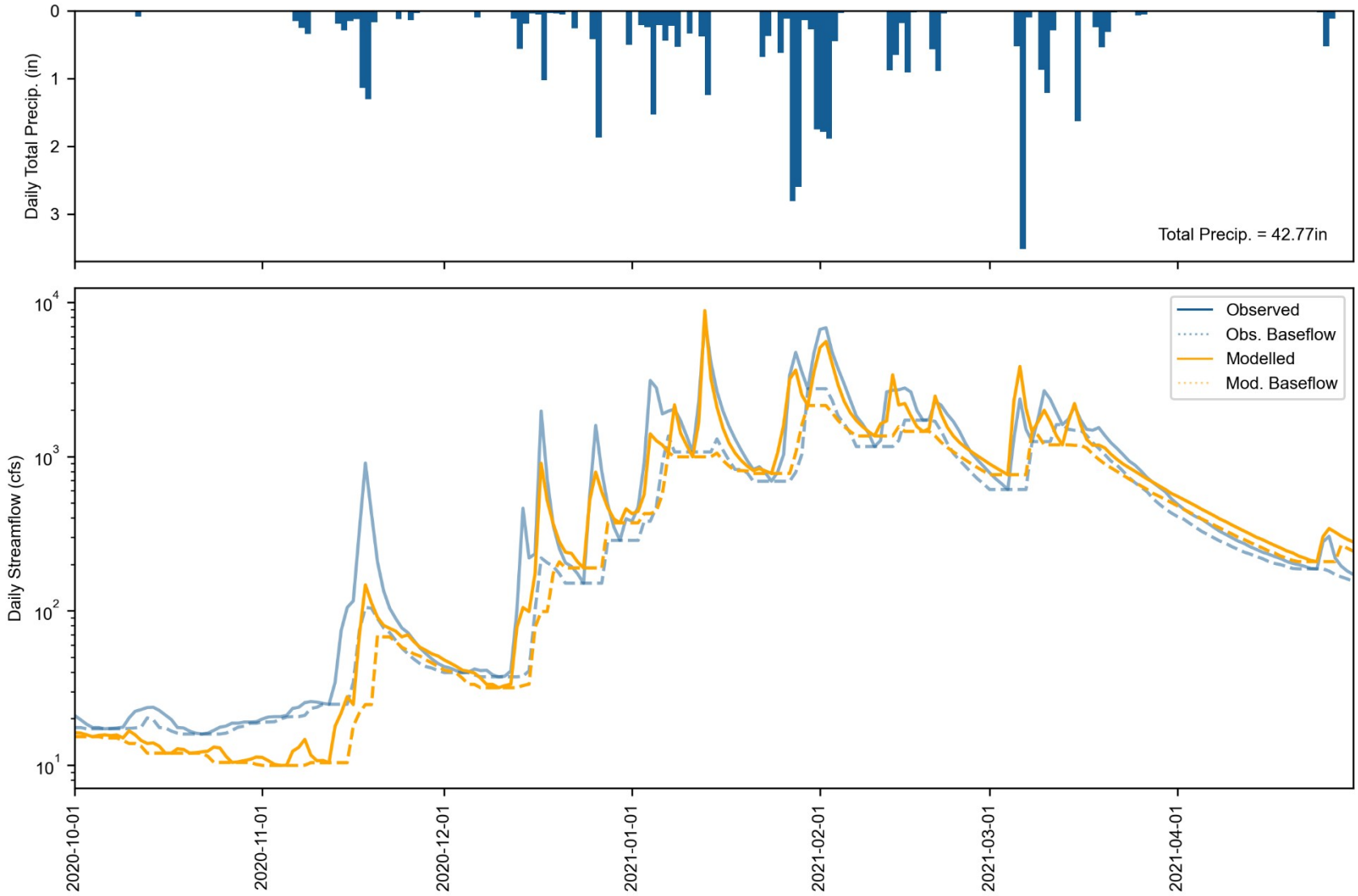

Figure 7-21. Water Year 2021 Wet season daily total precipitation (top) and streamflow (bottom) at MATTOLE R NR PETROLIA CA (11469000). Observed and simulated baseflow are calculated with HYSEP.

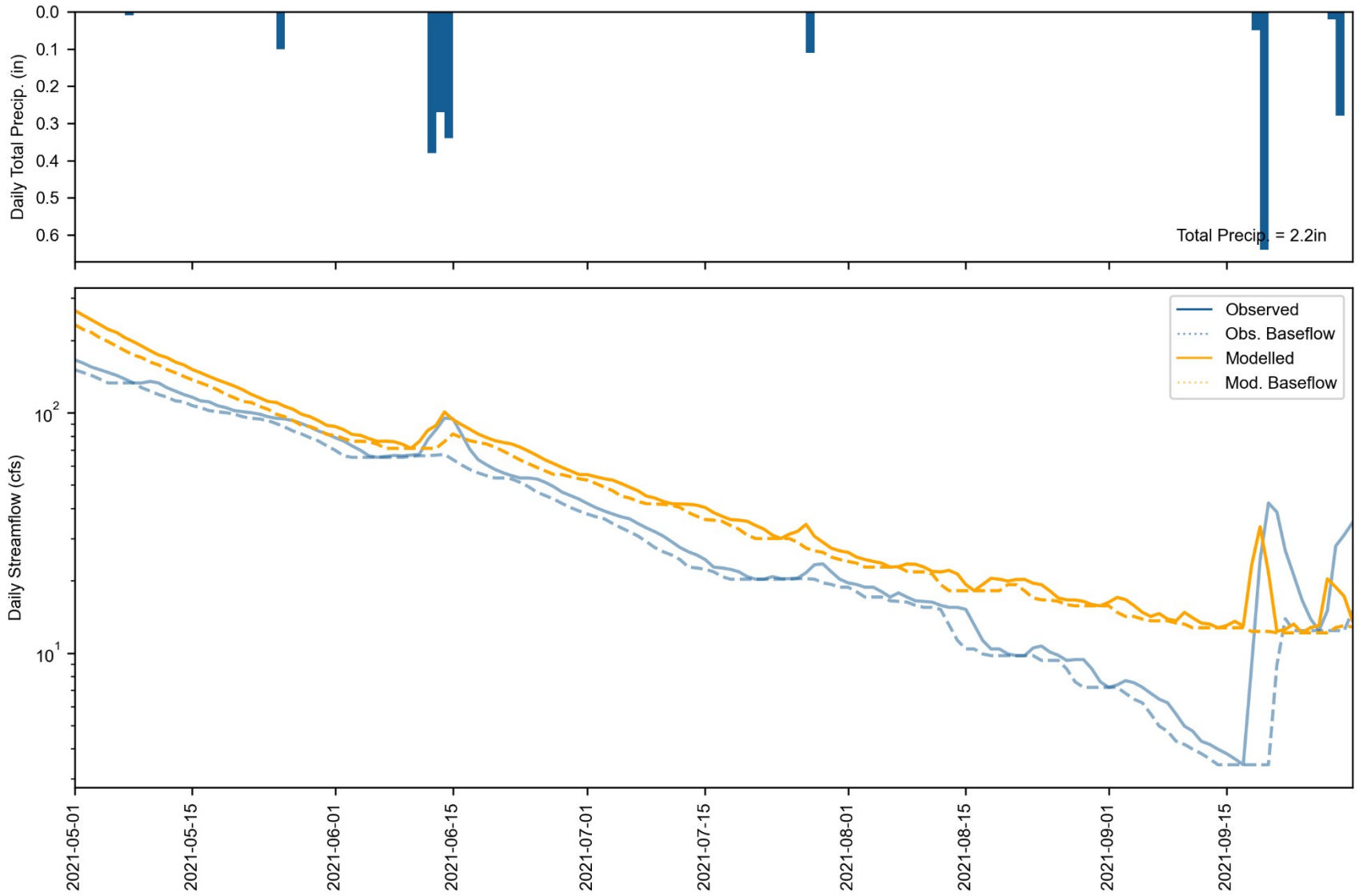

Figure 7-22. Water Year 2021 Dry season daily total precipitation (top) and streamflow (bottom) at MATTOLE R NR PETROLIA CA (11469000). Observed and simulated baseflow are calculated with HYSEP.

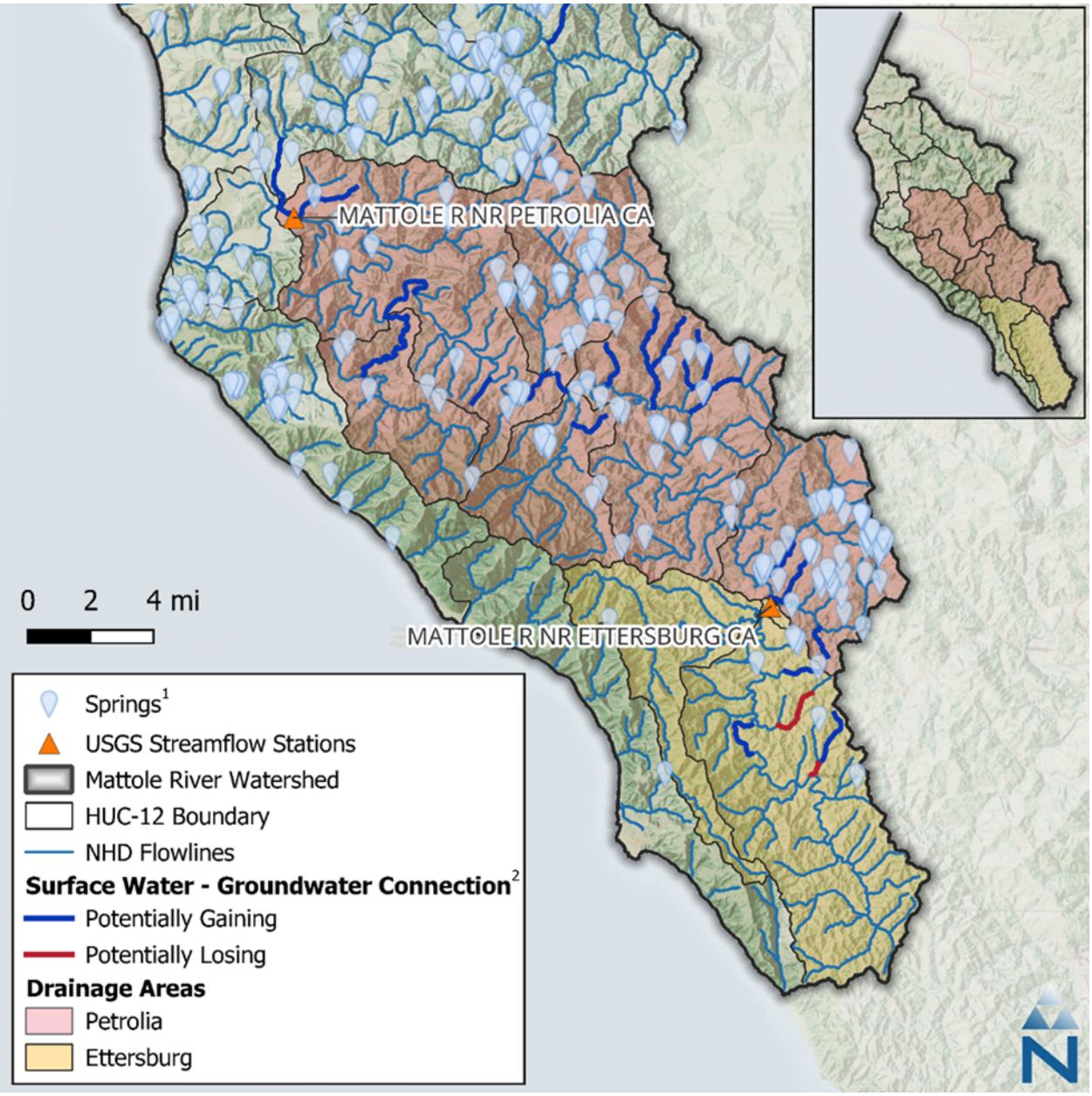

1. (USGS 2025)
2. (Jasechko et al. 2021)

Figure 7-23. Springs and interconnected surface flow conditions within the USGS station drainage areas.

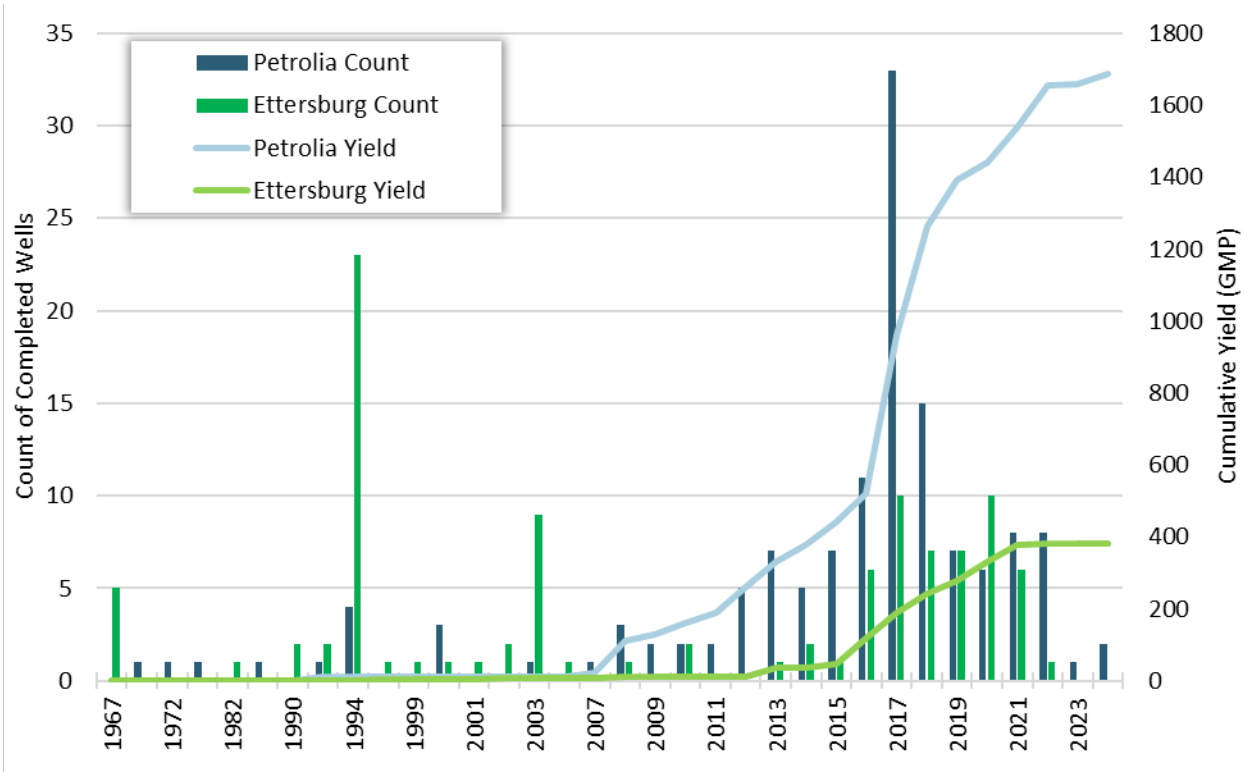

Figure 7-24. DWR well completion report data for the Petrolia (excluding Ettersburg) and Ettersburg drainage areas within the Mattole River watershed. Note that yield is estimated from well pumping tests and was not available for every well completion record.

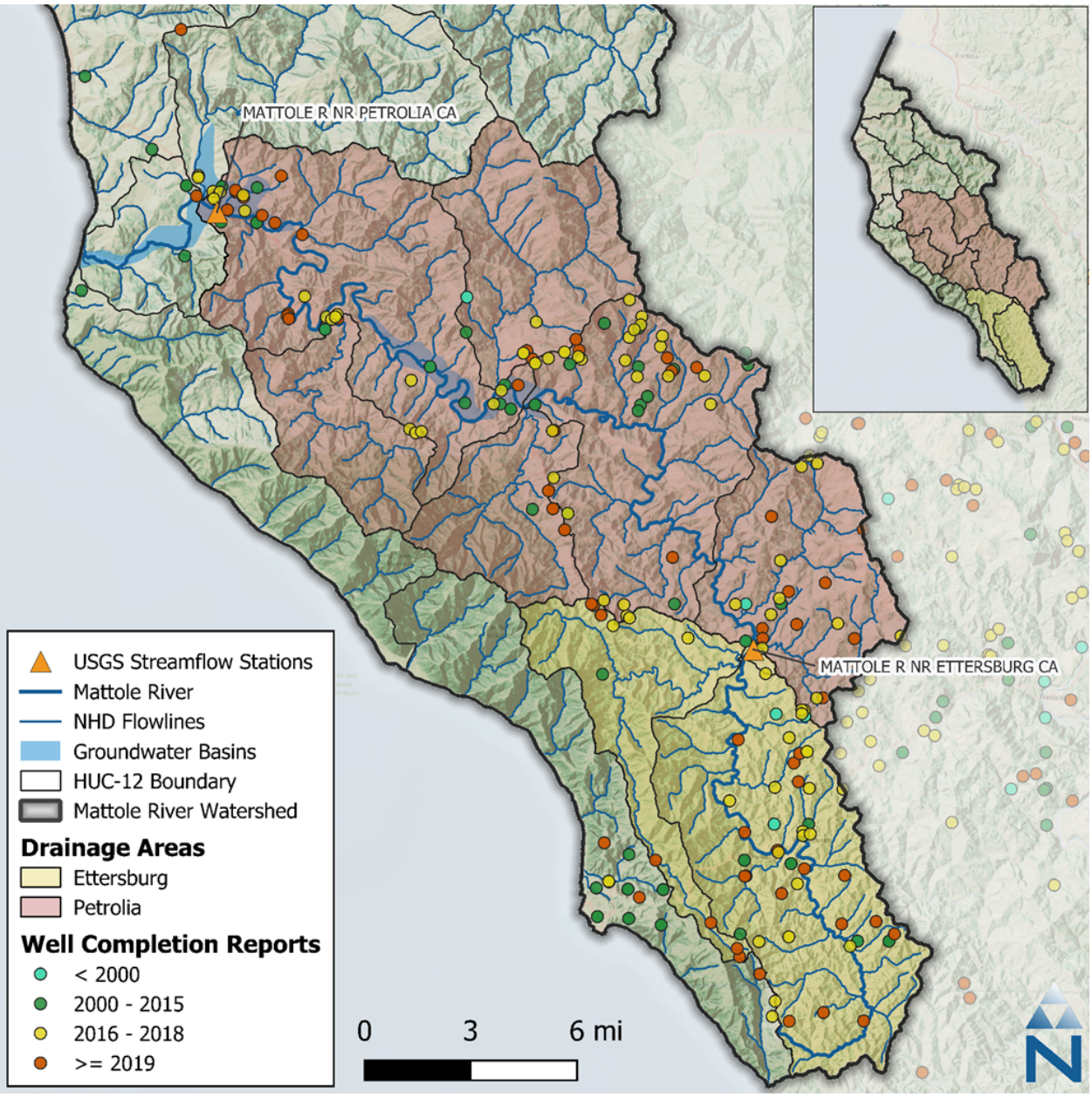

Figure 7-25. Spatial distribution of well completion reports, by time period of interest, for the Petrolia and Ettersburg drainage areas within the Mattole River watershed.

8 MODEL VALIDATION

The model was calibrated for water years 2018-2023 (6 years) and validated for water years 2004-2017 (previous 13 years) at both the Mattole River near Ettersburg station and the Mattole River near Petrolia station. It should be noted that the validation period includes several very wet years with yearly precipitation values greater than those in the calibration period, as shown in Figure 7-3. Validation included several steps. First, a water budget analysis was conducted for water years 2005-2023 for the Petrolia drainage area. Next, the irrigation water budget was confirmed by normalizing associated inputs and outputs by total irrigated area. This validation check was to confirm that applied

irrigation water and withdrawals as represented using the coefficients, rates, and methods described in Section 5.1 produced a reasonable and representative average monthly distribution relative to the precipitation and evapotranspiration meteorological forcing data. Irrigation was simulated for the full period from 2004-2023. This section presents results for the water budget analysis (Section 8.1) and the validation period performance at the Ettersburg headwaters station and the Petrolia downstream station (Section 8.2.1 and 8.2.2, respectively).

8.1 Water Budget

A water budget analysis was conducted to validate a match between the sum of model inputs and outputs. Water inputs include precipitation (both to land segments and water body surfaces) and applied irrigation water. Water outputs include terminal outflow at the Mattole River near Petrolia station, total actual evapotranspiration (from land segments + direct evaporation from water bodies), deep aquifer losses, and total withdrawals (i.e., irrigation and non-irrigation diversion). The water budget was calculated from October 2005 through September 2023 to be representative of long-term conditions within the watershed. The water budget validation showed a close match between all model inputs and outputs—there is a 0.26% difference between inflow and outflow, which represents net volume to/from system storage over the 19-year simulation period; this is an expected difference for water balances at the watershed scale. Figure 8-1 shows the simulated water balance expressed as total volumes and area-normalized annual average depths. These values are within +/- 1.5% of the observed values over the same time period, as shown in Table 6-3. The area-normalized annual average depths shown in Figure 8-1 include the intermediate values for edge-of-stream outflows prior to stream routing (i.e., surface runoff + interflow outflow + active groundwater outflow) and inflow to active groundwater storage to illustrate the relative scale of those components. Figure 8-2 shows monthly average area-normalized simulated water balance components for the same period and illustrates the expected system lag of approximately 5-6 months between peak rainfall (December) and peak evapotranspiration (June).

Because of the importance of forests on the hydrology of the Mattole River watershed given their stage of recovery from logging, density, and composition, an additional analysis of simulated ET pathways was carried out for the Petrolia drainage area for WY2005-2023. This is illustrated as annual average and monthly summaries in Figure 8-3. On an annual average basis, ET from the lower soil zone represents nearly 60% of simulated Total Actual ET (TAET). ET from canopy interception, which is dominated by forests, accounts for 28% of TAET; this is well within the range of reported values from studies on Douglas fir forests (see Table 6 of Pypker et al. 2005). On a monthly basis, the impact of the monthly LZETP, as discussed in Section 7.2.1, can be seen in the dry months when potential ET is highest and water availability may be lowest; during July and August, for example, lower soil zone ET accounts for 96% and 94% of TAET, respectively. Conversely, the impact of ET from canopy interception is closely tied to precipitation and is highest in wetter months (e.g., December, January). While ET from canopy interception can make up a large proportion of TAET during the wet season, it should be noted that TAET volume is lowest during those same periods.

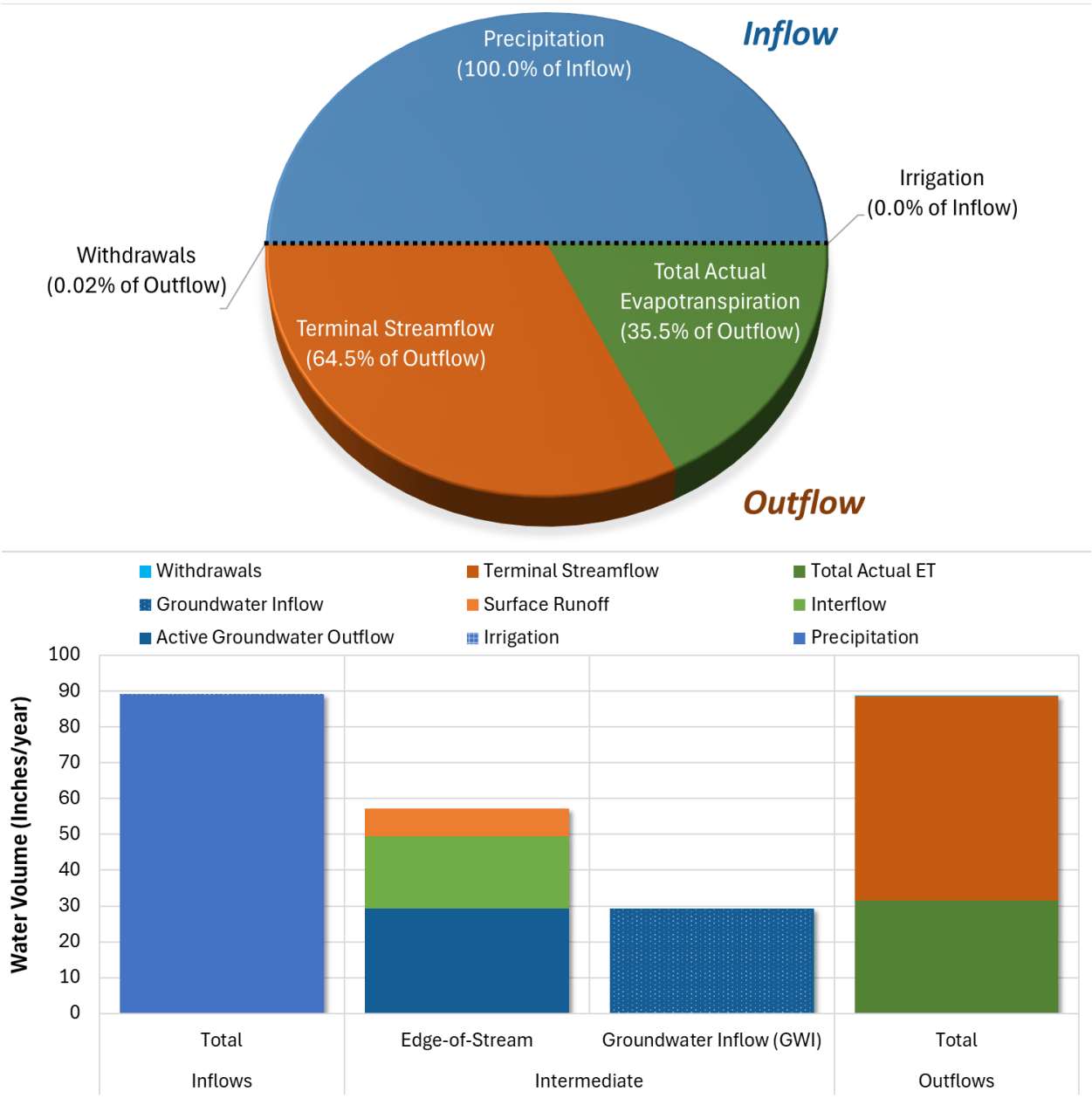

Figure 8-1. Simulated water balance expressed as total volumes and area-normalized annual average depths for the calibration period (water years 2005-2023) at the MATTOLE R NR PETROLIA CA (11469000) station.

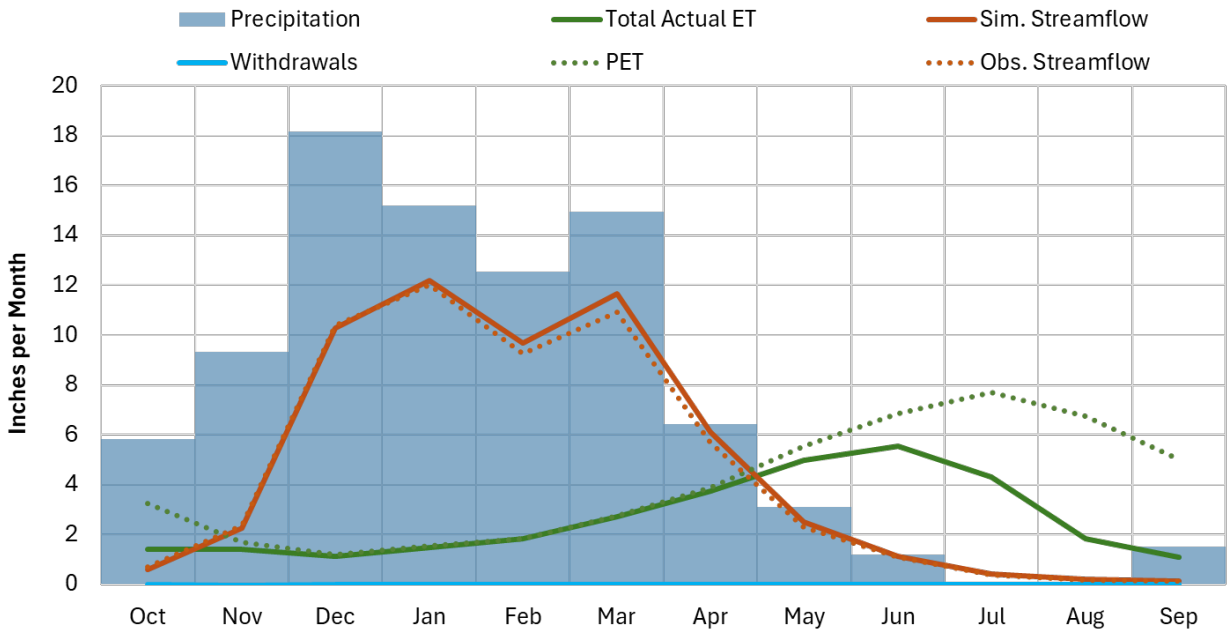

Figure 8-2. Monthly average area-normalized simulated water balance components for water years 2005-2023 at the MATTOLE R NR PETROLIA CA (11469000) station. Note that withdrawals are a minor portion of the total water balance within this drainage area.

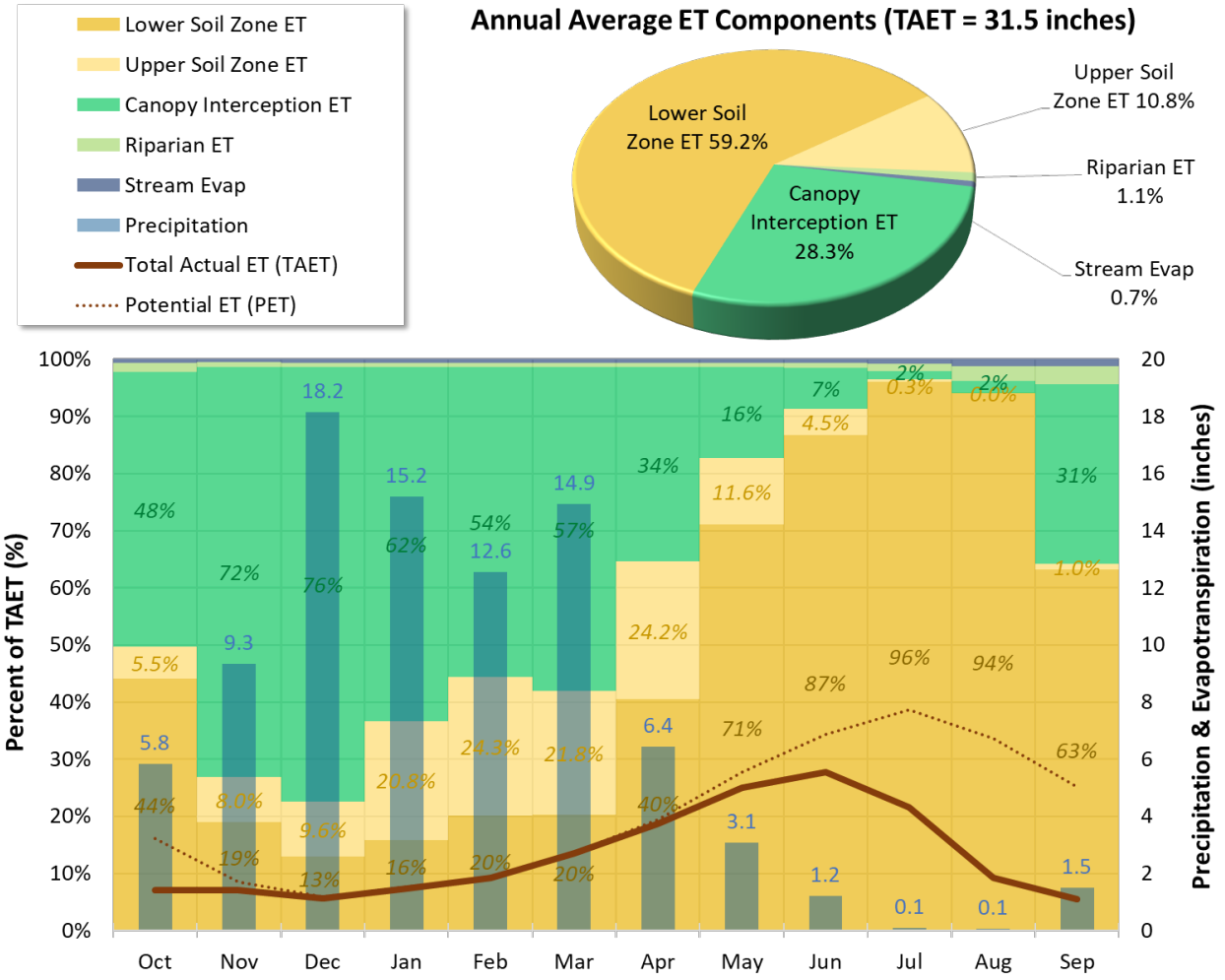

Figure 8-3. Analysis of ET components as a percentage of Total Actual ET (TAET) on an annual average (pie chart) and monthly average (bar chart) basis for water years 2005-2023 at the MATTOLE R NR PETROLIA CA (11469000) station. Area-normalized precipitation, Potential ET (PET) and TAET are included for reference. Note that for each month, the percentage of ET components fits under the TAET curve when considered as a depth.

The water budget for applied irrigation volume was also summarized from calibrated model outputs. On average, a total of 47.2 acre-feet of irrigation water per year was applied on 28.9 acres of land in the Petrolia drainage area, which equates to an irrigation depth of 19.6 inches over the year. Irrigation volume was temporally distributed with monthly evaporative coefficients (described in Section 5.1.3) so that more irrigation occurred during the drier months, as shown in Figure 8-4. The total simulated volume of applied irrigation water represents 20.1% of the total simulated surface water withdrawn for all uses; this is reasonably close to the 30% that can be calculated from the eWRIMS reported data for the entire Mattole River watershed (2017-2023) given that the Petrolia drainage area accounts for 80% of the annual average irrigation withdrawal volume. It should be noted that, on an annual average basis, the reported volume of irrigation withdrawal for the entire watershed (109 ac-ft; Figure 5-2) is a negligible portion of the total water budget at the Petrolia station where streamflow averages over 700,000 ac-ft/yr (Table 6-3). Irrigation withdrawals and application will still have localized impacts, especially around smaller tributaries.

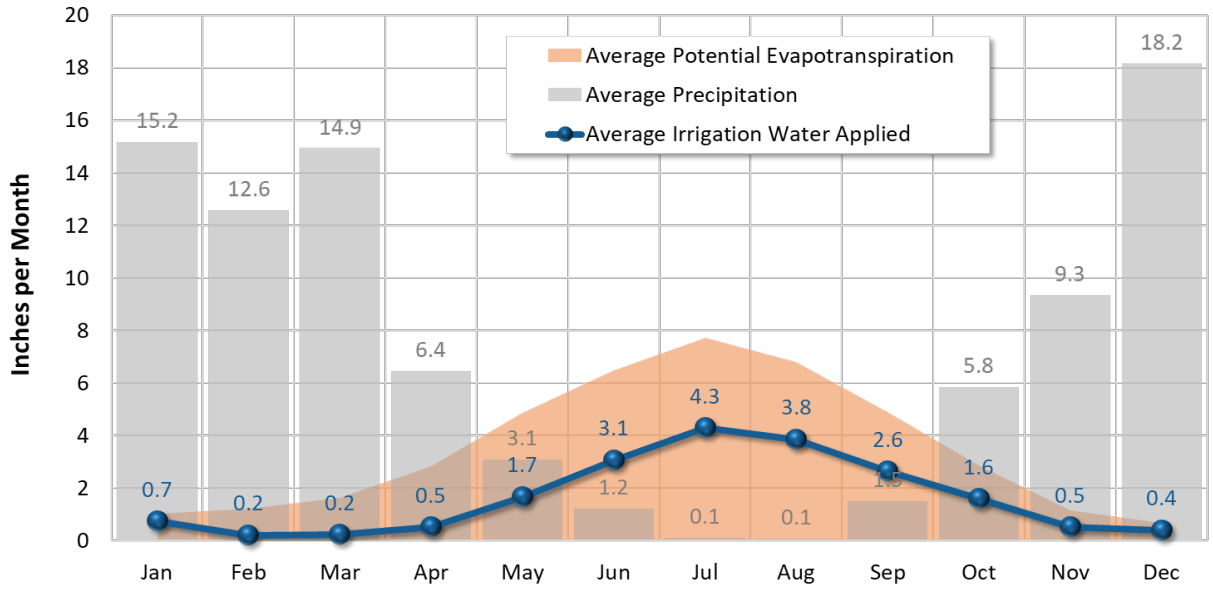

Figure 8-4. Irrigation monthly average area-normalized water balance for irrigated HRUs in the Mattole River near Petrolia drainage area (average precipitation for the entire drainage area is also plotted for reference).

8.2 Hydrology

8.2.1 Upstream – Mattole River near Ettersburg

Across the validation period (water years 2005 to 2017), hydrologic performance at the Mattole River near Ettersburg was generally improved compared to the calibration period with flows slightly overestimated during the wet and still slightly underpredicted during the dry season. Note that all results below exclude observed average daily flows < 1 cfs, where there may be more uncertainty in gauge readings. Over the long-term simulation, PBIAS is "Very Good" (Table 8-1); seasonal PBIAS values were "Very Good" and "Good" for the wet and dry seasons, respectively. Stormflows and baseflows were also well captured with "Very Good" PBIAS.

Table 8-2 presents a summary of model calibration vs. validation performance metrics computed using monthly time series, as recommended by Moriasi et al. (2015). As expected, PBIAS is not impacted by the time step change, however, RSR and NSE both show notable improvement in performance compared to using daily average time series.

Table 8-1. Summary of daily validation performance metrics for MATTOLE R NR ETTERSBURG CA (11468900)

Hydrology Monitoring Locations	Performance Metrics (10/01/2004 - 09/30/2017)														
	PBIAS						RSR			NSE			KGE[1]		
	All	Wet Season	Dry Season	>10th %ile Flows	Storm Flows	Baseflow	All	Wet Season	Dry Season	All	Wet Season	Dry Season	All	Wet Season	Dry Season
MATTOLE R NR ETTERSBURG CA	-0.4%	-1.5%	13.1%	4.3%	-2.6%	2.0%	0.48	0.51	0.52	0.77	0.74	0.73	0.95	0.94	0.75

[1] Monthly, as specified in Table 7-3.

Table 8-2. Summary of calibration performance metrics using monthly averages MATTOLE R NR ETTERSBURG CA (11468900)

Calibration Metrics for Monthly Flow (10/01/2004 - 09/30/2017)	Hydrological Condition		
	All (n = 156)	Wet Season (n = 91)	Dry Season (n = 65)
Percent Bias (PBIAS)	-0.4%	-1.5%	13.1%
Nash-Sutcliffe Efficiency (NSE)	0.94	0.93	0.91
RMSE-Std-Dev. Ratio (RSR)	0.24	0.27	0.31
Kling–Gupta Efficiency (KGE)	0.95	0.94	0.75

Very Good Good Fair Poor
\- Overpredicts + Underpredicts

As with the calibration period, flow time series plots, monthly aggregate figures, and the FDC were also created for the validation period, and are shown in Figure 8-5 to Figure 8-9. PBIAS, NSE, and RSR performance values by season and flow regime are shown in Table 8-3, Table 8-4, and Table 8-5, respectively; the count of values used to calculate each of these metrics is provided in Table 8-6. In general, performance metric scores showed some improvement between calibration and validation periods, which is likely an artifact of having the longer 13-year averaging period for computing validation metrics, compared to 6 years for the calibration period. It should be noted that metrics like the PBIAS for the highest 10% of flows, for example, can be skewed by a small sample set, especially during the dry season when differences in small numbers can translate to large percentage differences. The wet and dry season daily hydrographs exhibit similar responses as were seen for the calibration period (Figure 8-10 and Figure 8-11) and illustrate performance during a year with precipitation near the median (47th percentile) for the modeled period. On average, the performance assessments demonstrate that the model performs well across both wet and dry conditions and is a robust predictor of hydrological conditions in the Mattole River near Ettersburg drainage area and the transition periods between both individual storms and wet/dry seasons.

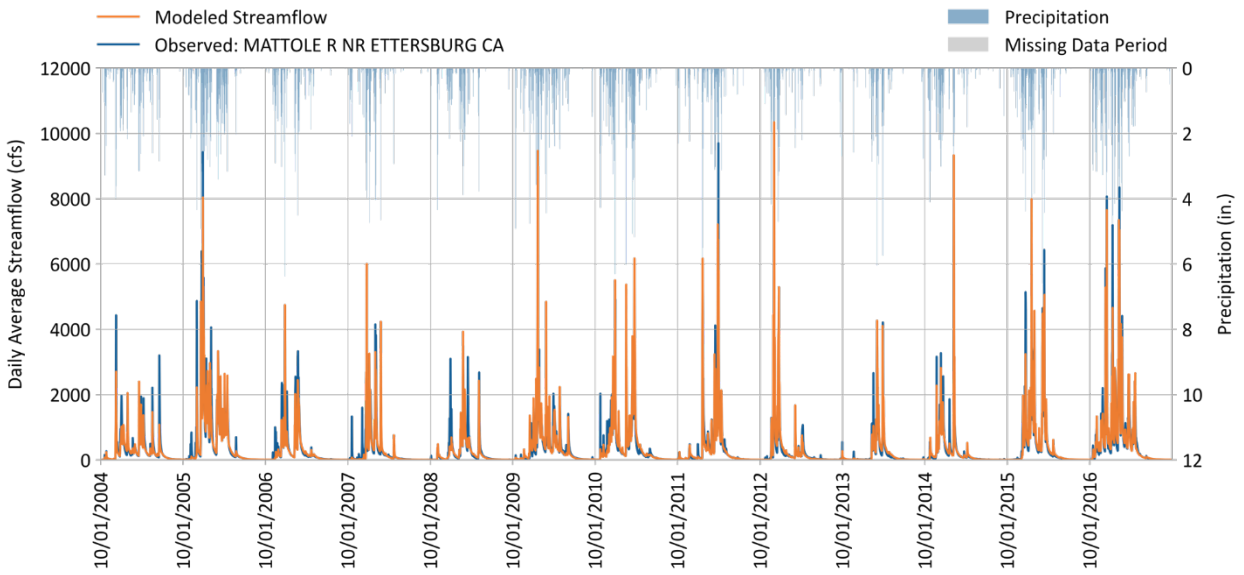

Figure 8-5. Daily simulated vs. observed streamflow for MATTOLE R NR ETTERSBURG CA (11468900).

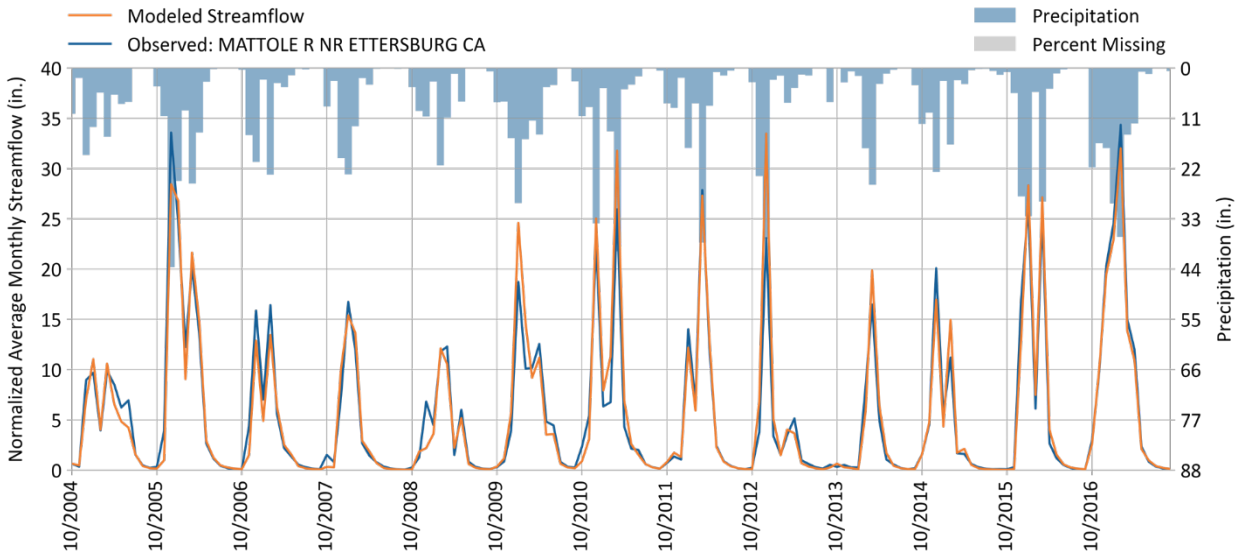

Figure 8-6. Monthly simulated vs. observed streamflow for MATTOLE R NR ETTERSBURG CA (11468900).

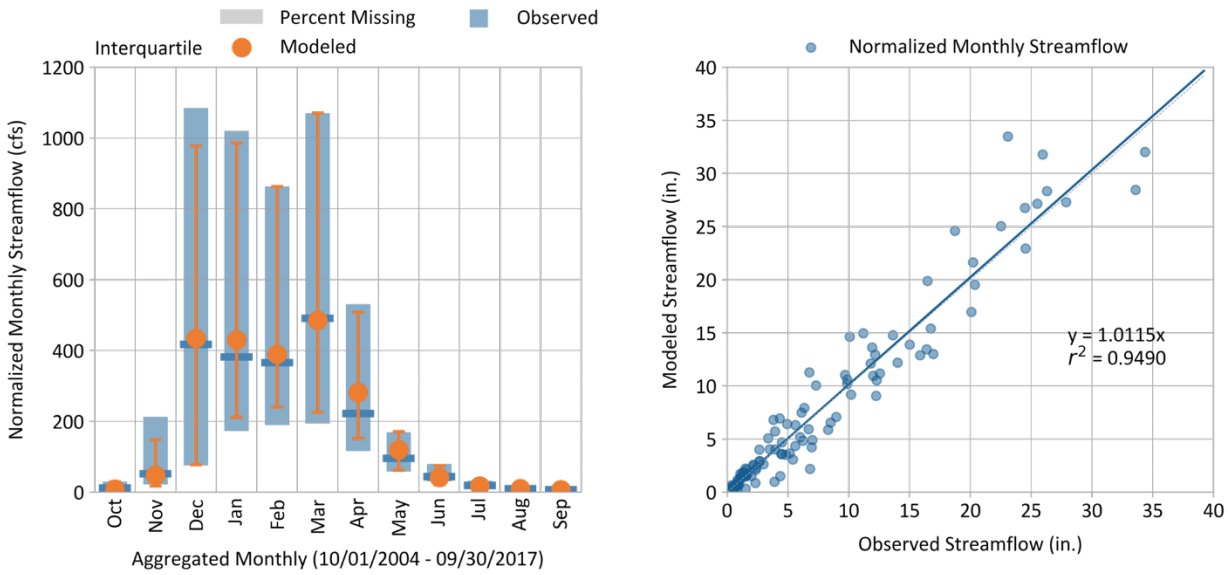

Figure 8-7. Monthly normalized simulated vs. observed streamflow for MATTOLE R NR ETTERSBURG CA (11468900).

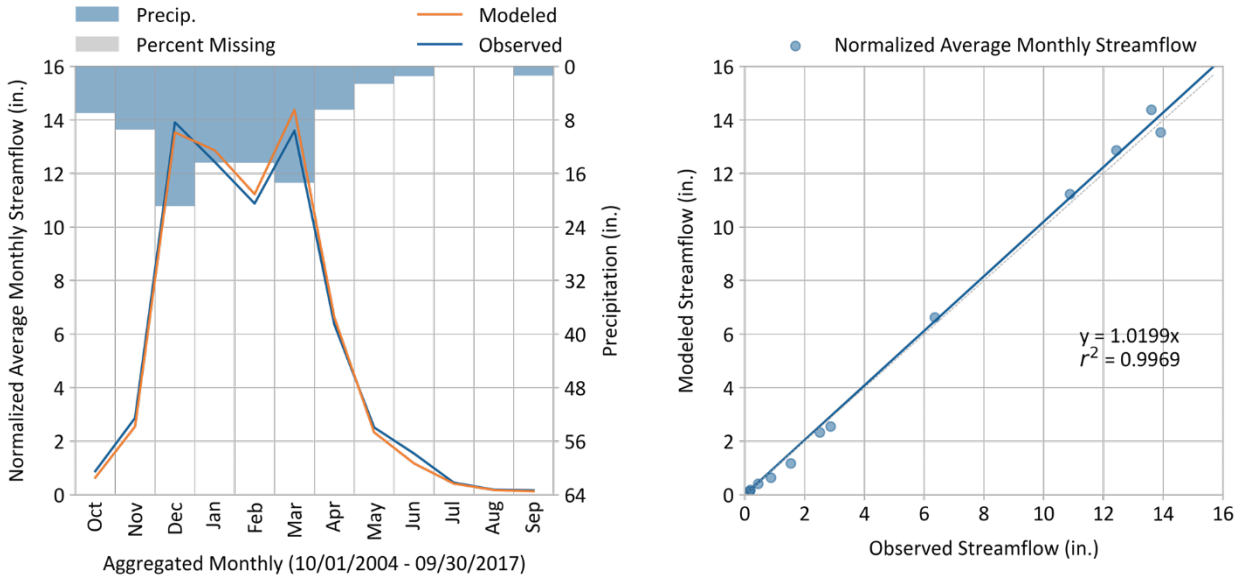

Figure 8-8. Average monthly simulated vs. observed streamflow for MATTOLE R NR ETTERSBURG CA (11468900).

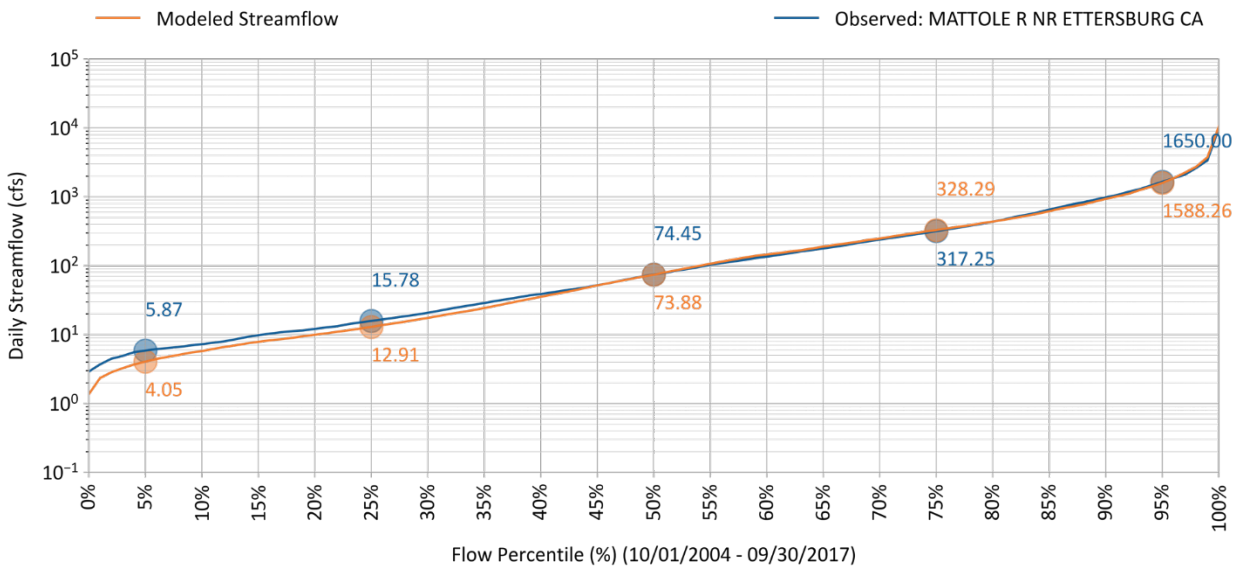

Figure 8-9. Simulated vs. observed flow duration curve for MATTOLE R NR ETTERSBURG CA (11468900).

Table 8-3. Simulated vs. observed daily streamflow PBIAS at MATTOLE R NR ETTERSBURG CA (11468900)

Validation Metrics *(10/01/2004 - 09/30/2017)*	Percent Bias (PBIAS)		
	All Seasons	Wet Season	Dry Season
All Conditions	-0.4%	-1.5%	13.1%
Highest 10% of Daily Flow Rates	4.3%	3.8%	33.7%
Days Categorized as Storm Flow	-2.6%	-3.8%	23.7%
Days Categorized as Baseflow	2.0%	1.3%	8.1%

Table 8-4. Simulated vs. observed daily streamflow NSE at MATTOLE R NR ETTERSBURG CA (11468900)

Validation Metrics *(10/01/2004 - 09/30/2017)*	Nash-Sutcliffe Efficiency (NSE)		
	All Seasons	Wet Season	Dry Season
All Conditions	0.77	0.74	0.73
Highest 10% of Daily Flow Rates	0.37	0.38	-1.11
Days Categorized as Storm Flow	0.7	0.67	0.69
Days Categorized as Baseflow	0.85	0.83	0.85

Table 8-5. Simulated vs. observed daily streamflow RSR at MATTOLE R NR ETTERSBURG CA (11468900)

Validation Metrics *(10/01/2004 - 09/30/2017)*	RMSE-Std-Dev. Ratio (RSR)		
	All Seasons	Wet Season	Dry Season
All Conditions	0.48	0.51	0.52
Highest 10% of Daily Flow Rates	0.8	0.79	1.45
Days Categorized as Storm Flow	0.55	0.58	0.56
Days Categorized as Baseflow	0.38	0.41	0.39

Very Good Good Fair Poor
\- Overpredicts + Underpredicts

Table 8-6. Count of values used to calculate daily validation metrics at MATTOLE R NR ETTERSBURG CA (11468900)

Validation Metrics *(10/01/2004 - 09/30/2017)*	Data Count		
	All Seasons	Wet Season	Dry Season
All Conditions	4748	2759	1989
Highest 10% of Daily Flow Rates	475	465	10
Days Categorized as Storm Flow	1552	1084	468
Days Categorized as Baseflow	3196	1675	1521

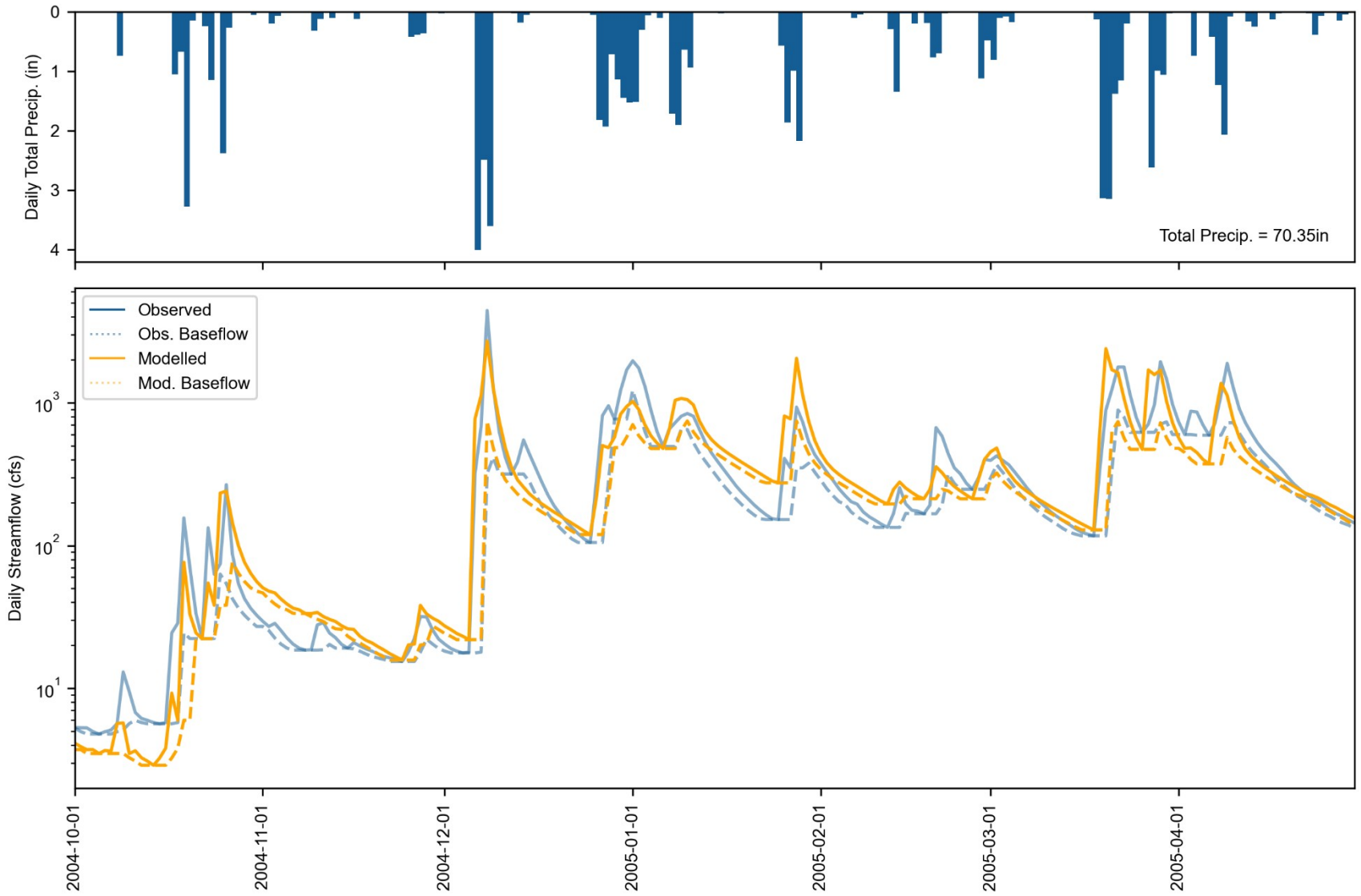

Figure 8-10. Water Year 2005 Wet season daily total precipitation (top) and streamflow (bottom) at MATTOLE R NR ETTERSBURG CA (11468900). Observed and simulated baseflow are calculated with HYSEP.

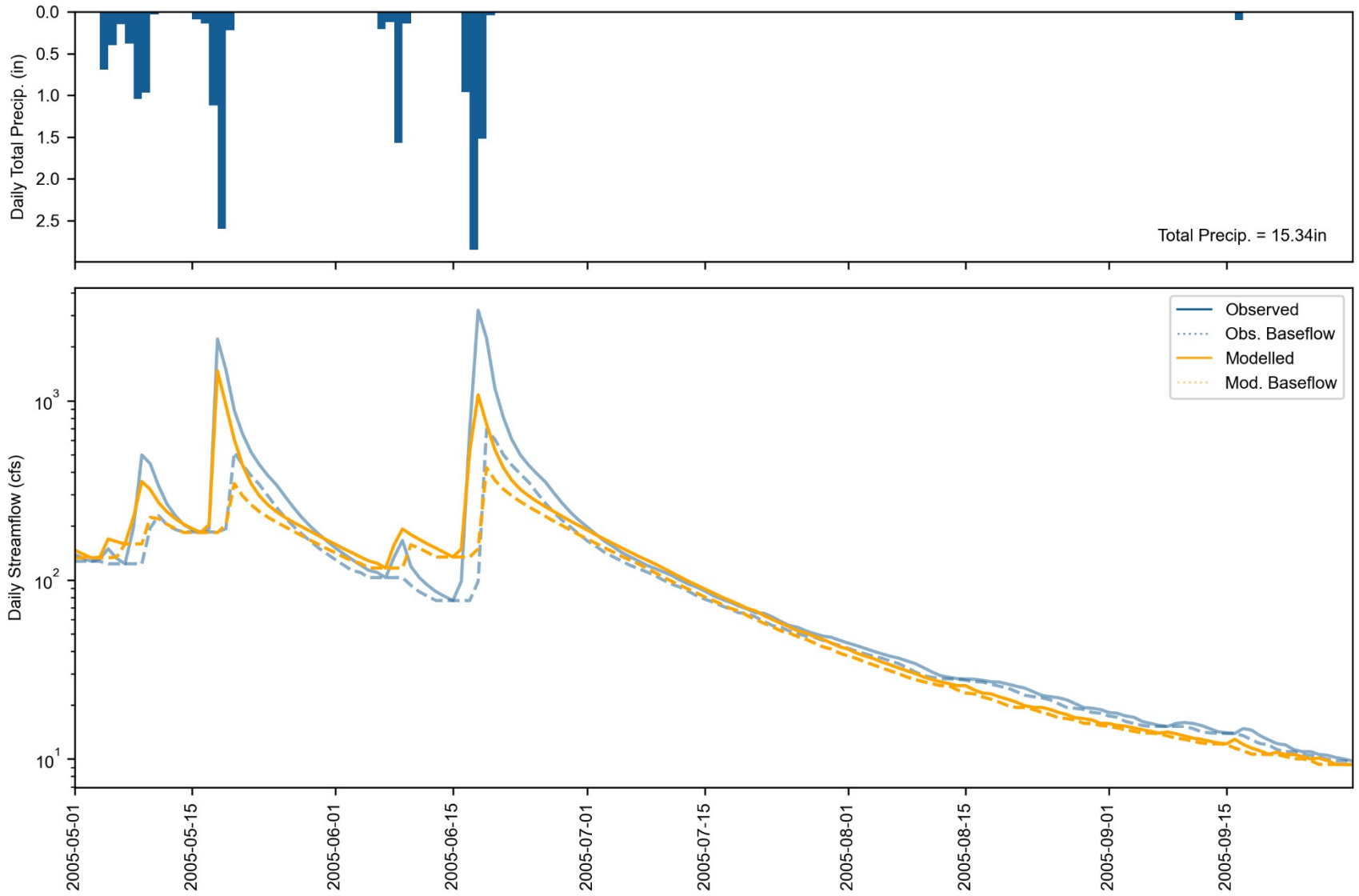

Figure 8-11. Water Year 2005 Dry season daily total precipitation (top) and streamflow (bottom) at MATTOLE R NR ETTERSBURG CA (11468900). Observed and simulated baseflow are calculated with HYSEP. Note that the preceding wet season is very wet.

8.2.2 Downstream – Mattole River near Petrolia

Across the validation period (water years 2005 to 2017), hydrologic performance at the Mattole River near Petrolia station was generally similar and somewhat improved compared to the calibration period with flows still slightly overpredicted. Note that all results below exclude observed average daily flows < 1 cfs, where there may be more uncertainty in gauge readings. Based on the daily average time series, hydrologic performance is "Very Good" for all metrics (Table 8-7) and "Very Good" for all metrics based on monthly averages (Table 8-8) with the exception of "Good" dry season KGE.

Flow time series plots, monthly aggregate figures, and the FDC were created for this period and are shown in Figure 8-12 to Figure 8-16; the count of values used to calculate each of these metrics is provided in Table 8-12. These figures illustrate a high degree of correspondence between simulated and observed values. PBIAS, NSE, and RSR performance values by season and flow regime are shown in Table 8-9, Table 8-10, and Table 8-11, respectively. The stormflow and baseflow values for these metrics are "Very Good" to "Good", except for "Poor" dry season performance for the highest 10% of flows and "Fair" dry season stormflow RSR.

Table 8-7. Summary of daily validation performance metrics for MATTOLE R NR PETROLIA CA (11469000)

Hydrology Monitoring Locations	Performance Metrics (10/01/2004 - 09/30/2017)														
	PBIAS						RSR			NSE			KGE[1]		
	All	Wet Season	Dry Season	>10th %ile Flows	Storm Flows	Baseflow	All	Wet Season	Dry Season	All	Wet Season	Dry Season	All	Wet Season	Dry Season
MATTOLE R NR PETROLIA CA	-2.2%	-2.2%	-1.7%	2.1%	-6.1%	3.1%	0.41	0.44	0.49	0.83	0.81	0.76	0.96	0.96	0.89

[1] Monthly, as specified in Table 7-3.

Table 8-8. Summary of calibration performance metrics using monthly averages at MATTOLE R NR PETROLIA CA (11469000)

Calibration Metrics for Monthly Flow (10/01/2004 - 09/30/2017)	Hydrological Condition		
	All (n = 156)	Wet Season (n = 91)	Dry Season (n = 65)
Percent Bias (PBIAS)	-2.2%	-2.2%	-1.7%
Nash-Sutcliffe Efficiency (NSE)	0.95	0.94	0.93
RMSE-Std-Dev. Ratio (RSR)	0.22	0.25	0.26
Kling–Gupta Efficiency (KGE)	0.96	0.96	0.89

Very Good Good Fair Poor
\- Overpredicts + Underpredicts

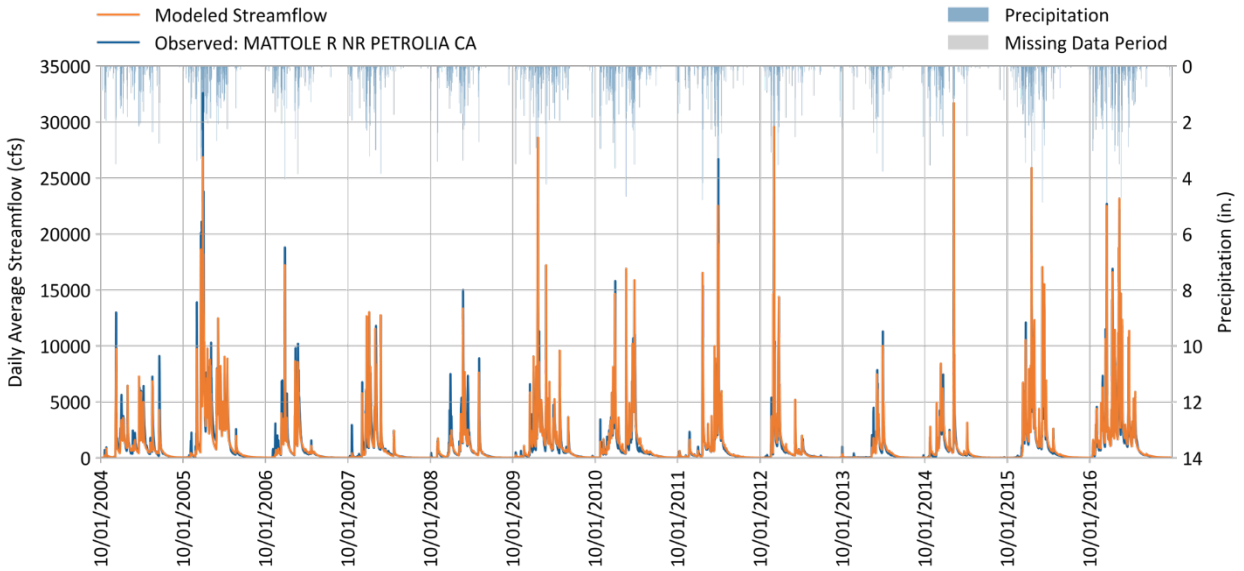

Figure 8-12. Daily simulated vs. observed streamflow for MATTOLE R NR PETROLIA CA (11469000).

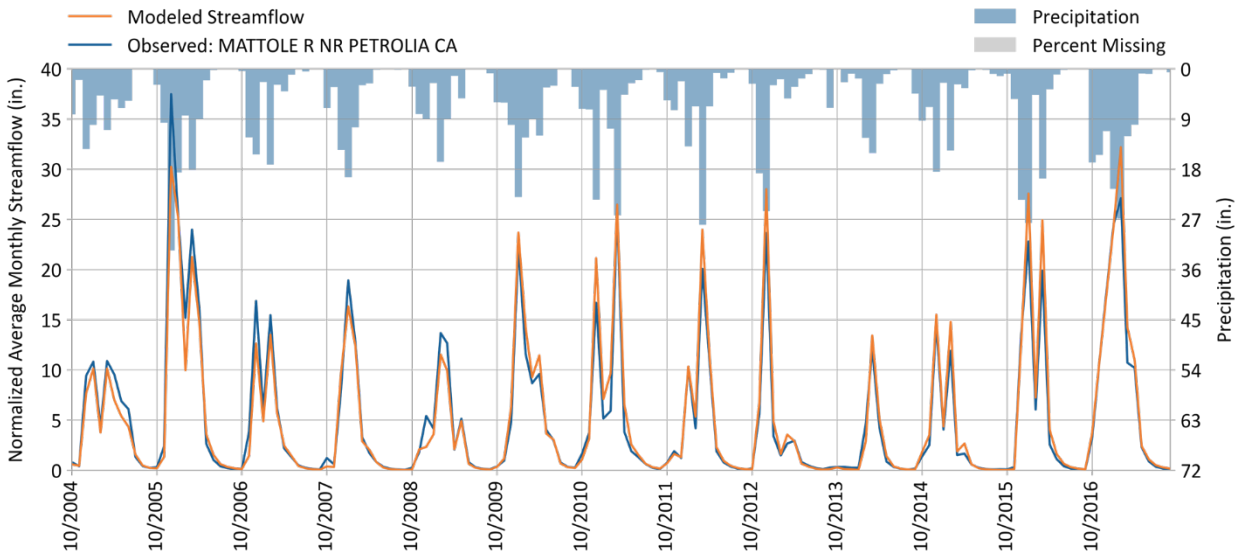

Figure 8-13. Monthly simulated vs. observed streamflow for MATTOLE R NR PETROLIA CA (11469000).

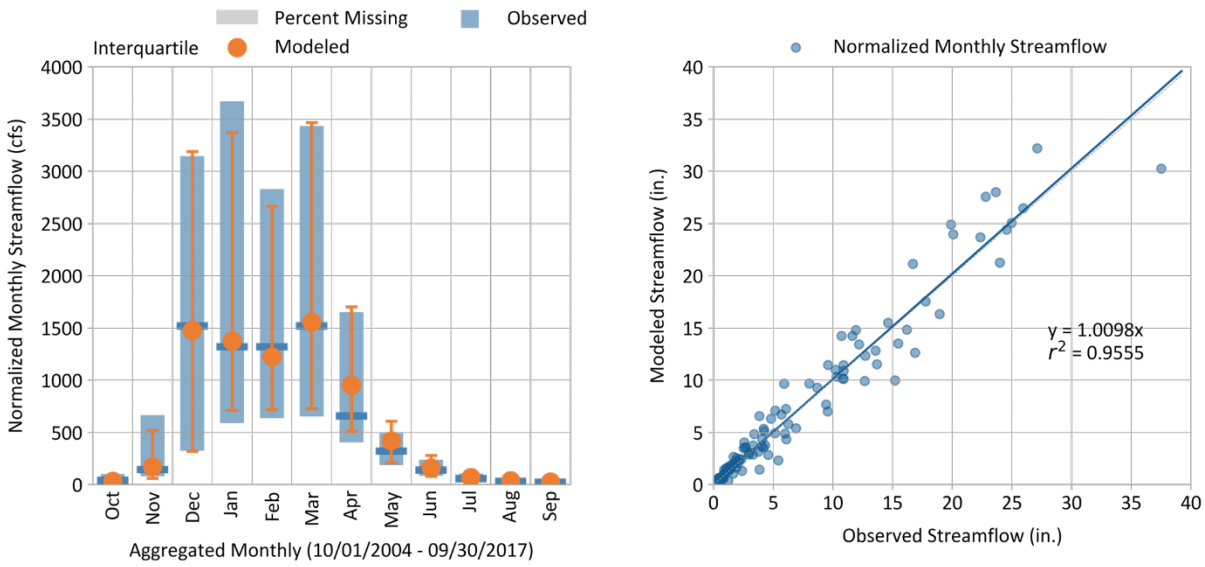

Figure 8-14. Monthly normalized simulated vs. observed streamflow for MATTOLE R NR PETROLIA CA (11469000).

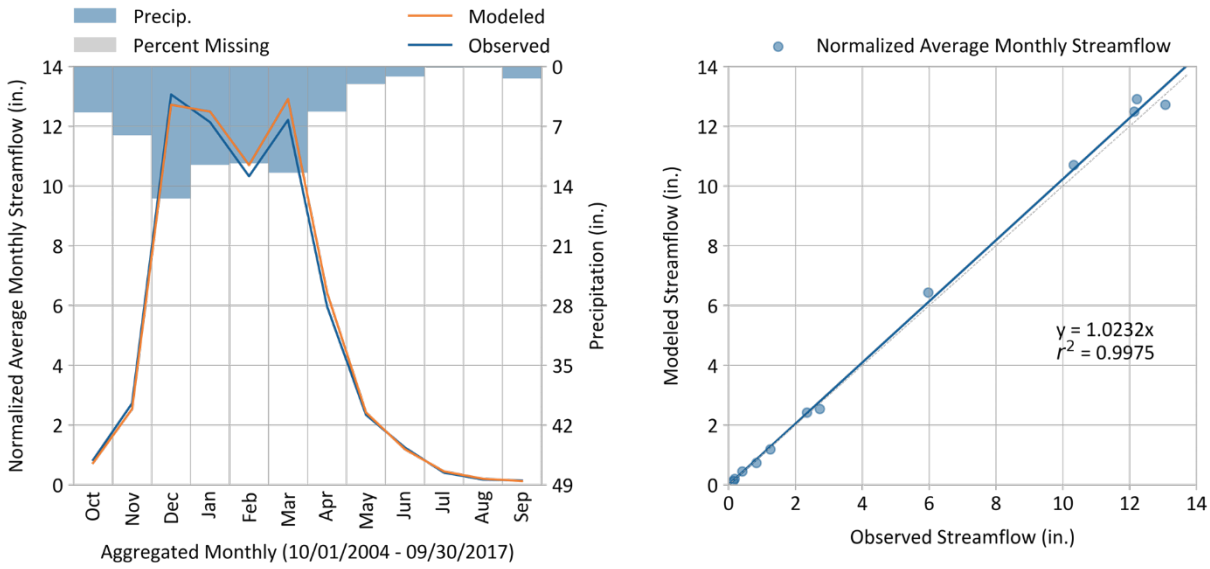

Figure 8-15. Average monthly simulated vs. observed streamflow for MATTOLE R NR PETROLIA CA (11469000).

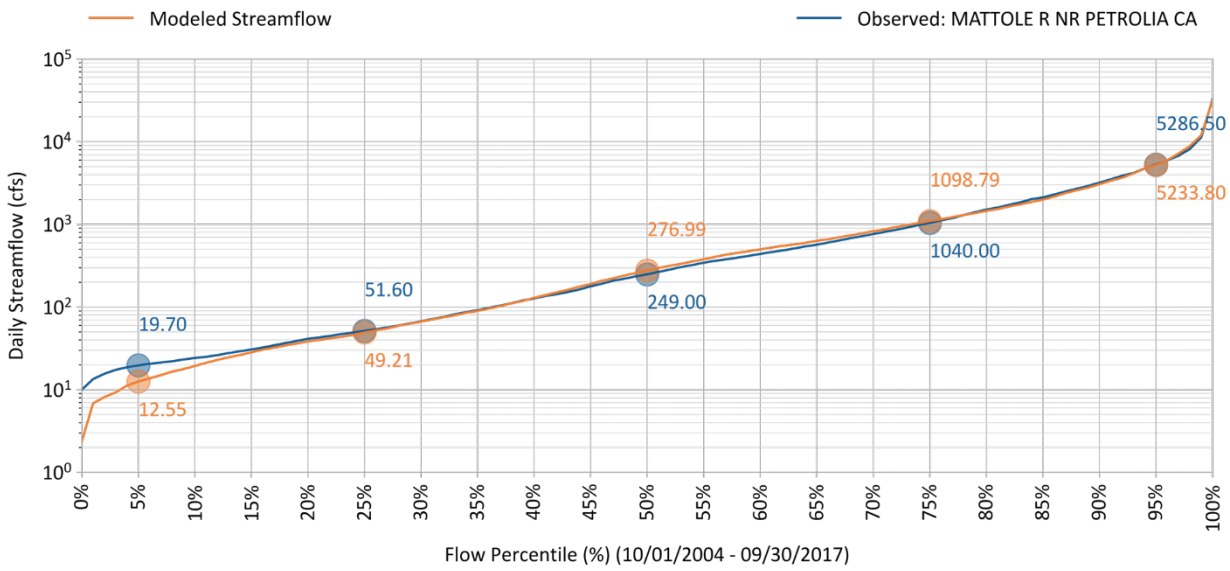

Figure 8-16. Simulated vs. observed flow duration curve for MATTOLE R NR PETROLIA CA (11469000).

Wet and dry season daily hydrographs for water year 2005 are provided in Figure 8-17 and Figure 8-18, respectively, to illustrate model performance during a year with near median precipitation (53rd percentile) across the modeled period. Also included is the daily hydrograph for the water year 2014 wet season. This year was very dry (11th percentile for total precipitation) and exhibits sustained baseflow that is visible because the majority of the wet season storm events were delayed until February. This behavior could indicate more groundwater storage and interactions that are not currently represented in the model. On average, these validation assessments demonstrate that the model performs very well across both wet and dry conditions and is a robust predictor of hydrological conditions in the Mattole River near Petrolia drainage area and the transition periods between both individual storms and wet/dry seasons.

Table 8-9. Simulated vs. observed daily streamflow PBIAS at MATTOLE R NR PETROLIA CA (11469000)

Validation Metrics *(10/01/2004 - 09/30/2017)*	Percent Bias (PBIAS)		
	All Seasons	Wet Season	Dry Season
All Conditions	-2.2%	-2.2%	-1.7%
Highest 10% of Daily Flow Rates	2.1%	1.5%	39.5%
Days Categorized as Storm Flow	-6.1%	-6.8%	10.4%
Days Categorized as Baseflow	3.1%	4.5%	-8.1%

Table 8-10. Simulated vs. observed daily streamflow NSE at MATTOLE R NR PETROLIA CA (11469000)

Validation Metrics *(10/01/2004 - 09/30/2017)*	Nash-Sutcliffe Efficiency (NSE)		
	All Seasons	Wet Season	Dry Season
All Conditions	0.83	0.81	0.76
Highest 10% of Daily Flow Rates	0.52	0.53	-1.08
Days Categorized as Storm Flow	0.78	0.77	0.74
Days Categorized as Baseflow	0.9	0.89	0.86

Table 8-11. Simulated vs. observed daily streamflow RSR at MATTOLE R NR PETROLIA CA (11469000)

Validation Metrics *(10/01/2004 - 09/30/2017)*	RMSE-Std-Dev. Ratio (RSR)		
	All Seasons	Wet Season	Dry Season
All Conditions	0.41	0.44	0.49
Highest 10% of Daily Flow Rates	0.69	0.69	1.44
Days Categorized as Storm Flow	0.46	0.48	0.51
Days Categorized as Baseflow	0.31	0.34	0.37

Very Good Good Fair Poor
\- Overpredicts + Underpredicts

Table 8-12. Count of values used to calculate daily validation metrics at MATTOLE R NR PETROLIA CA (11469000)

Validation Metrics *(10/01/2004 - 09/30/2017)*	Data Count		
	All Seasons	Wet Season	Dry Season
All Conditions	4748	2759	1989
Highest 10% of Daily Flow Rates	472	464	8
Days Categorized as Storm Flow	1758	1307	451
Days Categorized as Baseflow	2990	1452	1538

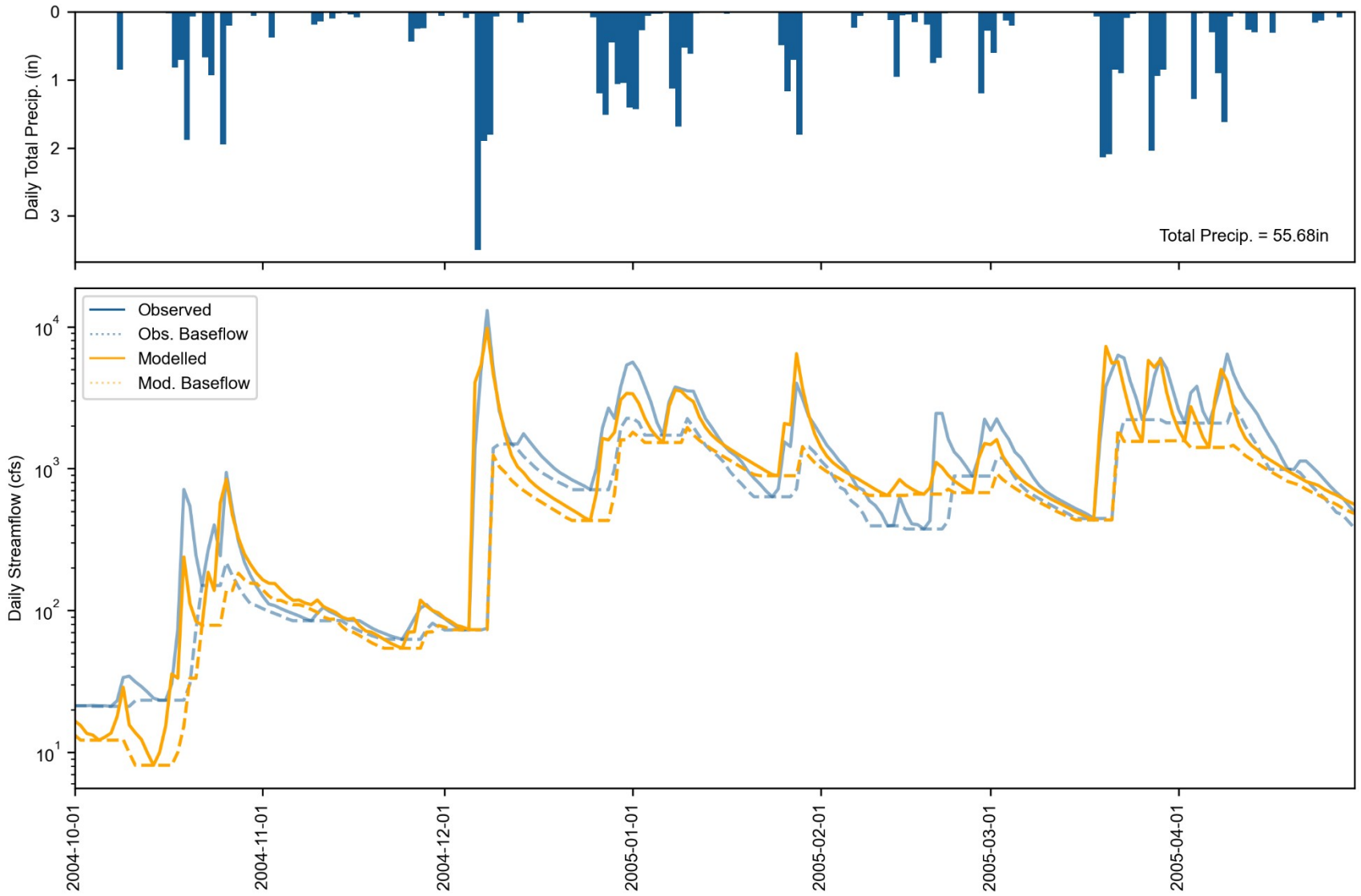

Figure 8-17. Water Year 2005 Wet season daily total precipitation (top) and streamflow (bottom) at MATTOLE R NR PETROLIA CA (11469000). Observed and simulated baseflow are calculated with HYSEP.

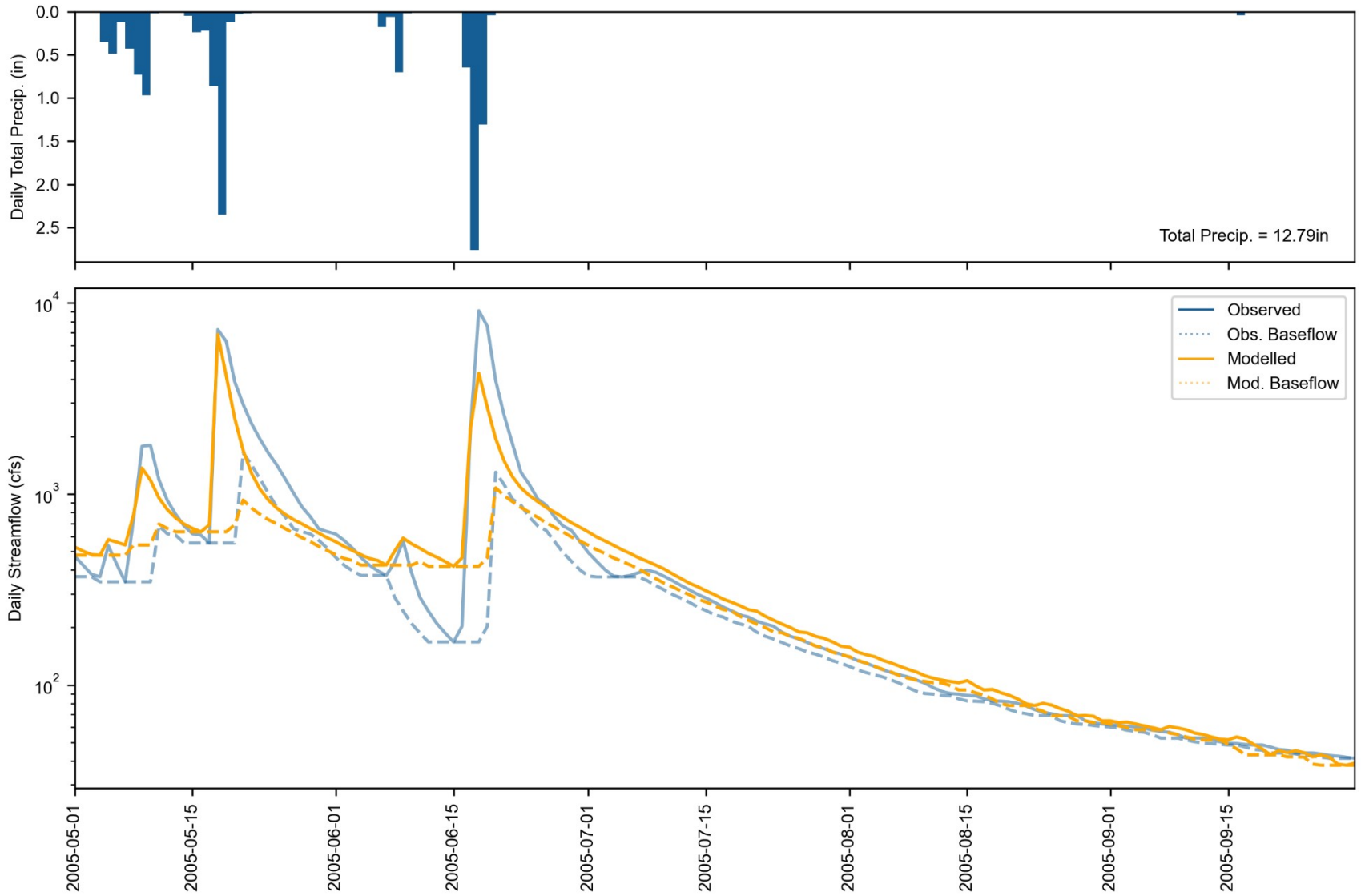

Figure 8-18. Water Year 2005 Dry season daily total precipitation (top) and streamflow (bottom) at MATTOLE R NR PETROLIA CA (11469000). Observed and simulated baseflow are calculated with HYSEP.

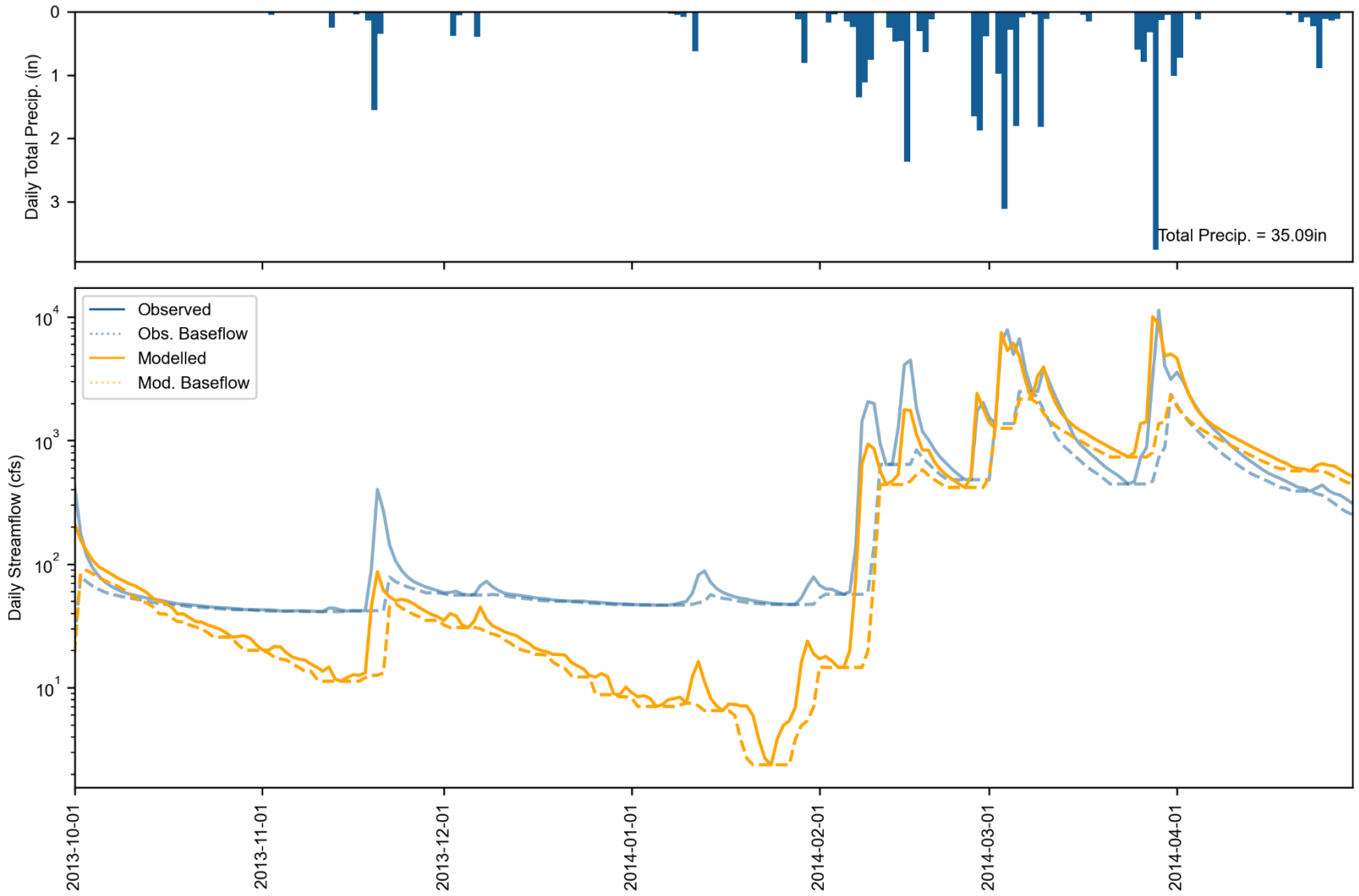

Figure 8-19. Water Year 2014 Wet season daily total precipitation (top) and streamflow (bottom) at MATTOLE R NR PETROLIA CA (11469000). This is a very dry year with delayed wet season storm events that make a sustained baseflow behavior observable.

9 SUMMARY

This report documented the configuration, calibration, and validation of an LSPC hydrology model for the Mattole River watershed. The Water Board will use this model to facilitate water use planning to ensure adequate, minimal water supplies for critical purposes. The Mattole River watershed model provides a comprehensive planning and decision-making tool by serving as an evaluation platform for (1) simulating existing instream flows that integrate current water management activities and consumptive uses and (2) evaluating the range of impacts of alternative management scenarios, including water allocation, changes in demand, and the impact of extreme events (e.g., droughts, atmospheric rivers, etc.).

The Mattole River watershed model was configured based on authoritative and comprehensive data sets suitable for characterizing hydrology within the region. The model is based on HRUs, which capture physical attributes controlling the rainfall-runoff response and are driven by long-term meteorological forcing time series representing the spatial and temporal range of precipitation and evapotranspiration conditions in the watershed. The model was calibrated and validated at two USGS streamflow stations representing the headwaters (Ettersburg) and mainstem (Petrolia) of the Mattole River for the modeled period (Water Years 2004-2023). The overall model validation performance across the evaluated performance metrics was generally "Very Good" to "Good". There is some accepted underprediction of wet-weather flows at the Ettersburg headwaters station during the calibration period (2018-2023); however, this was necessary to balance overprediction at the larger downstream Petrolia station. Model performance at both Ettersburg and Petrolia during the validation period (2004-2017) were generally "Very Good" and "Good," with a reasonably representative water balance assessment. The difference in performance between the two gauges may indicate unrepresented processes in the Petrolia drainage area that could be further evaluated when additional information and data become available.

Some key findings on conditions within the Mattole River watershed that should be considered during use and potential future updates to the model are:

- **Forest recovery from logging**: The Mattole River watershed has been dynamically recovering from extensive logging sing the 1950s and 1960s. The current stage of forest growth, especially for Douglas fir, has been shown to use more water than older mature forests; however, this use may decline as forests mature and the density of trees declines from canopy closure and stem suppression (Stubblefield et al. 2011; Stubblefield and Reddy 2022).
- **Headwaters restoration efforts**: A consortium of organizations have been working in headwater regions of the Mattole River watershed with the aim to "improve coho spawning habitat and water supply conditions by restoring consistent summertime flows, enhancing riparian cover, and supporting groundwater recharge to result in beneficial floodplain habitat and flow regime in the upper Mattole" (California State Coastal Conservancy 2018). These projects are ongoing and have included instream restoration, rainwater capture and groundwater recharge ponds (TNC 2017), and will include forest thinning in riparian corridors (CDFW 2024). These organizations could provide important local knowledge of conditions within the watershed and may have additional data for future model refinements.
- **Representation of springs**: As discussed in Section 7.3.2, there are many springs within the Mattole River watershed, as well as other potential groundwater-surface water interactions that are not currently represented in the model. As a surrogate for enhanced groundwater modeling, springs could be represented in future refinements to help capture the steady baseflow seen in many years. While there is little to no available data on spring flows in the watershed generally, the BLM does provide occasional reports for select springs within the King Range Wilderness (e.g., King Range National Conservation Area: Roads & Trails Report). These reports are

generally qualitative and the accuracy of flow rates, when provided, is uncertain. Engagement with King Range BLM staff may provide additional details.

In conclusion, the Mattole River watershed model is a robust platform for representing existing conditions and setting up future management scenarios. An important benefit of the model development approach used to build the watershed model and described in this report is that it is designed in a modular way, where key components can be refined and improved over time as new and better information becomes available.

10 REFERENCES

Arcement, G.J. Jr., Schneider, V.R., 1989. Guide for selecting Manning's roughness coefficients for natural channels and flood plains. USGS Water-Supply Paper 2339.

Arnold, J.G., Allen, P.M., Muttiah, R., Bernhardt, G., 1995. Automated Base Flow Separation and Recession Analysis Techniques. Groundwater 33, 1010–1018. https://doi.org/10.1111/j.1745-6584.1995.tb00046.x

Bent, G.C., Waite, A.M., 2013. Equations for Estimating Bankfull Channel Geometry and Discharge for Streams in Massachusetts. U.S. Geological Survey Scientific Investigations Report 2013–5155 62. https://doi.org/https://doi.org/10.3133/sir20135155

California State Coastal Conservancy, 2018. Mattole Headwaters Groundwater, Streamflow and Habitat Enhancement. Project No. 18-007-01. https://scc.ca.gov/webmaster/ftp/pdf/sccbb/2018/1805/20180524Board06_Mattole_Headwaters.pdf

CDFW (California Dept. of Fish and Wildlife), 2024. California Environmental Quality Act Statutory Exemption for Restoration Projects: Mattole Headwaters Enhancement and Planning Project. https://nrm.dfg.ca.gov/FileHandler.ashx?DocumentID=223838&inline

Cosgrove, B.A., Lohmann, D., Mitchell, K.E., Houser, P.R., Wood, E.F., Schaake, J.C., Robock, A., Marshall, C., Sheffield, J., Duan, Q., Luo, L., Higgins, R.W., Pinker, R.T., Tarpley, J.D., Meng, J., 2003. Real-time and retrospective forcing in the North American Land Data Assimilation System (NLDAS) project. Journal of Geophysical Research: Atmospheres 108, 8842. https://doi.org/10.1029/2002jd003118

Daly, C., G. H. Taylor, W. P. Gibson, T. W. Parzybok, G. L. Johnson, P. A. Pasteris, 2000. High-Quality Spatial Climate Data Sets for the United States and Beyond. Transactions of the ASAE 43, 1957–1962. https://doi.org/10.13031/2013.3101

Daly, C., Neilson, R.P., Phillips, D.C., 1994. A Statistical-Topographic Model for Mapping Climatological Precipitation over Mountainous Terrain. J Appl Meteorol Climatol 33, 140–158.

Daly, C., Taylor, G., Gibson, W., 1997. The Prism Approach to Mapping Precipitation and Temperature, in: 10th AMS Conf. on Applied Climatology. Reno, NV, pp. 10–12.

Doherty, J., 2015. Calibration and Uncertainty Analysis for Complex Environmental Models - PEST: complete theory and what it means for modelling the real world. Brisbane, Australia.

Duda, P.B., P.R. Hummel, A.S. Donigian, and J.C. Imhoff, 2012. BASINS/HSPF: Model Use, Calibration, and Validation. Trans ASABE 55, 1523–1547. https://doi.org/10.13031/2013.42261

DWR (California Department of Water Resources), 2025. i07 Well Completion Reports. DWR GIS. https://data.ca.gov/dataset/i07-wellcompletionreports1

EPA (U.S. Environmental Protection Agency), 2000. BASINS Technical Note 6 Estimating Hydrology and Hydraulic Parameters for HSPF, Office of Water 4305. EPA-823-R00-012.

Gibson, W.P., Daly, C., Kittel, T., Nychka, D., Johns, C., Rosenbloom, N., McNab, A., Taylor, G.H., 2002. Development of a 103-Year High-Resolution Climate Data Set for the Conterminous United States, in: Proceedings of the 13th AMS Conference on Applied Climatology. Portland, OR, pp. 181–183.

Gupta, H. V., Kling, H., Yilmaz, K.K., Martinez, G.F., 2009. Decomposition of the mean squared error and NSE performance criteria: Implications for improving hydrological modelling. J Hydrol (Amst) 377, 80–91. https://doi.org/10.1016/j.jhydrol.2009.08.003

Henn, B., Newman, A.J., Livneh, B., Daly, C., Lundquist, J.D., 2018. An assessment of differences in gridded precipitation datasets in complex terrain. J Hydrol (Amst) 556, 1205–1219. https://doi.org/10.1016/j.jhydrol.2017.03.008

Houtman, R.M., Leatherman, L.S.T., Zimmer, S.N., Housman, I.W., Shrestha, A., Shaw, J.D., Riley, K.L., 2025. TreeMap 2022 CONUS: A tree-level model of the forests of the conterminous United States circa 2022. Forest Service Research Data Archive. https://doi.org/10.2737/RDS-2025-0032

Jasechko, S., Seybold, H., Perrone, D., Fan, Y., Kirchner, J.W., 2021. Widespread potential loss of streamflow into underlying aquifers across the USA. Nature 591, 391–395. https://doi.org/10.1038/s41586-021-03311-x

Kim, S., Paik, K., Johnson, F.M., Sharma, A., 2018. Building a Flood-Warning Framework for Ungauged Locations Using Low Resolution, Open-Access Remotely Sensed Surface Soil Moisture, Precipitation, Soil, and Topographic Information. IEEE J Sel Top Appl Earth Obs Remote Sens 11, 375–387. https://doi.org/10.1109/JSTARS.2018.2790409

Knoben, W.J.M., Freer, J.E., Woods, R.A., 2019. Technical note: Inherent benchmark or not? Comparing Nash–Sutcliffe and Kling–Gupta efficiency scores. Hydrol Earth Syst Sci 23, 4323–4331. https://doi.org/10.5194/hess-23-4323-2019

Kouchi, D.H., Esmaili, K., Faridhosseini, A., Sanaeinejad, S.H., Khalili, D., Abbaspour, K.C., 2017. Sensitivity of calibrated parameters and water resource estimates on different objective functions and optimization algorithms. Water (Basel) 9. https://doi.org/10.3390/w9060384

LACFCD (Los Angeles County Flood Control District), 2020. WMMS Phase I Report: Baseline Hydrology and Water Quality Model. Prepared for the Los Angeles County Flood Control District by Paradigm Environmental. Alhambra, CA.

Looper, J.P., Vieux, B.E., 2012. An assessment of distributed flash flood forecasting accuracy using radar and rain gauge input for a physics-based distributed hydrologic model. J Hydrol (Amst) 412–413, 114–132. https://doi.org/10.1016/j.jhydrol.2011.05.046

McCandless, T.L., 2003a. Maryland stream survey: Bankfull discharge and channel characteristics in the Allegheny Plateau and the Valley and Ridge hydrologic region. Annapolis, MD.

McCandless, T.L., 2003b. Maryland Stream Survey: Bankfull Discharge and Channel Characteristics in the Coastal Plain Hydrologic Region. Annapolis, MD.

McCandless, T.L., Everett, R.A., 2002. Maryland stream survey: Bankfull discharge and channel characteristics in the Piedmont hydrologic region. Annapolis, MD.

McGourty, G., Lewis, D., Metz, J., Harper, J., Elkins, R., Christian-Smith, J., Papper, P., Schwankl, L., Prichard, T., 2020. Agricultural water use accounting provides path for surface water use solutions. Calif Agric (Berkeley) 74, 46–57. https://doi.org/10.3733/CA.2020A0003

Mitchell, K.E., Lohmann, D., Houser, P.R., Wood, E.F., Schaake, J.C., Robock, A., Cosgrove, B.A., Sheffield, J., Duan, Q., Luo, L., Higgins, R.W., Pinker, R.T., Tarpley, J.D., Lettenmaier, D.P., Marshall, C.H., Entin, J.K., Pan, M., Shi, W., Koren, V., Meng, J., Ramsay, B.H., Bailey, A.A., 2004. The multi-institution North American Land Data Assimilation System (NLDAS): Utilizing multiple GCIP products and partners in a continental distributed hydrological modeling system. Journal of Geophysical Research: Atmospheres 109. https://doi.org/10.1029/2003jd003823

Moriasi, D.N., Arnold, J.G., Van Liew, M.W., Bingner, R.L., Harmel, R.D., Veith, T.L., 2007. Model Evaluation Guidelines for Systematic Quantification of Accuracy in Watershed Simulations. Trans ASABE 50, 885–900. https://doi.org/10.13031/2013.23153

Moriasi, D.N., Gitau, M.W., Pai, N., Daggupati, P., 2015. Hydrologic and water quality models: Performance measures and evaluation criteria. Trans ASABE 58, 1763–1785. https://doi.org/10.13031/trans.58.10715

Nash, J.E., Sutcliffe, J. V., 1970. River flow forecasting through conceptual models part I - A discussion of principles. J Hydrol (Amst) 10, 282–290. https://doi.org/10.1016/0022-1694(70)90255-6

Nathan, R.J., McMahon, T.A., 1990. Evaluation of automated techniques for base flow and recession analyses. Water Resour Res 26, 1465–1473. https://doi.org/10.1029/WR026i007p01465

Pypker, T.G., Bond, B.J., Link, T.E., Marks, D., Unsworth, M.H., 2005. The importance of canopy structure in controlling the interception loss of rainfall: Examples from a young and an old-growth Douglas-fir forest. Agric For Meteorol 130, 113–129. https://doi.org/10.1016/j.agrformet.2005.03.003

Quirmbach, M., Schultz, G.A., 2002. Comparison of rain gauge and radar data as input to an urban rainfall-runoff model. Water Science and Technology 45, 27–33. https://doi.org/10.2166/wst.2002.0023

Riley, K.L., Grenfell, I.C., Shaw, J.D., Finney, M.A., 2022. TreeMap 2016 Dataset Generates CONUS-Wide Maps of Forest Characteristics Including Live Basal Area, Aboveground Carbon, and Number of Trees per Acre. J For 120, 607–632. https://doi.org/10.1093/jofore/fvac022

Sloto, R.A., Crouse, M.Y., 1996. HYSEP: A Computer Program for Streamflow Hydrograph Separation and Analysis: U.S. Geological Survey Water-Resources Investigations Report 1996–4040. https://doi.org/10.3133/wri964040

Smakhtin, V.U., 2001. Low flow hydrology: a review. J Hydrol (Amst) 240, 147–186. https://doi.org/10.1016/S0022-1694(00)00340-1

Stubblefield, A., Kaufman, M., Blomstrom, G., Rogers, J., 2011. Summer Water Use by Mixed-Age and Young Forest Stands, Mattole River, Northern California, U.S.A., in: Standiford, R.B., Weller, T.J., Piirto, D.J., Stuart, john D. (Eds.), Proceedings of the Coast Redwood Forests in a

Changing California: A Symposium for Scientists and Managers. United States Forest Service, Santa Cruz, pp. 173–184.

Stubblefield, A.P., Reddy, K., 2022. Measurement and prediction of water consumption by Douglas-fir, Northern California, USA. Ecohydrology 15. https://doi.org/10.1002/eco.2388

Sutherland, R.C., 2000. Methods for Estimating the Effective Impervious Area of Urban Watersheds, Technical Note 58, in: Scueler, T.R., Holland, H.K. (Eds.), The Practice of Watershed Protection. Center for Watershed Protection, Ellicot City, MD, pp. 193–195.

SWRCB (State Water Resource Control Board), 2024. Watershed Supply and Demand Allocations: Mattole River Work Plan. https://www.waterboards.ca.gov/waterrights/water_issues/programs/supply-and-demand/docs/mattole-river-workplan.pdf

SWRCB (State Water Resource Control Board), 2025. Supply and Demand Assessment (SDA) – Navarro River. Watershed Supply and Demand Allocations. https://www.waterboards.ca.gov/waterrights/water_issues/programs/supply-and-demand/navarro-river.html.

TNC (The Nature Conservancy), 2017. Humboldt County | Near-Stream Recharge: Reconnecting Surface and Groundwater. https://www.groundwaterresourcehub.org/content/dam/tnc/nature/en/documents/GWR_Hub_Mattole_Creek_case_study.pdf

USGS (United States Geological Survey), 2025. USGS TNM HydroLocation - Sink, Spring, Waterbody Outlet (ID: 20). https://3dhp.nationalmap.gov/arcgis/rest/services/usgs_3dhp_all/FeatureServer/20.

USDA (United States Department of Agriculture), 2024. Cropland Data Layer. https://croplandcros.scinet.usda.gov/.

Xia, Y., Mitchell, K., Ek, M., Cosgrove, B., Sheffield, J., Luo, L., Alonge, C., Wei, H., Meng, J., Livneh, B., Duan, Q., Lohmann, D., 2012a. Continental-scale water and energy flux analysis and validation for North American Land Data Assimilation System project phase 2 (NLDAS-2): 2. Validation of model-simulated streamflow. Journal of Geophysical Research Atmospheres 117. https://doi.org/10.1029/2011JD016051

Xia, Y., Mitchell, K., Ek, M., Sheffield, J., Cosgrove, B., Wood, E., Luo, L., Alonge, C., Wei, H., Meng, J., Livneh, B., Lettenmaier, D., Koren, V., Duan, Q., Mo, K., Fan, Y., Mocko, D., 2012b. Continental-scale water and energy flux analysis and validation for the North American Land Data Assimilation System project phase 2 (NLDAS-2): 1. Intercomparison and application of model products. Journal of Geophysical Research Atmospheres 117, 3109. https://doi.org/10.1029/2011JD016048